Bull. Inst. r. Sci. nat. Belg. Bull. K. Belg. Inst. Nat. Wet.	Bruxelles Brussel	31-V-1972
48	B I O L O G I E	6

EXPERIMENTAL ALTERATION OF THE NAUTILUS SHELL BY FACTORS INVOLVED IN DIAGENESIS AND IN METAMORPHISM

Part III. — Thermal and hydrothermal changes in the organic and mineral components of the mural mother-of-pearl

BY

Charles GRÉGOIRE (Liège)

(with 2 Tables and 133 Figures)

ERRATUM

Page 12, third paragraph from below : read rounding up of the fragments *instead of* rounding up the fragments.

Page 18, fourth paragraph : read girder *instead of* girdle.

Page 53, in the middle of the page, : 2 ..... *read* girder-like *instead of* girdle-like.

Page 81, second line : read girder- *instead of* girdle-.

1801

Bull. Inst. r. Sci. nat. Belg. Bull. K. Belg. Inst. Nat. Wet.	Bruxelles Brussel	31-V-1972
48	B I O L O G I E	6

EXPERIMENTAL ALTERATION OF THE NAUTILUS SHELL BY FACTORS INVOLVED IN DIAGENESIS AND IN METAMORPHISM

Part III. — Thermal and hydrothermal changes in the organic and mineral components of the mural mother-of-pearl

BY

Charles GRÉGOIRE (Liège)

(with 2 tables and 133 Figures)

(Reçu le 24 septembre 1971)

CONTENTS

I. INTRODUCTION

As shown previously (GRÉGOIRE, 1964, 1966 b, 1968; GRÉGOIRE and VOSS-FOUCART, 1970), dry pyrolysis of mother-of-pearl of the modern *Nautilus* produced in the conchiolin matrices modifications in structure and in biochemical composition which simulated changes observed in the remnants of fossil nacreous conchiolin (GRÉGOIRE, 1958, 1959 a, b, 1966 a, 1968; GRÉGOIRE and VOSS-FOUCART, 1970; VOSS-FOUCART, 1970; VOSS-FOUCART and GRÉGOIRE, 1971).

Part I of this study was a description of the alterations in the conchiolin matrices of the *Nautilus* mural mother-of-pearl pyrolysed dry in the range of 150 °C to 900 °C in open vessels, under vacuum in sealed tubes, and boiled at 100 °C in sea water.

As wet pyrolysis realizes a closer approach than dry heating to the conditions of natural diagenesis, it has been performed, in new sets of experiments, in sealed tubes in the presence of sea and of distilled water.

As reported in Part I, the samples heated dry at 300 °C were still aragonitic, those heated at 400 °C were calcitic. In other sets of experiments, the temperature of conversion of aragonite into calcite has been precised, using series of samples heated dry and wet at 325 °C, 350 °C and 375 °C.

The present Part III is chiefly a study with the transmission and scanning electron microscopes of the pyrolytic changes in the microtexture of the mineral components of the whole material. These changes have been compared to those recorded in mother-of-pearl of fossil specimens of different ages.

Abstracts of fragmentary results have been given elsewhere (GRÉGOIRE, GISBOURNE and HARDY, 1969; GRÉGOIRE and LORENT, 1971).

II. MATERIAL AND METHODS

The fragments of mural mother-of-pearl of *Nautilus pompilius* LINNÉ and of *Nautilus macromphalus* SOWERBY used in these investigations were collected in the living chamber, more adorally than the region of insertion of the shell muscles.

The fragments were deposited in open ceramic boats or introduced, dry or mixed with sea or distilled water, in quartz tubes (vitriosil) which were then sealed under vacuum or under argon atmosphere. Heating was performed by boiling at 100 °C or in electric ovens and in muffle furnaces in the range of 150 °C to 900 °C for different periods of time (5 minutes to 53 days).

The value of the methods of preparation used for obtaining reliable records in the transmission electron microscope of the structures of the brittle altered conchiolin matrices in fossil and in the pyrolysed modern nacres has been discussed elsewhere (GRÉGOIRE, 1966 a, b, p. 13; 1968, p. 10 and 11; GRÉGOIRE and LORENT, 1971).

Two procedures of preparation have been used.

1. Decalcification of the fragments by EDTA (titriplex III, Merck, Darmstadt, pH 4.0 and 7.5). The conchiolin residues were collected directly on formvar coated screens. Agglutinated interlamellar matrices, opaque to the electron beam, were gently delaminated into single sheets by teasing with needles or were exposed for a few seconds to the ultrasonic radiations.

2. The interlamellar conchiolin matrices were also observed in their original topography in the form of pseudoreplicas adhering to the replicas of surfaces of polished and etched tangential sections of mother-of-pearl and to the surfaces of cleavage along the interlamellar planes (see Part I, p. 10).

The changes in the microtexture and in the microstructure of the mineral components were studied using positive carbon-platinum replicas (double-stage replication : BRADLEY, 1956; single-stage, self-shadowed replication : TOWE and CIFELLI, 1967), of surfaces of fresh fracture and cleavage, and of surfaces of polished and etched sections of the samples in transverse and tangential orientations.

The samples pyrolysed over 300 °C are brittle and powdery. Direct replication of the rough surfaces of fracture of these samples was impossible in most cases. In these materials, the changes in the microstructures were studied with a scanning electron microscope (SEM) (STEREOSCAN. Cambridge Scientific Instruments Limited).

The nature of the minerals composing the samples has been determined by X-ray powder diffraction analysis (see GRANDJEAN, GRÉGOIRE and LUTTS, 1964). As already reported, the results indicate the predominant

substance found in the samples : minerals in lesser amounts than 3 per cent could not be recorded with the diffractometer used. Under these conditions, ultramicroscopic islands of aragonite or of recrystallization into calcite escaped detection in samples identified respectively as calcitic or aragonitic in composition.

The transmission electron microscopy (TEM) was carried out using a R C A - E M U - 2 and chiefly a SIEMENS-ELMISKOP I, using a double condenser, a voltage of 80 kV, a 200 microns condenser aperture, a 30 microns objective aperture and a cold stage.

All the transmission electron micrographs were taken by Ch. GRÉGOIRE, the scanning electron micrographs by Chr. GISBOURNE and Ann HARDY. The micrographs of Figs. 119-124 were taken by Mr. G. DETILLOUX.

III. OBSERVATIONS

A description of the hydrothermal changes in mother-of-pearl of the shell wall of *Nautilus* is given in table 1. The micrographs are a sampling of about 8,000 transmission electron micrographs and 800 scanning electron micrographs.

1. Microtexture and microstructure of the nacre in the shell wall of Nautilus

The considerable literature on the texture of mother-of-pearl in modern shells has been frequently reviewed (see GRÉGOIRE, 1957, 1967, 1971; WILBUR and SIMKISS, 1968; WISE, 1970; MUTVEI, 1970) and will not be again examined.

Mother-of-pearl appears as a brickwork, in which aragonite crystals are the bricks and a conchiolin matrix the mortar (EHRENBAUM, 1885; SCHMIDT, 1923, 1924). Tabular, euhedral or rounded crystals of aragonite form a single mineral layer or lamella. Numerous lamellae are piled upon each other horizontally, parallel to the inner shell surface. Stacking of the crystals into vertical columns characterizes mother-of-pearl in *Nautilus* (VON NATHUSIUS-KÖNIGSBORN, 1877; BIEDERMANN, 1902; SCHMIDT, 1923, 1924; AHRBERG, 1935; GRÉGOIRE, 1962, 1966 a; STENZEL, 1964; MUTVEI, 1964, 1970; ERBEN, FLAJS and SIEHL, 1969; WISE, 1970).

As in case of crystals of calcite in the calcitostracum (WATABE, SHARP and WILBUR, 1958; WADA, 1961, 1963) the individual tabular crystals of aragonite in the nacreous layers of different shells have been considered as mosaic aggregates of aragonite microcrystals, oriented polycrystalline aggregates (WADA, 1961, 1966, 1968; GRÉGOIRE, 1966b; GRÉGOIRE, GISBOURNE and HARDY, 1969; MUTVEI, 1970), as monocrystals constructed of primary subunits, 500-600 Å of average size (TOWE and HAMILTON, 1968) and as coherent optical units (WISE, 1970). According to MUTVEI (1970) microcrystallites or aragonitic laths form a single layer in each

aragonite crystal and are oriented parallel to its crystallographic a-axis. The laths are themselves composed of smaller acicular elements (MUTVEI, 1972). These laths appear on the 001 planes of the aragonite crystals in the form of parallel ridges or rod-like elevations (Figs. 15, 16, 17). In parts of the nacreous layer, where the aragonite crystals seem to lack an uniform orientation, the laths show a different orientation in adjacent crystals (MUTVEI, 1970; see also GRÉGOIRE, 1959, in fossils, Pl. 2, Fig. 11).

Circular or elongate elevations (« tubercles » : MUTVEI, 1970) identical to the crystal seeds described on the growth surfaces of the nacre (see discussion : IV 2 B b), are superposed on the ridges in parallel rows or scattered at random on the 001 facets of the tabular crystals. Some of these crystal seeds have euhedral, hexagonal outlines (not shown).

2. Microstructure of the mural nacreous conchiolin

The literature on the organic components of mother-of-pearl has been reviewed elsewhere (GRÉGOIRE, 1957, 1967, 1971; MUTVEI, 1969). Conchiolin matrices separate the lamellae (interlamellar conchiolin) and the crystals (intercrystalline conchiolin).

Among the taxonomic patterns of ultrastructure recognized with the TEM in the interlamellar conchiolin matrices (GRÉGOIRE, DUCHÂTEAU and FLORKIN, 1950, 1955; GRÉGOIRE, 1957, 1962; MUTVEI, 1969), the nautiloid pattern is characterized by a rather loosely knit texture, sturdy, irregularly cylindrical trabeculae in the form of knobby cords (1), sprinkled with hemispheral protuberances or tuberosities, and a broad, frequently elongate fenestration (2) (see GRÉGOIRE, 1962, Fig. 39; 1966a, Figs. 1-4; 1968, Fig. 1). According to MUTVEI (1969), the intertrabecular areas in the matrices are not openings, but are occupied by a thin membrane.

In the samples decalcified without mechanical dislocation of the conchiolin membranes, and especially in the pseudoreplicas left on the surfaces of cleavage or on the polished and etched tangential sections of the nacre, the interlamellar conchiolin matrices appear in the form of mosaics of polygonal fields delimited by cords of intercrystalline conchiolin. These structures which reveal the outlines of the flagging formed by the original polygonal crystals between which the matrices were sandwiched before decalcification were called crystal imprints by GRÉGOIRE (1959 a, Figs. 1 and 2; 1959 b, Fig. 1; 1962, Figs. 46, 80, 81; 1966 a, Fig. 44), GRÉGOIRE and TEICHERT (1965, Pl. III, Fig. 1; Pl. VI,

(1) Recent additional results on the fibrillar microstructure of the trabeculae will be examined in a further paper (see GRÉGOIRE, 1966a, p. 16 and 1967).

(2) Erben (1971, Plate 4, Figs. 3 and 4; 1972, Plate 6, Figs. 1 and 2; Plate 4, Fig. 2) using the SEM, dit not observe in the nacreous interlamellar conchiolin membranes of various molluscs the characteristic structures of the patterns (trabeculae, fenestration). The discrepancy between these and former observations is probably due to the fact that the power of resolution of the SEM does not permit to record the ultrastructures detected by means of the TEM (see also Part I, discussion, p. 11).

Figs. 1 and 2) and crystal scars by MUTVEI (1969) (3). In the central portions of these polygonal fields (« central transparent elevations areas », MUTVEI, 1969) the trabeculae are narrower and the intertrabecular areas broader than in the peripheral portions.

After a period of controversy (see WATABE, 1963, 1965; TOWE and HAMILTON, 1968), there seems to be now a general agreement that an intracrystalline matrix does exist, in a still unsufficiently known form, within the aragonite crystals. According to MUTVEI (1970), this matrix would probably encase, not only the aragonite laths, but also their acicular crystalline elements.

3. Conchiolin matrices of the pyrolysed mother-of-pearl (Plates 9, 10, 11, 16, 20, 21, 26, 29, 36 and 39)

A. Dry heat in open vessels and under vacuum in sealed tubes (Figs. 25, 26, 28, 29, 44, 45, 61, 79, 88, 106 and 107)

On the basis of an additional material, the present observations confirm and extend the former descriptions of the successive stages of alteration in the nautiloid pattern of conchiolin in the samples dry pyrolysed in the range of 150 °C to 900 °C, in open vessels and in sealed tubes (GRÉGOIRE, 1964, 1966 b and 1968, Part. I). These changes in the trabeculae of the conchiolin matrices consist of inflation, shrinkage, flattening and widening into loose networks of ribbon like structures (Figs. 25, 26, 29, 44, 88, 91 and 107), followed by coalescence into continuous or perforated membranes in which the holes are the traces of the original fenestration (Figs. 27 and 106) (4). In the 600 °C-900 °C stages, the membranes or the clusters composed of their debris have frequently polygonal shapes, and appear in the form of casts of facets of euhedral crystals (see below, hydrothermal alterations, Plate 39, and Part I, Figs. 92 and 95).

In agreement with the former observations, the samples heated in open vessels were more brittle and their conchiolin matrices were more altered than in the samples heated in sealed tubes. Flattening of the trabeculae into networks of ribbon-like structures develop also, as in sealed tubes, in the material heated in open vessels (Fig. 44), but these trabecular ribbons are extremely brittle and generally fragmented into twisted segments, lenticular or spheroidal, pebble-shaped corpuscles. These corpuscles remain agglutinated in their original position, especially in pseudo-replicas (Fig. 79) or are dispersed or clustered at random, especially in suspensions of the decalcified samples (Figs. 28, 45, 61) (5).

(3) The statement of Mutvei (1969) « that the crystal scars... have not been reported in the preparations of the demineralized interlamellar conchiolin membranes studied by GRÉGOIRE (1962) » is not consistent with these former observations on modern and fossil materials.

(4) See also in Part I, Figs. 51, 68, 69, 70, 75-80, 83-85 and 92.

(5) See also Part I, Figs. 20, 21-27 and 33.

Collection of several samples after a short exposure to heat (e.g. 5 to 60 minutes), revealed, as already shown in Part I (6) that the changes observed in the conchiolin matrices after a longer exposure (5 hours, 21 days) had already developed and seemed to be stabilized, except for further subsidiary structural differences (Figs. 88 and 91). In samples heated for example at 600 °C, the changes already appeared during preheating (after 5 minutes) and did not differ from those recorded at 300 °C-700 °C for varying periods of time (15 minutes to 5 hours).

All the samples were biuret-positive (see Part I).

B. Hydrothermal changes

The results are based on examination of 30 groups of samples heated for 5 hours in presence of sea or distilled water in tubes sealed under vacuum at temperatures in the range of 150 °C to 900 °C.

The changes observed in the conchiolin matrices of the samples heated wet were identical or did not distinctly differ from those seen in the samples heated dry under identical conditions of temperature : flattening of the trabeculae into loose networks of strips (Figs. 27, 30, 31, 32, 33, 46, 47, 62 and 80) and coalescence into continuous or fenestrate membranes (Figs. 46, 59, 63, 64, 65, 89, 90, 113, 114, 115) were predominant.

Compare Fig. 26 (275 °C, dry in open vessels) to Fig. 27 (275 °C, distilled water, 1090), Fig. 29 (300 °C, dry in sealed tubes, 782) to Fig. 30 (300 °C, sea water, 992), Fig. 44 (325 °C in open vessels, 1041) to Figs. 46 and 47 (325 °C, distilled water, 1044).

As in the samples heated dry in sealed tubes, the changes observed in samples heated wet, e.g. for 5 hours, were not modified by prolonged heating (compare Fig. 31 : 300 °C in distilled water, 5 hours, 976, to Figs. 32 and 33 : 300 °C, sea water, 21 days, 986).

The structure of the conchiolin in the samples heated wet at high temperatures (700 °C-900 °C) greatly varied, as in the samples heated dry (see Part. I, Figs. 86-95), and consisted of veils sprinkled with straight parallel rows of corpuscles (Fig. 114), thinly granular and vesiculated membranes (Figs. 113 and 115), clusters of agglutinated corpuscles (Figs. 124, 125 and 126), arranged into geometrical figures suggesting casts of facets of euhedral crystals (crystal ghosts).

In several samples heated dry and wet in the range of 600 °C-900 °C, elongate structures in the form of collapsed tubes were mixed with the other remnants of conchiolin (Figs. 104 and 105). These structures were composed of membranes perforated by rectangular openings surrounded by thickenings in the form of pads and more or less regularly aligned in parallel rows.

(6) Compare in Part I, Figs. 54, 57 and 59 (400 °C, 60 minutes in sealed tubes) to Figs. 55 and 56 (5 hours) and Figs. 58, 60 and 61 (21 days); Figs. 69 and 70 (600 °C, 5 minutes in sealed tubes) to Figs. 73 and 74 (30 minutes) and Figs. 75 and 76 (5 hours); Figs. 78 and 81 (800 °C, 5 minutes in sealed tubes) to Figs. 79 and 80 (30 minutes) and Figs. 82 to 85 (5 hours).

4. Hydrothermal changes in the microtexture of the nacre

A. Physical characteristics of the mineral components

The boiled fragments of nacre did not distinctly differ in colour and consistency from the normal nacre.

As reported previously (GRÉGOIRE, 1964, 1968; p. 4), the originally hard and compact nacreous substance of *Nautilus*, iridescent with pale greenish and faintly pink hues, is transformed by dry pyrolysis in open vessels and in sealed tubes into a brittle material, intensely coloured with glowing metallic tints. At 300 °C and over, this substance is spontaneously cleaved during pyrolysis into booklets of parallel mineral sheets which are composed of a varying number of parallel lamellae (Figs. 37, 38, 84, 85, 98, 99, 119, 128, 131).

In the samples heated over 500 °C, these sheets disintegrate into ash-grey and snow-white, lustreless, powdery material (in open vessels) or into extremely breakable, bright snow-white slabs and flakes (in sealed tubes). In sealed tubes, traces of iridescence could still be detected in the fragments heated at 800 °C for 5 minutes.

The hardness and colour of the samples heated dry and wet in sealed tubes did not distinctly differ. Several samples heated wet were possibly less brittle and remained more compact than their controls heated dry.

As seen in Part I (p. 4 and 7) X-ray powder diffraction analysis revealed preservation of the original aragonite in the 150-300 °C samples and transformation into calcite in the 400 °C and up samples, heated dry in open vessels and in sealed tubes. Calcium hydroxide, with decreasing amounts of calcite, was recorded in several 600 °C, 700 °C, 800 °C and 900 °C samples heated in open vessels.

Examination of an additionnal material has specified the temperature of transformation of the aragonite into calcite in samples heated for 5 hours in the range of 300 °C to 400 °C.

In open vessels, the samples were still aragonitic at 325 °C and were calcitic at 350 °C and 375 °C. The samples heated with distilled water in sealed tubes, were aragonitic at 300 °C, aragonitic, or calcitic with traces of aragonite, at 325 °C, and calcitic at 350 °C and 375 °C. Over these temperatures (up to 900 °C) calcite was recorded in all the samples, heated dry or wet in sealed tubes.

B. Transmission (TEM) and scanning (SEM) electron microscopy of the pyrolytic changes in the nacre (Plates 1, 2, 8, 12, 13, 17, 18, 19, 22, 23, 26, 27, 30, 31, 32, 34, 35, 37, 38, 40, 41, 42)

Owing to frequently periodic variations in the regularity of the nacreous stratification (see GRÉGOIRE, 1962, p. 9), in the thickness of the crystals

composing the lamellae and especially in the orientation of groups of lamellae, the changes which take place in mother-of-pearl during pyrolysis at relatively low temperatures (150 °C-250 °C), are difficult to appreciate. The brickwork texture seems to be unchanged in the samples boiled for 42 hours (Figs. 4, 5 and 6) or heated at 150 °C for 5 hours (Fig. 2). The first alterations seem to affect scattered individual crystals of aragonite without modifying the brickwork architecture. These alterations consist of loosening of the lamellae (Fig. 24), separation of contiguous crystals, inflation of portions of crystals, fragmentation, development of polygonal notches, pits, polyhedral elevations resembling inclusions in etched preparations (Figs. 24, 54, 56). Similar changes appeared in parts of nacreous layers in which the brickwork or the lamellar textures had been preserved in samples pyrolysed at 500 °C for 5 minutes (Fig. 92) and for 5 hours (Fig. 93).

On the surfaces of cleavage, which expose the 001 planes of the tabular crystals of aragonite, the changes in the parallel ridges and in the crystal seeds greatly vary in the different samples and in the different regions of a single sample. The modifications in these structures in samples pyrolysed at 200 °C - 350 °C for 5 hours consist of inflation, rounding up, fragmentation and coalescence, loss of orientation and disappearance in scattered areas (Figs. 22, 23). Clusters of similar seeds seemed to persist longer in the centre of the polygonal areas, corresponding to MUTVEI's « central elevations areas », of the aragonite crystals (Fig. 55).

The elements of texture involved in the sequence of changes with increase of temperature (300 °C and over) are essentially the characteristic columnar stacks of crystals (Figs. 35 and 36).

The nacreous layer was dissociated into groups of agglutinated parallel contiguous fragments of lamellae (Fig. 68) or columns of crystals (Figs. 34 and 57) forming foliate aggregates in which the parallel elements are the relics of the original nacreous lamellation (Fig. 38). The frequent random orientation of these aggregates of parallel elements is not an artifact of fracture, as for instance a displacement of groups of lamellae : replicas of the surfaces exposed by the spontaneous cleavage into sublayers of the nacre along the interlamellar planes reveal identical aggregates oriented at random at a distance from the region of fracture (see GRÉGOIRE *and al.*, 1969, Fig. 10 and p. 229).

The mineral sheets of cleavage are chiefly composed of these foliate aggregates. However, as shown in Figs. 37 and 48, parts of the original brickwork texture can subsist in contiguity to the altered regions. This « complex of alterations » was found not only in samples still composed of aragonite (250 °C, 275 °C, 300 °C) but also in further stages, in predominantly calcitic samples, in which aragonite was identified in individual crystals by X-ray diffraction analysis (Figs. 53, 57, 93, 95, 95 a).

Foliate aggregates constitute also the most typical changes in microtexture of the samples heated at higher temperatures (Figs. 49 and 50 : 325 °C; Figs. 84 and 85 : 400 °C; Figs. 98 and 99 : 500 °C).

In a further step of alteration, (Figs. 49, 57, 66) which can already take place in scattered portions of the samples heated at 300 °C - 325 °C the constituents of the aggregates (fragments of lamellae, crystal stacks) undergo a progressive coalescence, illustrated in Fig. 39. This field shows portions of columns of crystals in which fusion of the crystals into blocks has obliterated the interlamellar spaces. These spaces appear reduced to scattered oval holes.

In the foliate aggregates shown in Figs. 84, 85 (400 °C), 98 and 99 (500 °C), inflation of the crystals composing the mineral sheets seemed to accompany the process of coalescence.

With the progress of coalescence and fusion of their constitutive structures (600 °C - 900 °C), the foliate aggregates were transformed into blocks in which traces of the foliation are still recognizable (Fig. 116).

At this stage of the changes, the parallel mineral sheets of cleavage resemble in transverse fracture walls of ragstones and appear to be composed of mosaics of interlocking, coarse (14-22 microns), polyhedral, anhedral or subhedral crystals (Figs. 116, 117, 118, 119, 120-122, 123). As in case of crystalline grains composing coarse-grained limestones, observed by HARVEY (1966) with the electron microscope, these crystals have smooth edges, straight, curvilinear, concave or convex boundaries. Some surfaces of contact are in part concave toward one crystal and in part convex toward an adjacent crystal. Some of these crystals present hemispheric or elongate holes (Figs. 117, 122, 131, 133), which give them the appearance of fragments of swiss cheese (Fig. 120). Decoration patterns are visible on the contact surfaces of several crystals (Figs. 131 and 133).

Information on the changes described above were chiefly obtained from TEM and SEM records of surfaces of transverse fracture and of polished and etched transverse section.

The sequences in the pyrolytic changes developed on the 001 planes of the original aragonite crystals have been chiefly studied on direct replicas of surfaces of cleavage of the parallel mineral sheets, produced spontaneously during pyrolysis along the interlamellar planes, and on preparations of polished and etched tangential sections of the samples.

These changes shown in Figs. 51, 52, 54-56, 58, 60, 67, 71, 72, 81-83, 94, 100, 108-112, 129 and 132 may be summarized as follows :

1. The tabular 001 planes of the original crystals of aragonite are progressively replaced by loose or tight mosaics of smaller crystals, either by fragmentation or by another mechanism (Figs. 51, 52 : 325 °C; Fig. 60 : 350 °C; Figs. 67 and 68 : 375 °C; Figs. 81, 82 and 83 : 400 °C; Fig. 100 : 500 °C; Fig. 108 : 600 °C, 30 minutes : Fig. 109 : 600 °C, 60 minutes; Fig. 111 : 600 °C, 5 hours. Except for the samples shown in Figs. 51 and 52 (325 °C), which still contained aragonite, all the other samples were calcitic. Some of these smaller crystals appear elongate and disposed in bundles (Figs. 51 and 52). Fig. 83 shows a disposition res-

sembling an enfacial junction, described by BATHURST (1964) (see discussion). As in preparations of transverse fracture, decoration patterns appear on the surfaces of several crystals (Figs. 51 and 52).

2. In still aragonitic and in calcitic samples, single coarse crystals or groups of crystals and acicular blades, generally of large size, and differing thoroughly in their appearance from the surrounding elements, were scattered in different parts of the surfaces (Figs. 58, 71, 72).

3. Etching of the surfaces of cleavage along the interlamellar planes revealed in aragonitic and calcitic samples polyhedral elevations standing out in relief on the surfaces of the large crystals exposed by cleavage (Fig. 54) and polygonal pits perforating other crystals (Fig. 56, see discussion, IV, 2 B b). Identical microstructures were found on the 001 planes of the aragonite crystals in a sample after 5 minutes, during preheating to 500 °C (771 : Fig. 94).

4. In the samples heated in the range of 600 °C - 900 °C, mosaics of bulging, coarser, dome-shaped polygonal elements (Fig. 110) compose, instead of the mosaics of small crystals described above, the surfaces of cleavage, which resemble pavements of cobblestones (Figs. 112, 119, 123, 129, 132). These bulging crystal surfaces are the facets, exposed on the surfaces of cleavage, of the polyhedral crystals shown in transverse fracture in Figs. 116, 117, 118, 119, 121, 122).

Particular structures

1. Decoration patterns were scattered on some facets of crystals in the mosaics described above (Figs. 51 and 52).

2. In several samples heated dry and wet in the range of 600 °C - 900 °C and composed of calcite, needle-, rod- or girdle- like crystals were erected at different angles on the cleavage surfaces of the mineral sheets (Figs. 96, 97 and 103). These crystals resemble the whiskers described in other materials.

3. Efflorescences in the form of rosettes of diverging flat crystals developed on the surfaces of transverse fracture in some samples in which metallization before examination in the scanning microscope had not been performed immediately after fracture.

5. Microtexture of fossil nacreous layers in ammonoids and in nautiloids

(Plates 1, 3, 4, 5, 7, 14, 15, 24, 25, 28 and 33)
(see also GRÉGOIRE, 1966 a, Figs. 47 to 54)

Data obtained with the conventional and polarisation microscopes on the topography and on the microarchitecture of the fossil nacres (BØGGILD,

1930; HÖLDER, 1952; HÖLDER and MOSEBACH, 1950) have been confirmed and extended with the TEM and SEM (GRÉGOIRE, 1959 a, 1966 a; BIRKELUND, 1967; HUDSON, 1967; MUTVEI, 1967, 1970; ERBEN, FLAJS and SIEHL, 1969).

With a view to comparing with the pyrolytic changes in the microtexture of the nacre of the modern *Nautilus*, a few examples of diagenetic textural alterations have been selected in a material of Pennsylvanian, Permian, Jurassic, Cretaceous and Miocene nautiloids and ammonoids (unpublished results 1957-1971, and 1966 a, pp. 8-11 and 19-20).

A. Nacreous layers with integral or predominant preservation of the aragonite

Stacking in columns of the aragonite crystals as in the modern *Nautilus* is shown in the Jurassic *Leioceras* (Fig. 3) and in the Cretaceous *Baculites* (Fig. 10).

In the fossil material used, all grades of alteration were found in the aragonitic nacreous layers, from an apparently intact mineral microtexture to disappearance of the lamellation. Fig. 7 shows in a Pennsylvanian ammonoid (*Wellerites mohri*, Buckhorn Asphalt, 769) the characteristic stacking of the crystals, still associated with a whole conchiolin (interlamellar and intercrystalline) equipment. A similar preservation of the microtexture is shown in the Cretaceous nautiloid *Eutrephoceras* sp. (999, Fig. 11), in the Cretaceous ammonoids *Baculites ovatus* (356; Fig. 12) and *Acanthohoplites* sp. (499 : Fig. 14).

In the nacreous layers of other fossils, changes in the microtexture consist of discontinuities in portions of the interlamellar conchiolin matrices produced by inflation and local coalescence of contiguous crystals or columns of crystals (e.g. in the Jurassic *Ammonites lineatus penicillatus*, 785, Fig. 13; in a sample from the Cretaceous ammonoid *Placenticeras* : 1006, Fig. 8). Fragmentation of the crystals with rounding up the fragments, is shown in Figs. 9 and 10 (Cretaceous *Baculites claviformis* : 998, 393).

In these well preserved nacreous layers, replicas of cleavage surfaces along the interlamellar planes revealed, as in the normal nacre, mosaics of polygonal crystal surfaces, apparently unchanged in their structure, on to which crystal seeds were scattered (Fig. 18 : *Leioceras*, Jurassic; Fig. 19 : a Pennsylvanian orthoconic nautiloid; Figs. 20 and 21 : two different Cretaceous *Placenticeras*).

In other predominantly aragonitic nacreous layers or in scattered portions of otherwise intact microtextures, more advanced stages of alteration consist of coalescence of columns of crystals into anhedral blocks or grains in which the original lamellation and the form of the original crystals are progressively obliterated by fusion. This type of alteration is shown in Fig. 40 (Jurassic *Ammonites lineatus penicillatus*,

785), in Fig. 41 (Cretaceous ammonoid *Placenticeras* sp., 1006), and in Fig. 43 (Jurassic ammonoid *Psiloceras planorbis*, 988), in which the successive steps towards formation of subhedral or euhedral crystals from anhedral grains are visible.

In a still more advanced stage of alteration, the stacks of originally tabular crystals fused into blocks appear in the form of coarse polyhedral, subhedral or euhedral crystals with several plane facets (Fig. 42 : *Ammonites lineatus penicillatus*, Jurassic, 785, aragonite and calcite). In the field seen in this figure, the traces of the original crystals, still visible in the blocks shown in Figs. 40, 41 and 43, have disappeared and the disposition of the polyhedral crystals in rows is the only trace of the original columnar arrangement.

B. Recrystallized nacreous layers (Plates 24, 25 and 33)

Mosaics of interlocking coarse crystals oriented at random characterize the texture of the recrystallized fossil nacreous layers (BØGGILD, 1930; MOORE, LALICKER and FISCHER, 1952; HÖLDER, 1952; HÖLDER and MOSEBACH, 1950; BATHURST, 1964; GRÉGOIRE, 1966 a; DODD, 1966; ERBEN and *al.*, 1969).

In the samples selected for comparison with the pyrolysed nacre, persistance of relics of the original aragonitic crystal fabrics indicate, as reported in former petrographic studies of FLOWER (1961), HUDSON (1962) and BATHURST (1964) that transformation of aragonite into calcite had occurred in situ.

Figs. 77 and 78 (Permian nautiloid *Domatoceras* sp., 422), Figs. 73, 74 and 75 (Jurassic ammonoid *Ludwigia murchisonae*, 836), Fig. 76 (Jurassic ammonoid *Hildoceras* sp. 1008) and Fig. 101 (Jurassic *Ammonites lineatus penicillatus*, 785) show different aspects of these mosaics in preparations of transverse fracture of the nacreous layers of the shell wall, and especially parallel lamellation and striation in the individual crystals. The orientation of this striation differs or not (see Fig. 101) in the contiguous crystals. In Fig. 78, three parallel straight lines (ridges, grooves ?) subdivide the field into four mineral sheets. Each of these sheets consists of blocks (grains), differently oriented, made up of thinly parallel mineral lamels. These lamels run in some places across the straight lines without discontinuity.

C. Conchiolin remnants

Flattening, widening and coalescence of the trabeculae into continuous or fenestrate membranes, dislocation into corpuscles are the predominant structural changes observed in the remnants of the interlamellar conchiolin matrices of the fossil nacres from different ages investigated till now (GRÉGOIRE, 1958, 1959 a, b, 1966, 1968; GRÉGOIRE and VOSS-FOUCART, 1970; VOSS-FOUCART and GRÉGOIRE, 1971).

Fig. 85 shows such remnants in the Cretaceous ammonoid *Collignoniceras*, in the form of loose networks of flattened trabeculae, fused into membranes by coalescence.

IV. DISCUSSION

1. Conchiolin matrices of pyrolysed mother-of-pearl

The results of the present study confirm and extend former observations (see Part I) and can be summarized as follows :

a. In the four groups of samples (ebullition, heating in open vessels, heating dry and wet in sealed tubes) the present results confirm the remarkable thermoresistance of conchiolin, which has not yet disappeared in the samples heated at 900 °C for 5 hours and was still biuret-positive, though altered in its biochemical composition.

b. In the remnants of decalcification of the pyrolysed samples, and in the structures left in the form of pseudoreplicas on the cleaved, polished and etched surfaces along the interlamellar planes, mosaics of polygonal fields, characterize, as in normal nacre, the structure of the interlamellar matrices of conchiolin (Figs. 32, 46, 63 to 65, 87, 91, 107). Loosening of the original conchiolin networks, flattening of trabeculae into angulate strips and coalescence of this material into continuous or fenestrate membranes, especially at the periphery of the polygonal areas, are the predominant hydrothermal changes observed within these areas in the samples heated in sealed tubes. (Figs. 25-27, 29-31, 46, 47, 88, 91, 106.) Pyrolysis in open vessels alters more the conchiolin matrices than in sealed tubes, in producing disintegration of the trabeculae into corpuscles (Fig. 45; compare also Figs. 61 and 62). As the pyrolytic organic material is very brittle, especially in the samples heated in open vessels, the polygonal areas formed by the interlamellar conchiolin matrices are frequently dislocated, especially in the samples collected from suspensions of the decalcified nacre and the fragments of trabeculae are dispersed at random on the screens.

c. The structural changes in the conchiolin matrices did not distinctly differ in samples heated dry or wet in sealed tubes.

d. The structural changes in the conchiolin matrices developed rapidly in the pyrolysed samples, within a few minutes, in still integrally or predominantly aragonitic nacreous layers. From the 275 °C - 300 °C stages up, these changes seemed to be stabilized and did not show further important modification during prolonged heating (21 days) at the same or at higher temperatures. A similar stabilization has been also observed in the biochemical composition of this material (GRÉGOIRE and VOSS-FOUCART, 1970; VOSS-FOUCART and GRÉGOIRE, 1971 a, b).

2. Hydrothermal changes in the microtexture of the nacre and in the microstructure of its crystals

A. Previous work on inversion of skeletal aragonite into calcite

The thermal inversion of skeletal aragonite into calcite has been investigated experimentally and in the nature by means of crystallographic, petrographic, thermodynamic and physico-chemical techniques (SORBY, 1879, in *Anodonta* and *Pinna*; MÜGCE, 1901, in *Nautilus pompilius*; LAND, 1967, in corals, pelecypod shells and the Gastropod *Polinices*; KUNZLER and GOODELL, 1970, in the gastropod *Oliva*). The problem of aragonite-calcite relations has been reviewed by FAUST (1950), MACDONALD (1956), CURL (1962), BROWN, FYFE and TURNER, 1962, FYFE and BISCHOFF (1965), KENNEDY and HALL (1967), HALL and KENNEDY (1967), BOETTCHER and WYLLIE (1967, 1968), LAND (1967).

In their experimental investigations using the electron microscope on transformation of heated and compressed wet mud from the Bahamas, composed of aragonite needles, HATHAWAY and ROBERTSON (1961) observed a rapid transformation of the needles into a mosaic of large globular-shaped calcite crystals.

In their studies on the kinetics of transformation of aragonite into calcite, AVRAMI (1939), KUNZLER and GOODELL (1970) report that calcite nucleation must occur within the aragonite crystallites at preferred sites corresponding to aragonite germ nuclei. The most probable sites are at individual aragonite grain surfaces and boundaries. Under these conditions, the calcite will form a casing around the individual grains and grow inward.

As shown by BATHURST (1964), confirmed by DODD (1966), replacement of aragonite by calcite in fossil mollusc shells took place in two ways : solution-deposition or recrystallization in situ. The latter mechanism is characterized by the preservation of relics or ghosts of the original architectures (HUDSON, 1962; BATHURST, 1964).

BATHURST (1964) described in details the criteria permitting recognition of the drusy calcite developed by solution-deposition from the calcite formed in situ from aragonite shell walls (solid state inversion). One of the criteria used is the proportion of the places where three intercrystalline boundaries meet. In drusy mosaics of calcite developed by solution-deposition, the proportion of these triple junctions with one of the three angles equal to 180° reaches more than 50 per cent of these triple junctions. In the calcite mosaics evolved in situ from aragonitic shell walls, the proportion of 180° triple junctions (enfacial junctions) is less than 5 per cent.

It has long been observed (see BUCKLEY, 1950; WOLF, CHILINGAR and BEALES, 1967) that the presence of impurities in various polymorphs, such as coatings of organic compounds (WILBUR and WATABE, 1960, 1963; KITANO and HOOD, 1961, 1965; SUESS, 1970), adsorbed Mg ions (TAFT, 1967; Lit. in WEBER, 1969) or included trace elements (CLOUD, 1962) modify the physical properties of the surfaces of carbonates and increase the resistance to transformation of the unstable form into the stable form (BLOOM and BUERGER, 1937).

Crystallographically pure aragonite is rapidly transformed into calcite at temperatures lower than 100 °C (WRAY and DANIELS, 1957; HALL and KENNEDY, 1967). The biochemical (skeletal) aragonite seems to be more stable (7) than the inorganic aragonite to the thermal conversion to calcite. Preservation of aragonite in many fossils, especially Mesozoic shells (GRANDJEAN, GRÉGOIRE and LUTTS, 1964; KENNEDY and HALL, 1967; HALL and KENNEDY, 1967) has been explained by the protective effect of the conchiolin matrices associated with the mineral components (NEWELL *and al.*, 1953; MACDONALD, 1956; WRAY and DANIELS, 1957; KENNEDY and HALL, 1967; HALL and KENNEDY, 1967).

Data on the temperature at which inversion takes place in pure dry aragonite have been reviewed by HINTZE (1930) and by FAUST (1950). Conversion of pure dry aragonite takes place in a few minutes in air in the range of 450 - 470 °C and three hours at 400 °C (JOHNSTON, MERWIN and WILLIAMSON, 1916). It takes place between 387 °C and 488 °C at a heating rate of 12 °C per minute (FAUST, 1950). Recrystallization rate of aragonite to calcite in contact with distilled water is directly affected by temperature of the solution (TAFT, 1967).

The samples of *Nautilus* mother-of-pearl heated dry by MÜGGE (1901) were still aragonitic at 300 °C and already showed development of twinning lamellation, those heated at 350 °C and 400 °C were calcitic.

B. Personal results

The crystallographic interpretation, at the microtextural, microstructural and molecular levels, of the pyrolytic changes in the mineral components of the nacre described in this paper, is left to the competent specialists. As a direct determination of the different types of crystals shown in the plates has not been made, the interpretations are based on comparisons with the data of the literature. The problem of the trace-element content of the materials used has not been examined in this study.

a. Pyrolytic changes in the microtexture of mother-of-pearl

Under the experimental conditions of pyrolysis realized in this study, conversion of aragonite into calcite took place by a solid-solid reaction

(7) According to Land (1967, p. 918), the skeletal aragonite inverts more rapidly than more dense non skeletal aragonite.

in the range of 325 °C (wet heating in sealed tubes for 5 hours) and of 375 °C (heating in open vessels for 5 hours). These results do not differ greatly from those obtained by MÜGGE (1901) in the heated shell of *Nautilus*. If some grade of solution of aragonite developed at the periphery of the samples heated with sea or with distilled water, the process was negligible when compared with the amounts of material remaining in a solid state. No distinct change in size of the fragments occurred. Preservation, among the mosaics of large polyhedral crystals in dry and wet heated materials, of relics of the original brickwork architecture and the rarity or absence of enfacial junctions in the recrystallized samples (see Fig. 83) meet the criteria established by BATHURST (1964) concerning identification of the process of recrystallization in situ.

The present results suggest that the characteristic stacking in columns of the aragonite crystals in the *Nautilus* nacre plays an important part in the mechanism of the pyrolytic changes in the microtexture of mother-of-pearl.

In the process of conversion of the original brickwork of tabular crystals of aragonite into a mosaic of interlocking polyhedral crystals, coalescence of columns of crystals into foliate aggregates began when the samples were still predominantly aragonitic. As shown in Fig. 37, the new structures can be seen in contiguity to still preserved brickwork textures. These original textures can persist in later calcitic stages. The subsequent, progressive transformation of the foliate aggregates into polyhedral crystals — formation of anhedral blocks by coalescence, development of single euhedral facets on these blocks resulting finally in formation of subhedral of euhedral crystals — occurred in a material identified in the final stages by X-ray diffraction analysis as calcitic.

Transitional stages during which small islands of recrystallization were scattered among the elements of the foliate aggregates (see Fig. 58) might have developed when the X-ray diffraction of the samples still indicated aragonite but could not be detected owing to the limited sensitivity of the diffractometer used (see Material and Methods).

The mechanism of the process taking place within the foliate aggregates during their transformation into coarse polyhedral crystals was not solved in this study. It probably consisted of progressive fusion of the lamellar and crystalline components of the aggregates (see Fig. 116).

In the present pyrolysed material, the coarse polyhedral crystals deriving from the foliate aggregates display several features of the crystals of calcite from different sources (e.g. crystals of inorganic calcite : PFEFFERKORN, 1952; d'ALBISSIN and DE RANGO, 1962; calcite crystals of the eggshells : SCHMIDT, 1962, HEYN, 1963; mosaics of grains or coarse crystals composing the inversion products or aragonite shells : SHOJI and FOLK, 1964; inversion products of the limestones : CAYEUX, 1931; SEELIGER,1956; GRÉGOIRE and MONTY, 1963; TEICHERT, 1965; HARVEY, 1966; CHILINGAR, BISSELL and WOLF, 1967; WOLF, CHILINGAR and BEALES, 1967; WOLF, EASTON and WARNE, 1967; TAFT, 1967; FISCHER, HONJO and GARRISSON, 1967; FLÜGEL, 1967; FLÜGEL, FRANZ and OTT, 1968; transformation of mud needles : HATHAWAY and ROBERTSON (1961).

In the limestones, these tightly packed crystals or grains of calcite, 0.3 to 10 microns in size, vary from polyhedral, subangular to subround forms, with straight, slightly concave or convex, contact or true crystallographic planes, and are crossed

by parallel striations or cleavages lines. On broken surfaces, these grains appear to be composed of thin lamellae, as in the material shown in Figs. 116 and 117.

The similarity of structure between the thermally developed polyhedral crystals observed in this material and the crystalline grains described by HARVEY (1966) in the coarse-grained limestones has been already mentioned above.

Nearly identical textures also appear in a micrograph of FISCHER and al., 1967, Fig. 83, of an Upper triassic limestone and suggesting, according to the authors, a thermal recrystallization, and in a micrograph of a pyrolysed sample of *Nautilus* mother-of-pearl of the present material, heated in an open vessel at 500 °C for 5 hours (Fig. 101).

The significance of the crystalline arrangement shown in Fig. 127 in the form of a ring of small euhedral around large, dome-shaped elements could not be established in this study. Similar crystal assemblages have been mentioned by KUNZLER and GOODELL (1970) as regards certain phases of solid-solid transformation or aragonite into calcite.

The girdle- or needle-shaped crystals which protrude from the lateral surfaces of cleavage in samples heated in the range of 400 °C - 800 °C (see table 1 : 721-400; 975; 993; 721-500; 721-600; 977, 995; 778; 816 and 817) developed rapidly (e.g. 5, 10 and 15 minutes). These needles differ in their appearance (except for a single needle-like crystal) and crystallographic nature from the club-shaped aragonitic calcareous pillars (Kalkpfeilerchen) scattered on the adoral surfaces of the septa in *Nautilus* (APPELLÖF, 1892-1893; ERBEN *and al.*, 1969, table 12, Fig. 2).

On the other hand, the tufts of spear-like structures, appearing in the form of efflorescences of protruding and diverging blades on the surfaces of transverse fracture of the pyrolysed nacre (Fig. 69) closely resemble those observed by ERBEN *and al.* (1969, Fig. 3) on the adoral septal surfaces of the *Nautilus* shell in the neighbourhood of the sipho.

LOWENSTAM (1964) has reviewed the independent sources of sedimentary aragonite needles. Some of these needles are physico-chemical precipitates. In the present material, the needles belonged to samples in which X-ray diffraction analysis revealed the presence of calcite only. As needles of identical structure were observed in samples heated not only with sea water but also dry in open vessels and in sealed tubes, a process different from precipitation of sea salts was probably involved in their formation.

b. Pyrolytic changes in the microstructure of the nacre crystals

The present observations on the pyrolytic modifications in the microcrystallites composing the crystals of aragonite and emerging in the form of ridges on their 001 facets were not conclusive. The thermal changes in these structures consisted probably of inflation and coalescence. The nature of the relations between these microcrystallites and the etch patterns (polygonal elevations and perforations) developed on the surfaces of transverse (Figs. 24, 92 and 93) and tangential polishing (Figs. 54, 56 and 94) of the pyrolysed crystals also requires further investigation. Identical polygonal patterns were observed on etched surfaces of nacre cleavage in an australian Middle Miocene nautiloid (*Eutrephoceras balcombensis)* (unpublished).

In the present material, a part, if not all of the etching perforations seem to be artifacts of preparation, caused by mechanical elimination, during preparation of the replicas, of the portions of the metallic replicas corresponding to true elevations. Some of these detached « covers » are still visible at the edge of the pits and other perforations (Fig. 56).

Some of the elevations might be inclusions with a solubility in the etchant used differing from that of the contiguous mineral substance. True pits of small size might be liquid inclusions (water bubbles), similar to those, which can be euhedral or subhedral (negative crystals) described by FISCHER *and al.* (1967) on the surfaces of limestones.

Inflation, fragmentation and coalescence were the pyrolytic changes observed in the crystal seeds (MUTVEI's « tubercles ») scattered on the tabular facets of the crystals in the present material (see III 4 B).

According to MUTVEI (1970), the tubercles are in part the outer faces of the intracrystalline laths. However, as shown in different crystalline materials composed also of oriented laths (TOWE, 1967, echinoderm calcite, see his Fig. 3) the ends of these structures merging at the surfaces differ in their features from Mutvei's tubercles. On the other hand, the crystal seeds described in the present paper on the cleavage surfaces (see Figs. 15, 18-21, 22, 23 and 55) are obviously identical to the true crystal seeds growing on the basal 001 facets on exposed larger crystals in immature portions of mother-of-pearl and of calcitostracum (WATABE, SHARP and WILBUR, 1958; WATABE and WILBUR, 1961, Fig. 15; GRÉGOIRE, 1962, textfig. 3; WADA, 1968, Fig. 1; TOWE and HAMILTON, 1968, Figs. 13, 14 and 15). The seeds visible on the surfaces of cleavage were probably stopped in their growth by the compression exerted by overlapping, more newly grown crystals from the younger superposed consecutive lamellae (compare also Fig. 23 with Plate 1, Fig. 3, in TAYLOR, HALL and KENNEDY (1969) showing identical seeds growing all over the surface of an underlying lamella of nacre of *Neotrigonia dubia*).

In a thoughtful paper, just published (April 1972), TOWE emphasizes the difficulties encountered in describing the mineral phase and especially the intrastructure of the crystals involved in the architecture of the shells. As the data of literature on the normal crystal structure of the shells are still contradictory, the difficulties of interpretation are considerably enhanced when the material has been treated experimentally as it is the case in the present pyrolysed samples.

In a paper just out of press (April 1972) ERBEN discusses the literature on the inner configuration of the aragonite crystals in the nacre. On the basis of examination by means of the SEM of nacre crystals from shells of Gastropods, Pelecypods and Cephalopods, ERBEN concludes « that the tablet of nacre is not a complex aggregate containing acicular or lath-like microcrystals, but a crystal by itself. Although some of the tablets may represent monocrystals, in their majority they seem to be multiple twins. This is suggested by etching patterns (Mutvei's aragonite laths) as well as by tiny faces (appearing in the form of ridges on the 001 facets) of crystal growth ».

3. Conchiolin-mineral interactions during pyrolysis

The chief pyrolytic alterations in the conchiolin matrices of the modern *Nautilus* shell took place when the nacre was still predominantly aragonitic. These alterations seem to be unrelated to subsequent crystallographic changes of the aragonite into calcite (GRÉGOIRE and LORENT, 1971).

Flattening and coalescence of the trabeculae into ribbon-shaped structures consistently recorded in the fossil and in the pyrolysed *conchiolin* matrices over 275 °C - 300 °C (8) might have developed under the influence of a certain grade of compression, especially in the sealed tubes. As already suggested (GRÉGOIRE, 1966 a, p. 20; 1968, Part I, p. 12), pressure could be exerted in part in the interlamellar and intercrystalline planes before spontaneous cleavage of the nacre into sublayers, by the volatile products of the thermal decomposition of conchiolin during natural and experimental diagenesis. These volatile substances escape, frequently with explosion, on breaking the sealed tubes (see Part 1, table 1, third column, and this paper, table 1, third column). This interpretation seems to be consistent with observations of intense vesiculation within the trabecular cords in the pyrolysed samples (see Part I), or of release of small gas bubbles by the conchiolin included in different layers of heated shells, reported by RÖMER (1912) in mother-of-pearl, and by HUDSON (1962) in prism sheaths.

Compression could also be exerted under the influence of progressive changes in the mineral structures, which involve inflation and compaction of individual and groups of crystals in a still predominantly aragonitic material, followed by transformation of these structures into mosaics of large polyhedral crystals in a calcitic material. As reported in literature (HÖLDER and MOSEBACH, 1950; BATHURST, 1970), during their transformation into calcite, the aragonite crystals undergo an increase in volume amounting to 8.35 per cent. Squeezing of the conchiolin matrices by crystals seems to be confirmed by the detection, in samples heated at high temperatures (600 °C - 900 °C) (Figs. 124, 125 and 126; see also in Part. I, Figs. 86-92 and 95) of polygonal organic structures appearing in the form of casts of euhedral facets of the polyhedral crystals between which the conchiolin is sandwiched. Some of these organic remnants are shown in Fig. 130.

4. Pyrolytic changes in mother-of-pearl of the Nautilus shell and diagenetic changes in fossil nacres

In the pyrolysed modern material, used in the present and former studies, the conditions of alteration of the nacre thoroughly differed from those produced during natural diagenesis of fossil shells. The experimental

(8) In the diagram of the pressures and temperatures in the different metamorphic facies published by Winkler (1964. 1965), diagenesis is followed by burial metamorphism (with extensive changes in mineralogy and fabric of the rocks : see review of literature in TAYLOR, 1964) about a temperature of 300 °C and 2 to 6 kilobars. It is precisely about the same temperature (275 °C-300 °C for 5 hours), that in the material analysed in this and former studies, extensive changes occurred in sealed tubes in the interlamellar conchiolin matrices (flattening, coalescence of the trabeculae into membranes) and in the microarchitecture (constitution of foliate aggregates) of the pyrolysed samples.

material was not embedded in sediments as in late stages of diagenesis in fossils. It escaped the influence of several physical, biochemical and biomechanical factors of the burial environment (see LOWENSTAM, 1963, and Part I, p. 11). It remained at the atmospheric pressure in open vessels or was slightly compressed in sealed tubes (a few bars).

In spite of these differences in the environmental conditions, similarities appeared consistently in the changes in fossil and experimental materials.

A. Conchiolin matrices (see in Part I, disc. pp. 11-16 and table 2, p. 56)

The striking similarity shown in the changes (flattening and coalescence of the trabeculae) in the ultrastructure of the conchiolin remnants in a Cretaceous ammonite (*Collignoniceras* sp. Fig. 87) and in a sample of pyrolysed modern *Nautilus* nacre (Fig. 86) confirms former conclusions (GRÉGOIRE, 1964, 1966, 1968; GRÉGOIRE and VOSS-FOUCART, 1970; VOSS-FOUCART and GRÉGOIRE, 1971, a, b) that the diagenetic, structural and biochemical alterations of conchiolin in nacres of ammonoids and fossil nautiloids can be simulated by pyrolysis of modern *Nautilus* nacre.

As reported previously (GRÉGOIRE, 1966 a), in contrast with former statements in literature (ABELSON, 1957; MITTERER, 1968), natural (in fossils) and experimental (thermal) recrystallization does not destroy the conchiolin matrices. Conchiolin is a thermoresistant substance and is protected from the influence of diagenetic factors by its sheltering between mineral layers in the architecture of mother-of-pearl.

This high grade of thermoresistance of nacreous conchiolin suggests a cautious interpretation of results based on nacre materials in which the organic matter is considered to have been eliminated from the shells by heating for instance to 350 °C (PILKEY and GOODELL, 1967).

B. Microtexture of mother-of-pearl (see also Part I, disc., p. 13).

Several alterations recorded in the micro-architecture of the pyrolysed modern nacre and also found in diagenetically altered fossil shells are listed in table 2.

1. As in fossil shells, « complexes of alteration products » (TUREKIAN and ARMSTRONG, 1963) the thermal changes produced experimentally in modern nacre vary greatly in different, in some cases contiguous, parts of the samples (see Fig. 37).

2. As in several aragonitic, Jurassic and Cretaceous specimens, the columnar architecture is preserved with few alterations in samples of modern *Nautilus* nacre heated at moderate temperatures (150 °C - 275 °C).

3. As in predominantly aragonitic, more altered Jurassic and Cretaceous samples of nacre, columns of crystals fused into foliate aggregates,

with preservation of relics of the original architecture, in samples of modern nacre heated over 275 °C.

4. As in recrystallized, predominantly calcitic, Permian and Jurassic samples of nacre, mosaics of interlocking grains or polyhedral, subhedral crystals with parallel cleavage or lamellation striations (9) are formed in samples of modern nacre heated at 375 °C - 900 °C. In the diagenetically altered Permian material shown in Fig. 78 and in the pyrolysed nacre of *Nautilus* (Figs. 38, 68, 84, 85, 98, 99), parallel mineral sheets, former original sublayers of the nacre, seem to be similarly composed of foliate blocks.

5. Spontaneous cleavage of the pyrolysed nacre into booklets of mineral sheets of varying thickness (10) simulates the diagenetic process of disintegration in the sea of the modern mother-of-pearl into its micro-architectural units : layers (200-250 microns), sublayers (32-40 microns) and crystals (FORCE, 1969).

I thank Dr. D. COUTSOURADIS for permitting use of the furnaces and ovens of his Department. I am greatly indebted to Dr. A. DAVIN and to Mr. G. CASIER for their help in the preparation of the pyrolysed material.

I thank Mr. J. GRANDJEAN, who recorded and identified the X-ray diffraction patterns of the material, and Mr. A. CORNET, who took and analyzed the electron diffraction pattern shown in Fig. 95 a.

I am grateful to the persons who took the STEREOSCAN micrographs used in this paper : Miss Christine M. GISBOURNE, Miss Ann HARDY †, from the Laboratories of the CAMBRIDGE SCIENTIFIC INSTRUMENTS LIMITED (Figs. 34 to 38, 48, 49, 53, 57, 66, 69, 73 to 78, 84, 85, 96 to 99, 103, 116 to 118, 128 to 130, 131 to 133) and Mr. Gilbert DETILLOUX (from the C. R. M.) (Figs. 119 to 123).

I thank the paleontologists who gave me the fossil specimens used in this study : Prof. Dr. Rousseau H. FLOWER (422), Prof. William M. FURNISH and Prof. Brian F. GLENISTER (769, 356), Dr. P. L. MAUBEUGE (362),

(9) In Fig. 101 (Jurassic *Ammonites lineatus penicillatus*) three adjacent crystals have their cleavage or lamellation parallel striations similary oriented.

In Fig. 102 (sample of modern *Nautilus nacre pyrolysed* at 500 °C for 5 hours), orientation of these structures differs in contiguous crystals.

This divergence between fossil and experimental materials may be explained by the fact that in recrystallized fossil shells and rocks, as reported by FRIEDMAN and CONGER (1964), CARTER, CHRISTIE and GRIGGS (1964), a strongly preferential orientation of twin lamellation in crystals is related to the direction of the loading stress, a factor which is absent in our present experimental material.

(10) This preferential dissociation of the lamellation, which occurs in some cases at regular intervals, suggests a decrease in the cohesion of the lamellae at the site of cleavage, which possibly caused by local variations in the grade of thermal alteration of the interlamellar conchiolin cement. These differences in reaction to thermal stress could themselves be related to variations in the composition of the conchiolin cement during the process of formation of the lamellae. As reported previously (GRÉGOIRE, 1962, p. 41), similar variations could be the cause of interruption at periodic intervals of the regularity in the stratification of the lamellae (occurrence of thicker crystals), with an orientation differing from that of the crystals of the adjacent rows.

Prof. Raymond C. MOORE (433), Prof. O. H. SCHINDEWOLF †, Prof. Ad. SEILACHER, and Dr. Fr. WESTPHAL (785), Dr. Norman F. SOHL and Dr. G. Arthur COOPER (386, 393, 998, 999, 1006), Prof. Francis G. STEHLI (420).

I thank Mrs. Dr. M. F. VOSS-FOUCART, for reading the manuscript.

I thank Prof Gerh. PFEFFERKORN, for giving permission of reproducing the Figs. 15, 34, 73, 98 and 116.

I especially thank Prof. Dr. A. CAPART, Directeur of the Institut royal des Sciences naturelles de Belgique, for his help concerning the publication of the present paper.

The work is part of a research program financed by the Fonds de la Recherche Fondamentale Collective (Crédit 267) and by the Fonds National de la Recherche Scientifique (Crédits aux Chercheurs). The help of these organizations is gratefully acknowledged.

V. SUMMARY

1. The pyrolytic changes in the organic and mineral components of mother-of-pearl of the modern *Nautilus* have been studied with the transmission and scanning electron microscopes in 86 groups of samples.

2. Pyrolysis was performed in the range of 100 °C to 900 °C for periods extending from a few minutes to 53 days, in four sets of experiments : 1. samples boiled in sea water; 2. samples heated dry in open vessels; 3. samples heated dry in tubes sealed under vacuum; 4. samples heated with sea or distilled water in tubes sealed under vacuum.

3. The present observations confirm and extend those of previous studies on the thermal changes in the ultrastructure of the interlamellar conchiolin matrices :

a. Conchiolin is thermoresistant. It does not disappear and is still biuret-positive in samples pyrolysed at 900 °C for 5 hours.

b. The pyrolytic changes in the conchiolin ultrastructure in experiments of a few minutes to 21 days duration, consist of loosening of the lace-like networks, flattening, widening and coalescence of the trabeculae into continuous or fenestrate membranes (predominant in sealed tubes), fragmentation into corpuscles (predominant in the more altered samples heated in open vessels), and, in experiments of longer duration (e.g. 53 days), of disintegration into substantial tangled fibrils.

The factors possibly involved in these pyrolytic changes in conchiolin (compression by volatile constituents, increase in volume during recrystallization of the surrounding crystals) have been examined in the discussion.

The thermal conchiolin changes were similar or identical to those recorded till now in the organic remnants of nacreous layers in more than 250 species of fossil cephalopods (nautiloids and ammonoids).

c. The nature of the pyrolytic alterations in the conchiolin matrices did not distinctly differ in samples heated dry or wet in sealed tubes.

d. The hydrothermal changes developed in still aragonitic samples and, in agreement with former biochemical studies, seemed to be stabilized, except for subsidiary modifications in structure, at temperatures over 275 °C - 300 °C. At high temperatures (e.g. 600 °C), this stabilization was already established after a few minutes and the changes in structure of the conchiolin did not differ greatly from those recorded after 5 hours and 21 days.

e. In samples heated under 275 °C - 300 °C, protracted heating at a lower temperature (e.g. 225 °C - 21 days), produced changes identical to those obtained by heating at a higher temperature (e.g. 300 °C) for shorter periods of time (5 hours).

4. Except for scattered modifications (dissociation of the lamellae into individual crystals, inflation, fragmentation and coalescence of adjacent crystals), temperatures in the range of 150 °C - 300 °C did not distinctly modify the texture of mother-of pearl. Over 275 °C- 300 °C, the changes consisted of coalescence of single columnar stacks of crystals or of parallel groups of these structures characteristic of the *Nautilus* nacre. Coalescence of groups of crystals induced formation of well delimited, variously oriented foliate aggregates in which the original lamination of the nacre was temporarily preserved. In the range of 300 °C, the mineral components of the nacre were differently affected by pyrolysis in adjacent regions of a same sample; foliate aggregates were frequently contiguous to less altered parts of the samples in which the original columnar texture still subsisted.

In further stages (600 °C - 900 °C, the foliate aggregates were transformed progressively into mosaics of interlocking, polyhedral, anhedral, subhedral or euhedral crystals. Inflation and coalescence of the microcrystallites constituting the inner configuration of the original crystals of aragonite play possibly a part in this transformation.

5. Under the experimental conditions realized in this study, recrystallization of aragonite into calcite took place by a process of solid-solid reaction.

6. During pyrolysis, needle-like crystals resembling whiskers appeared on the surfaces of spontaneous cleavage into mineral sheets (sublayers) of the samples along the interlamellar planes. Decalcification of these crystals left organic ghosts in the form of perforated tubular sheaths of complex structure.

7. Several of these pyrolytic changes in the microtexture of mother-of-pearl are similar or identical to those recorded in the mineral components of aragonitic and recrystallized nacreous layers of fossil cephalopods of different ages (Permian, Jurassic, Cretaceous).

8. The present results suggest that simulation by pyrolysis of modern shells of diagenetic changes in fossil mother-of-pearl can be realized, not

only in the conchiolin matrices, as shown in previous studies, but also in the microtexture of this substance.

Experiments of longer duration than those performed till now, and in which samples of *Nautilus* nacre are subjected to heat and pressure are in progress.

VII. REFERENCES

ABELSON, PH. H.

1957. *Organic constituents of fossils.* (In Treatise on Marine Ecology and Paleoecology, II, Paleoecology, H. S. Ladd, ed., Geol. Soc. America, Mem. 67, pp. 87-92.)

ALBISSIN, M. D' and DE RANGO, C.

1962. *Etude de la microstructure des roches calcaires par l'observation au microscope électronique de l'orientation des figures de corrosion.* (Bull. Soc. franç. Miner. Cristallogr., vol. 85, pp. 170-176.)

AHRBERG, P.

1935. *Über den feineren Bau der Perlmutter von Schnecken und Cephalopoden.* (Arch. Molluskenk., vol. 67, pp. 1-20.)

APPELLÖF, A.

1892-1893. *Die Schalen von Sepia, Spirula und Nautilus. Studien über den Bau und das Wachstum.* (Kongl. Svenska Vetensk.-Akad. Handlingar, vol. 25, pp. 1-106.)

AVRAMI, M.

1939. *Kinetics of phase change. I. General theory.* (J. Chem. Phys., vol. 7, pp. 1103-1112) (quoted by Kunzler and Goodell, 1970.)

BATHURST, R. G. C.

1964. *The replacement of aragonite by calcite in the molluscan shell wall.* (In Approaches to Paleoecology, J. Imbrie and N. D. Newell, eds., John Wiley and Sons, Inc., New York, pp. 357-376.)

1970. *Problems of lithification in carbonate muds.* (Proc. geol. Assoc., vol. 81, pp. 429-440.)

BIEDERMANN, W.

1902. *Untersuchungen über Bau und Entstehung der Molluskenschalen.* (Iena. Zeitschr. Naturwiss. vol. 36, N. F. 29, pp. 1-164.)

BIRKELUND, T.

1967. *Submicroscopic shell structures in early growth-stage of Maastrichtian ammonites (Saghalinites and Scaphites.)* (Medd. Dansk Geol. Foren. København, vol. 17, 1, pp. 95-101.)

BISCHOFF, J. L.

1968. *The calcite-aragonite problem.* (Am. J. Science, vol. 266, p. 658.)

1969. *Temperature controls of aragonite-calcite transformation in aqueous solutions.* (Amer. Mineralog., vol. 54, pp. 149-155.)

BLOOM, M. C. and BUERGER, M. J.

1937. *On the genesis of polymorphous forms -Sb203.* (Zeitschr. Kristall., vol. 96, Abt. A, pp. 365-375.)

BØGGILD, O. B.

1930. *The shell structure of the mollusks.* (Kong. Danske Vidensk. Selsk. Skr., Naturvidensk, Math. afd., Raekke 9, 2, pp. 233-326.)

BOETTCHER, A. L. and WYLLIE, P. J.

1967. *Revision of the calcite-aragonite transition, with the location of a triple point between calcite I, calcite II and aragonite.* (Nature, Febr. 25, pp. 792-793.)

1968. *The calcite-aragonite transition measured in the system Ca0-C02-H20.* (J. Geol., vol. 76, pp. 314-330.)

BRADLEY, D. E.

1965. *Replica and shadowing techniques.* (In Techniques for Electron Microscopy, Desm. H. Kay, ed., 2nd. ed., Blackwell, Oxford, pp. 96-152.)

BROWN, W. H., FYFE, W. S. and TURNER, F. J.

1962. *Aragonite in California glaucophane schists, and the kinetics of the aragonite-calcite transformation.* (J. Petrology, vol. 3, pp. 566-582.)

BUCKLEY, H. E.

1950. *Crystal growth.* (J. Wiley & Sons, Inc., New York, 1-571.)

CAYEUX, L.

1931. *Introduction à l'étude pétrographique des roches sédimentaires.* (Paris, Imprimerie Nationale, 524 p.)

CARTER, N. L., CHRISTIE, J. M. and GRIGGS, D. T.

1964. *Experimental deformation and recrystallization of quartz.* (J. Geol., 72, pp. 687-733.)

CHILINGAR, G. V., BISSELL, H. J. and WOLF, K. H.

1967. *Diagenesis of carbonate rocks.* (In Diagenesis in sediments, Developments in sedimentology 8, Larsen Gunnar and Chilingar Geo. V. eds, Elsevier, Amsterdam, pp. 179-322.)

CLOUD JR., P. E.

1962. *Environment of calcium carbonate deposition west of Andros Island. Bahamas.* (U. S. Geol. Survey Profess. Paper 350, pp. 1-138.)

CURL, R. L.

1962. *The aragonite-calcite problem.* (Bull. Natl. Speleol. Soc., vol. 21, pp. 57-73.)

DODD, J. R.

1966. *Processes of conversion of aragonite to calcite with examples from the Cretaceous of Texas.* (J. sedim. Petrol., vol. 36, pp. 733-741.)

EHRENBAUM, E.

1885. *Untersuchungen über die Struktur und Bildung der Schale der in der Kieler Bucht haüfig vorkommenden Muscheln.* (Zeitschr. wiss. Zool. vol. 41, pp. 1-47.)

ERBEN, H. K.

1971. *Anorganische und organische Schalenkomponente bei Cittarium pica (L.) (Archaeogastropoda)* (Biomineral. Forschungsber., vol. 3, 51-64.)

1972. *Über die Bildung und das Wachstum von Perlmutt.* (Biomineral. Forschungsber., vol. 4, pp. 15-46.)

ERBEN, H. K., FLAJS, G. and SIEHL, A.

1969. *Die frühontogenische Entwicklung der Schalenstruktur ectocochleater Cephalopoden.* (Palaeontogr., Stuttgart, vol. 132, Abtg. A, pp. 1-54.)

FAUST, G. T.

1950. *Thermal analysis studies on carbonates. I. Aragonite and calcite.* (Amer. Mineralogist, vol. 35, pp. 207-224.)

FISCHER, A. G., HONJO, S. and GARRISON, R. E.

1967. *Electron micrographs of limestones and their nannofossils.* (Monogr. in Geol. Paleontol., vol. 1, pp. 1-141.)

FLOWER, R. H.

1961. *Personal communication.*

FLÜGEL, E.

1967. *Elektronenmikroskopische Untersuchungen an mikritischen Kalken.* (Geol. Rundschau, vol. 56, pp. 341-358.)

FLÜGEL, E., FRANZ, H. E. and OTT, W. F.

1968. *Review on Electron microscope studies of limestones.* (in Recent Developments in Carbonate Sedimentology in Central Europe, Springer-Verlag, Berlin-Heidelberg-New York, pp. 85-97.)

FORCE, L. M.

1969. *Calcium carbonate size distribution on the West Florida shelf and experimental studies on the microarchitectural control of skeletal breakdown.* (J. Sedim. Petrol, vol. 39, pp. 902-934.)

FRIEDMAN, M. and CONGER, F. B.

1964. *Dynamic interpretation of calcite twin lamellae in a naturally deformed fossil.* (J. Geol, 72, pp. 361-368.)

FYFE, W. S. and BISCHOFF, J. L.

1965. *The calcite-aragonite problem.* (In Pray, L. C. and Murray, R. C. eds, Dolomitization and limestones diagenesis : a symposium : Soc. Econ. Paleontolog. and Mineralog. spec. Publ., vol. 13, pp. 3-13.) (Quoted by Bathurst, 1964.)

GRANDJEAN, J., GRÉGOIRE, CH. and LUTTS, A.

1964. *On the mineral components and the remnants of organic structures in shells of fossil molluscs.* (Bull. Acad. roy. Belg., Cl. des Sciences, 5e série, vol. 50, 1964, pp. 562-595.)

GRÉGOIRE, CH.

1957. *Topography of the organic components in mother-of-pearl.* (J. Biophys. Biochem. Cytol., vol. 3, 1957, pp. 797-808.)

1958. *Essai de détection au microscope électronique des dentelles organiques dans les nacres fossiles. (ammonites, nautiloides, gastéropodes et pélécypodes).* (Arch. intern. Physiol. Biochim., vol. 66, pp. 674-676.)

1959a. *A study on the remains of organic components in fossil mother-of-pearl.* (Bull. Inst. roy. Sci. nat. Belg., vol. 35, fasc. 13, pp. 1-14.)

b. *Conchiolin remnants in mother-of-pearl from fossil Cephalopoda.* (Nature, vol. 184, pp. 1157-1158.)

1962. *On submicroscopic structure of the Nautilus shell.* (Bull. Inst. roy. Sc. nat. Belg., vol. 38, fasc. 49, pp. 1-71.)

1964. *Thermal changes in the Nautilus shell.* (Nature, London, vol. 203, pp. 868-869.)

1966a. *On organic remains in shells of Paleozoic and Mesozoic Cephalopods.* (Nautiloids and Ammonoids). (Bull. Inst. roy. Sci. nat. Belg., vol. 42, fasc. 39, pp. 1-36.)

1966b. *Experimental Diagenesis of the Nautilus shell.* (Advances in Organic Geochemistry. G. D. Hobson et G. C. Speers edit., Pergamon Press, pp. 429-442.)

1967. *Sur la structure des matrices organiques des coquilles de mollusques.* (Biol. Rev., vol. 42, 1967, p. 653-688.)

1968. *Experimental alteration of the Nautilus shell by factors involved in Diagenesis and Metamorphism. Part I. Thermal changes in conchiolin matrix of mother-of-pearl.* (Bull. Inst. roy. Sc. nat. Belg., vol. 44, (25) 69 p.)

1971. *Structure of Molluscan Shells.* (In Chemical Zoology, Florkin, M. and Scheer, B. T., edrs., Acad. Press Inc., New York, vol. VI.) (in the press.)

GRÉGOIRE, CH., DUCHÂTEAU, GH. and FLORKIN, M.

1950. *Structure, étudiée au microscope électronique, des nacres décalcifiées de mollusques.* (Archs. int. Physiol., vol. 58, 1950, pp. 117-120.)

1955. *La trame protidique des nacres et des perles.* (Ann. Inst. Océanogr., vol. 31, 1955, pp. 1-36.)

GRÉGOIRE, CH. and MONTY, CL.

1963. *Observations au microscope électronique sur le calcaire à pâte fine entrant dans la constitution des structures stromatolithiques du Viséen Moyen de la Belgique.* (Ann. Soc. géol. Belg., 10, pp. 389-397.)

GRÉGOIRE, Ch., GISBOURNE, Ch. and HARDY, A.

1969. *Über experimentelle Diagenese der Nautilusschale.* (Beitr. elektronenmikrosk. Direktabb. Oberfl., vol. 2, pp. 223-238.)

GRÉGOIRE, CH. and LORENT, R.

1971. *Alterations in conchiolin matrices of mother-of-pearl during conversion of aragonite into calcite under experimental conditions of pyrolysis and pressure.* (In the press.)

GRÉGOIRE, CH. and TEICHERT, C.

1965. *Conchiolin membranes in shell and cameral deposits of Pennsylvanian cephalopods, Oklahoma.* (Oklahoma Geol. Notes, vol. 25, pp. 175-201.)

GRÉGOIRE, CH. and VOSS-FOUCART, M. F.

1970. *Proteins in shells of fossil Cephalopods (Nautiloids and Ammonoids) and experimental simulation of their alterations.* (Arch. internat. Physiol. Bioch., vol. 78, 2, pp. 191-203.)

HALL, A. and KENNEDY, W. J.

1967. *Aragonite in fossils.* (Proc. roy. Soc. B, vol. 168, pp. 377-412.)

HALLAM, A. and O'HARA, M. J.

1962. *Aragonitic fossils in the Lower Carboniferous of Scotland.* (Nature, London, vol. 195, pp. 273-274.)

HARVEY, R. D.

1966. *Electron microscope study of microtexture and grain surfaces in limestones.* (Illinois State geol. Survey, vol. 404, pp. 1-18.)

HATHAWAY, J. C. and ROBERTSON, E. C.

1961. *Microtexture of artificially consolidated aragonitic mud.* (U. S. Geol. Survey, Professional Paper 424-C, art. 257, pp. C-301-304.)

HEYN, A. N. J.

1963. *The crystalline structure of calcium carbonate in the avian eggshell.* (J. Ultrastruct. Res., vol. 8, pp. 176-188.)

HINTZE,C.

1930. *Handbuch der Mineralogie.* (Walter de Gruyter & Co, Berlin-Leipzig, vol. I (3), p. 2982.)

HÖLDER, H.

1952. *Über Gehäusebau, insbesondere Hohlkiel jurassischer Ammoniten.* (Palaeontographica, Abh. A, vol. 102, pp. 18-48.)

HÖLDER, H. and MOSEBACH, R.

1950. *Die Conellen auf Ammonitensteinkernen als Schalenrelikte fossiler Cephalopoden.* (N. Jhrb. Geol. Paleont., vol. 92, Abh. B, pp. 367-414.)

HUDSON, J. D.

1962. *Pseudo-pleochroic Calcite in Recrystallized Shell-limestones.* (Geol. Mag., vol. 99, pp. 492-500.)

1968. *The microstructure and mineralogy of the shell of a Jurassic mytilid (Bivalvia).* (Palaeontology, vol. 11, pp. 163-182.)

JOHNSTON, J., MERWIN, H. E. and WILLIAMSON, E. D.

1916. *The several forms of calcium carbonate.* (Amer. J. Science, vol. 41, pp. 473-512.)

KENNEDY, W. J. and HALL, A.

1967. *The influence of organic matter on the preservation of aragonite in fossils.* (Proc. geol. Soc. London, nº 1643, pp. 253-255.)

KITANO, Y. and HOOD, D. W.

1961. *Effect of organic material on the polymorphic forms of CaCO3.* (Geol. Soc. Amer., Special papers, 72, pp. 86-87.)

1965. *The influence of organic material on the polymorphic crystallization of calcium carbonate.* (Geochim. Cosmochim. Acta, vol. 39, pp. 29-41.)

KUNZLER, R. H. and GOODELL, H. G.

1970. *The aragonite-calcite transformation : a problem in the kinetics of a solid-solid reaction.* (Amer. J. Science, vol. 269, pp. 360-391.)

LAND, L. S.

1967. *Diagenesis of skeletal carbonates.* (J. Sedim. Petrol., vol. 37, pp. 914-930.)

LOWENSTAM, H. A.

1963. *Biologic problems relating to the composition and diagenesis of sediments.* (The Earth Sciences. Thomas W. Donnelly ed., Rice University, Semicentennial Publ., Univ. Chicago Press, pp. 137-195.)

MACDONALD, G. J. F.

1956. *Experimental determination of calcite-aragonite equilibrium relations at elevated temperatures and pressures.* (Amer. Mineralogist, vol. 41, pp. 744-756.)

MITTERER, R. M.

1966. *Amino Acid and Protein Geochemistry in Mollusk Shell.* (The Florida State University, Ph. D. Thesis, 1966, pp. 1-151.)

MOORE, R. C., LALICKER, C. G. and FISCHER, A. G.

1952. *Invertebrate fossils.* (Mac Graw Hill Book Co, Inc. pp. 1-766.)

MUTVEI, H.

1964. *On the shell of Nautilus and Spirula with notes on the shell secretion in non-cephalopod molluscs.* (Arkiv. Zool., vol. 16, pp. 221-278.)

1967. *On the microscopic shell structure in some Jurassic ammonoids.* (N. Jhrb. Geol. Paläontol, Abh., vol. 129, pp. 157-166.)

1969. *On the micro-and ultrastructure of the conchiolin in the nacreous layer of some recent and fossil molluscs.* (Stockholm Contrib. in Geol., vol. XX, pp. 1-17.)

1970. *Ultrastructure of the mineral and organic components of molluscan nacreous layers.* (Biomineral. Forschungsber., vol. 2, pp. 49-72.)

1972. *Ultrastructural relationships between the prismatic and nacreous layers in Nautilus (Cephalopoda).* (Biomineral. Forschungsber., vol. 4, pp. 81-86.)

MÜGGE, O.

1901. *Krystallographische Untersuchungen über die Umlagerungen und die Struktur einiger mimetischer Krystalle.* (N. Jhrb. Miner., Beilage-Bd XIV, pp. 246-318.)

NEWELL, N. D., RIGBY, J. K., FISCHER, A. G., WHITEMAN, A. J., HICKOX, J. E. and BRADLEY, J. S.

1953. *The Permian reef complex of the Guadalupe Mountain Region, Texas and New Mexico.* [San Francisco, Freeman and Company, pp. 1-236 (quoted by Fischer & al., 1967.)]

OBST, K. H., MÜNCHBERG, W. and BLASCHKE, R.

1969. *Einsatzmöglichkeiten des Raster-Elektronenmikroskops für die Untersuchung basischer Roh- und Werkstoffe (Ein Beitrag zur Abbildung feinporöser nichtleitende Materialien.* (Beitr. elektronenmikrosk. Direktabb. Oberfl., vol. 2, pp. 265-273.)

PFEFFERKORN, G.

1952. *Untersuchungen zum Realbau von Kalkspat.* (N. Jhrb. Mineral., Abh., vol. 84, pp. 281-326.)

PILKEY, O. H. and GOODELL, H. G.

1964. *Comparison of the composition of fossil and recent mollusk shells.* (Bull. Geol. Soc. Amer., vol. 75, pp. 217-228.)

RÖMER, O.

1903. *Untersuchungen über den feineren Bau einiger Muschelschalen.* (Zeitschr. wissensch. Zool., vol. 75, pp. 437-472.)

SCHMIDT, W. J.

1923. *Bau und Bildung der Perlmuttermasse.* (Zool. Jahrb., Abt. Anat., vol. 45, pp. 1-148.)

1924. *Die Bausteine des Tierkörpers in polarisiertem Lichte.* (F. Cohen, ed. Bonn.)

1962. *Liegt der Eischalenkalk der Vögel als submikroskopische Kristallite vor.* (Zeitschr. Zellforschg. mikrosk. Anat. vol. 57, pp. 848-880.)

SEELIGER, R.

1956. *Übermikroskopische Darstellung dichter Gesteine mit Hilfe von Oberflächenabdrücken.* (Geol. Rundschau, vol. 45, pp. 332-336.)

SHOJI,R. and FOLK, R. L.

1964. *Surface morphology of some limestone types as revealed by electron microscopy.* (J. Sedim. Petrol., vol. 34, pp. 144-155.)

SORBY, H. C.

1878-1879. *The Anniversary Address of the President.* (Proc. Geol. Soc. London, pp. 39-95, in Quart. J. Geol. Soc. London, vol. 35, 1879.)

STENZEL, H. B.

1964. *Living Nautilus.* (in Moore, R. C. ed., Treatise on Invertebrate Paleontology, University of Kansas Press. Part K, Mollusca 3, pp. 59-93.)

STEHLI, F. G.

1956. *Shell mineralogy in Palaeozoic Invertebrates.* (Science, vol. 123, pp. 1031-1032.)

SUESS, E.

1970. *Interaction of organic compounds with calcium carbonate. I. Association phenomena and geochemical implications.* (Geochim. Cosmochim. Acta, vol. 34, pp. 157-168.)

TAFT, W. H.

1967. *Physical chemistry of formation of carbonates.* (in Carbonate Rocks, Developments in Sedimentology 9B, Chilingar, G. V., Bissell, H. J. and Fairbridge, R. W., eds, Elsevier, Amsterdam, pp. 151-167.)

TAYLOR, J. H.

1964. *Some aspects of diagenesis.* (Advanc. Science, vol. 20, pp. 417-436.)

TAYLOR, J. D., KENNEDY, W. J. and HALL, A.

1969. *The shell structure and mineralogy of the Bivalvia.* (Bull. British Museum (Natural History) Zoology, Suppl. 3, pp. 1-125.)

TEICHERT, C.

1965. *Devonian rocks and paleogeography of Central Arizona.* (U. S. Geol. Survey Professional Paper 464, U. S. Govern. Printing Office, Washington, pp. 1-181.)

TOWE, K. M.

1972. *Invertebrate Shell Structure and the organic matrix concept* (Biomineral. Forschungsber., vol. 4, pp. 1-14.)

TOWE, K. M. and CIFELLI, R.

1967. *Wall ultrastructure in the calcareous Foraminifera: Crystallographic aspects and a model for calcification.* (J. Paleont., vol. 41, pp. 742-762.)

TOWE, K. M. and HAMILTON, G. H.

1968. *Ultrastructure and inferred calcification of the mature and developing nacre in bivalve molluscs.* (Calc. Tissue Res., vol. 1, pp. 306-318.)

TUREKIAN, K. K. and ARMSTRONG, R. L.

1961. *Chemical and mineralogical composition of fossil molluscan shells from the Fox Hill formation, South Dakota (Cretaceous).* (Bull. Geol. Soc. America, vol. 72, pp. 1817-1828.)

VON NATHUSIUS-KÖNIGSBORN, W.

1877. *Untersuchungen über nicht-celluläre Organismen, namentlich Crustaceen-panzer, Molluskenschalen und Eihüllen.* (Berlin, 144 p.) (quoted by Schmidt, 1923.)

VOSS-FOUCART, M. F. and GRÉGOIRE, CH.

1971a. *Biochemical composition and submicroscopic structure of matrices of nacreous conchiolin in fossil cephalopods (Nautiloids and Ammonoids).* (Bull. Inst. roy. Sc. nat. Belg., vol. 47, fasc. 41, pp. 1-43.)

1971b. *On biochemical and structural alterations in fossil and in pyrolysed modern mother-of-pearl of molluscs.* (Biomineralisation, Forschungsberichte, in press.)

WADA, K.

1961. *Crystal growth of molluscan shells.* (Bull. nat. Pearl Res. Lab., vol. 7, pp. 703-828.)

1963. *Studies of the mineralization of the calcified tissue in molluscs. VI. Crystal structure of the calcite grown on the inner surface of calcitostracum.* (J. Electron microsc., vol. 12, pp. 224-227.)

1966. *Spiral growth of nacre* (Nature, London, vol. 211, p. 1427.)

1968. *Mechanism of growth of nacre in bivalvia.* (Bull. Natl. Pearl Res. Lab., vol. 13, pp. 1561-1596.)

WATABE, N.

1963. *Decalcification of thin sections for electron microscopical studies of crystal-matrix relationships in mollusc shells.* (J. Cell Biology, vol. 18, pp. 701-703.)

1965. *Studies on shell formation. XI. Crystal-matrix relationships in the inner layers of mollusc shells.* (J. Ultrastruct. Res., vol. 12, pp. 351-370.)
1968. *Mechanism of growth of nacre in Bivalvia.* (Bull. natl. Pearl Res. Lab., vol. 13, pp. 1561-1596.)

WATABE, N. and WILBUR, K. M.
1961. *Studies on shell formation. IX. An electron microscope study of crystal layer formation in the oyster.* (J. biophys. biochem. Cytol., vol. 9, pp. 761-772.)

WATABE, N., SHARP, D. G. and WILBUR, K. M.
1958. *Studies on shell formation. VIII. Electron microscopy of crystal growth in the nacreous layer of the oyster Crassostrea virginica.* (J. Biophys. biochem. Cytol., vol. 4, pp. 281-286.)

WEBER, J. N.
1969. *The incorporation of magnesium into the skeletal calcites of Echinoderms.* (Amer. J. Science, vol. 267, pp. 537-566.)

WILBUR, K. M. and WATABE, N.
1960. *Influence of the organic matrix on crystal type of molluscs.* (Nature, vol. 188, p. 334.)
1963. *Experimental studies on calcification in molluscs and the alga Coccolithus huxleyi.* (Ann. N. Y. Acad. Sc., vol. 109, pp. 82-112.)

WILBUR, K. M. and SIMKISS, K.
1968. *Calcified shells.* (in Florkin, M. and Stoltz, E. H., eds, Comprehensive Biochemistry, vol. 26 A, Elsevier, 1968, pp. 229-295.)

WINKLER, H. G. F.
1964. *Experimentelle Mineralogie.* (Naturwiss., vol. 51, pp. 303-307.)
1965. *Die Genese der metamorphen Gesteine.* (Springer, Berlin, ed. pp. 1-218.)

WISE, S. W.
1970. *Microarchitecture and mode of formation of nacre. (mother-of-pearl) in Pelecypods, Gastropods and Cephalopods.* (Eclogae geol. Helvet, vol. 63, pp. 775-797.)

WOLF, K. H., CHILINGAR, G. V. and BEALES, F. W.
1967. *Elemental composition of carbonate skeletons, minerals, and sediments.* (in Carbonate Rocks, Devel, in Sedimentology 9B, Chilingar, G. V., Bissell, H. J. and Fairbridge, R. W., eds., Elsevier Publ. Co, Amsterdam, pp. 23-149.)

WOLF, K. H., EASTON, A. J. and WARNE, S.
1967. *Techniques of examining and analyzing carbonate skeletons, minerals, and rocks.* (in Carbonate Rocks, Developments in Sedimentology, 9B, Chilingar, G. V., Bissell, H. J. and Fairbridge, R. W., eds, Elsevier, Amsterdam, pp. 253-341).

WRAY, J. L. and DANIELS, F.
1957. *Precipitation of calcite and aragonite.* (J. Am. Chem. Soc., vol. 79, 1957, pp. 2031-2034.)

DEPARTMENT OF BIOCHEMISTRY,
UNIVERSITY OF LIÈGE, BELGIUM,
17, PLACE DELCOUR, 4000 LIÈGE
AND
CENTRE DE RECHERCHES MÉTALLURGIQUES (C. R. M.)
ABBAYE DU VAL BENOÎT, 4000 LIÈGE.

TABLE

Thermal and hydrothermal changes in the mineral (crystals of aragonite)
(shell wall of the modern *Nautilus pompiliu*

Material File number (in parentheses) Temperature (in °C) Exposure time Conditions of pyrolysis	Mineral composition of the samples : X-ray powder diffraction	Physical characteristics of the samples
(721,449-40,1047) 20 °C (Control)	Aragonite	Very hard. Not easily cleavable. Iridescent, with pale pink-greenish hues.
100 °C	100 °C	100 °C
(886-3) (see Part I, p. 38 : 886-2)	Aragonite	See Part I, p. 38.
Repeated boiling in mixtures of sea mud and sea water. *Total boiling time* : 42 hours. Sample kept in sea mud for 42 months at room temperature.		
150 °C	150 °C	150 °C
(721-150; 1010) 5 hours Dry heating in open vessels.	Aragonite	Hard. More easily cleavable than unheat material. Slight burnishing of iridescence with i crease of the pink greenish hues.
(734) 13 days Dry heating in open vessels.	Aragonite	Burnishing of iridescence on outer surfac of samples. Bright metallic hues on freshly cleaved su faces.

nd organic (conchiolin matrix) components of the nacreous layer
INNÉ and *Nautilus macromphalus* SOWERBY)

1. Surfaces of transverse fracture. Polished and etched surfaces of transverse section. 2. Surfaces of cleavage along the interlamellar planes, exposing the 001 facets of the tabular crystals of aragonite. Polished and etched surfaces of cleavage. 3. Alterations in the ultrastructure (trabeculae and fenestration) of the conchiolin matrix (see Part I, Table 1).
1. Columnar architecture : stratified parallel lamellae composed of polygonal tabular crystals of aragonite disposed in single layers in each lamella (Fig. 1). Columnar stacking of the aragonite crystals in successive lamellae. 2. Microcrystallites (Crystal seeds), parallel or scattered at random, and imbricate parallel ridges stand out in relief on the 001 facets (Figs. 15, 16 and 17). 3. See Part 1, p. 21 and GRÉGOIRE 1962, Fig. 39. Nautiloid pattern : sturdy, irregularly cylindrical trabeculae, studded with hemispheric protuberances, mostly elongated fenestration.
100 °C
1. and 2. Main features of architecture unchanged (Figs. 4, 5 and 6). Possible changes (inflation, fragmentation ?) in the subunits in the superficial layers of the aragonite crystals (Figs 4 and 5). 3. See Part I, p. 39 (886-2).
150 °C
1. Original microtexture preserved. Possible loosening of the crystal cohesion. 2. No distinct modification of the topography of the ridges. Many rounded crystal seeds. 3. See Part I, p. 20-21. No distinct alteration in the nautiloid pattern in parts of the conchiolin matrices. In other areas, coalescence of contiguous parts of the trabeculae into thick ribbons onto which hemispheric protuberances are still visible.
1. Original architecture preserved. Scattered dislocation of lamellae into individual crystals. 3. See Part 1, p. 23.

TABLE

Material File number (in parentheses) Temperature (in °C) Exposure time Conditions of pyrolysis	Mineral composition of the samples : X-ray powder diffraction	Physical characteristics of the samples
(731-19) 19 days Dry heating in open vessels.	Aragonite	Brittle. Fragments easily cleavable in strongly iridescent sheets, with intense m tallic hues.
(801) 5 hours Dry heating in sealed tubes.	Aragonite	Hard. Fragments break without cleavage. Slight burnishing of iridescence on expos surfaces.
(997) 5 hours Heating with sea water in sealed tubes. (1086) (1099) Heating with distilled water in sealed tubes	Aragonite	Faint, transient smell of H2S and of burn horn on breaking tubes. Hard or moderately brittle (1086). Slig burnishing of iridescence with pinkgre shining hues.
(1100) 160 °C — 53 days Heating with distilled water in sealed tubes.	Aragonite	On breaking tubes, pungent smell of tar a of burned horn. Moderately brittle and cleavable. Slightly bronze - coloured fragments.
200 °C	200 °C	200 °C
(721-200) 5 hours Heating in open vessels	Aragonite	See Part. I, p. 22. Brittle. Fragments easily cleavable into bro ze-coloured, iridescent sheets with brig metallic hues.

1 *(contd.)*

1. Surfaces of transverse fracture. Polished and etched surfaces of transverse section. 2. Surfaces of cleavage along the interlamellar planes, exposing the 001 facets of the tabular crystals of aragonite. Polished and etched surfaces of cleavage. 3. Alterations in the ultrastructure (trabeculae and fenestration) of the conchiolin matrix (see Part I. Table 1).
1. Coalescence of parts of crystals. Scattered polygonal etch pits and elevations in the crystals. 2. Topography and shape of the crystal seeds and ridges not distinctly changed. Possibly some inflation of these structures. 3. See Part I, p. 22-23.
1. As in the samples heated in open vessels, architecture preserved (Fig. 2). 2. Possilby fragmentation and coalescence of the parallel ridges on the cleavage surfaces. Scattered hemispheric corpuscles. 3. See Part 1, p. 40. Alteration of the trabeculae, as in the samples heated in open vessels.
1 and 2. No distinct change in original architecture. In (1086), elongate polygonal notches appear in the crystals along the interlamellar spaces. 3. Transparent iridescent bluish shreds. Nautiloid pattern unchanged. Possibly diffuse flattening and local coalescence of some trabeculae. No appreciable difference with material heated dry in open vessels and in sealed tubes.
2. Coalescence of crystal seeds in the areas of central elevations. Parallel ridges still faintly visible. 3. Several types of alteration in the conchiolin matrices : interlaced bundles of fibrils, loose networks of varicose, slender or flattened trabeculae, fused in part into folded membranes. Spheroidal nodules.
200 °C
1 and 2. Original architecture preserved. Local inflation, fragmentation and fusion of crystals or of parts of crystals. 3. See Part I, p. 22-23.

TABL

Material File number (in parentheses) Temperature (in °C) Exposure time Conditions of pyrolysis	Mineral composition of the samples : X-ray powder diffraction	Physical characteristics of the samples.
(802) 5 hours Dry heating in sealed tubes.	Aragonite	See Part. I, p. 40. Decrease in hardness. Fragments cleavab into irridescent sheets, with intense, brc zed and green tints on the freshly cleav surfaces.
225 °C	**225 °C**	**225 °C**
(721-225-15) Preheating : 2 min. 30 sec. 225 °C : 10 min. Heating in open vessels.	Aragonite	Brittle. Fragments cleaved in part into th sheets. Diffuse burnishing of iridescence on ou and freshly cleaved surfaces.
(721-225) 5 hours Heating in open vessels.	Aragonite	Brittle. Beginning of spontaneous cleavage. Burnishing of iridescence on the exposed su faces. Intense metallic hues on the cleav surfaces.
(721-225-21) 21 days Heating in open vessels.	Aragonite	Very brittle; fragments spontaneously cleav into sheets. Exposed surfaces : smoke-brown. Cleavage surfaces : intense metallic hues.

(contd.)

1. Surfaces of transverse fracture. Polished and etched surfaces of transverse section. 2. Surfaces of cleavage along the interlamellar planes, exposing the 001 facets of the tabular crystals of aragonite. Polished and etched surfaces of cleavage. 3. Alterations in the ultrastructure (trabeculae and fenestration) of the conchiolin matrix (see Part I, Table 1).
1. Scattered dislocation of lamellae into free crystals. Local coalescence of adjacent crystals from the same or from contiguous lamellae. 2. Scattered dislocation of the flagging of polygonal crystals into free crystals. 3. See Part 1, p. 40-41.
225 °C
1. Original architecture preserved. Scattered fragmentation and coalescence of aragonite crystals. 2. Inflation, rounding up, fragmentation and fusion of the crystal seeds and ridges. Reduction in number of these structures in several areas of the 001 facets (Figs. 22 and 23). Etching reveals preservation of parallel oriented ridges in scattered areas. 3. See Part I, p. 22-23.
1, 2. Alterations as in 721-225-15 (10 minutes). 3. See Part I, p. 24-25. In pseudoreplicas, the trabeculae appear fused into fenestrate membranes.
1. Original architecture preserved. Diffuse changes in the aragonite crystals : inflation, shrinkage, beginning of fragmentation, displacement, fusion with adjacent crystals and conversely separation of individual crystals. Small polyhedral structures, stand out and in relief on the surfaces of fracture (Fig. 24). 2. Alteration of the crystal seeds and ridges as in (721-225-15) (10 minutes) (Fig. 23). 3. See Part I, p. 24-25. In pseudoreplicas, large parts of the original interlamellar conchiolin matrix appear in the forme of networks of membraneous flattened and widened trabeculae, in which the rounded corpuscles described in Part I are still held together (see also Fig. 9 in GRÉGOIRE, 1966a).

TABLE

Material File number (in parentheses) Temperature (in °C) Exposure time Conditions of pyrolysis	Mineral composition of the samples : X-ray powder diffraction	Physical characteristics of the samples
(770-772) 21 days. Dry heating in sealed tubes (Argon).	Aragonite	Decrease in hardness. Fragments cleavable into iridescent shee with intense metallic hues on the fresh cleaved surfaces.
250 °C	250 °C	250 °C
(721-250) 5 hours Heating in open vessels.	Aragonite	Brittle. Fragments cleavable into thin min sheets. Burnishing of iridescence on exposed surf ces. Freshly cleaved sheets strongly vari gate.
(803) 5 hours Dry heating in sealed tubes.	Aragonite	Decrease in hardness. Fragments moderate cleavable. Bronzed iridescence on the exposed surfac Intense metallic tints on the freshly cleav surfaces.
275 °C	275 °C	275 °C
(721-275) 5 hours Heating in open vessels.	Aragonite	Brittle. Portions of fragments cleaved into descent sheets, with intense metallic hu on the cleavage surfaces.

1 *(contd.)*

1. Surfaces of transverse fracture. Polished and etched surfaces of transverse section. 2. Surfaces of cleavage along the interlamellar planes, exposing the 001 facets of the tabular crystals of aragonite. Polished and etched surfaces of cleavage. 3. Alterations in the ultrastructure (trabeculae and fenestration) of the conchiolin matrix (see Part I, Table 1).
1. Original architecture preserved. 2. In the flaggings of polygonal surfaces, alterations in the crystal seeds and ridges as in (721-225-15) (10 minutes). 3. See Fig. 25 and Part I, p. 40-41. Observations confirmed in pseudoreplicas (loose networks of flattened trabeculae).
250 °C
1. Original architecture preserved. Disjunction of individual crystals in the lamellae. Alterations in the crystals as in (721-225-21) (225 °C, 21 days) and as in (803) (see below). 3. See Part I, p. 24-25
1. Original architecture preserved. Scattered dislocation of lamellae into free crystals. Alterations in tabular crystals : scattered smaller crystallites, appear in the replicas of transverse section in the form of polygonal or square pits and notches. 3. See Part I, p. 42-43.
275 °C
1. Original architecture preserved. Changes in aragonite crystals as in 721-225-21 (225 °C, 21 days). 3. See Part I, p. 26-27. In parts of the matrices, dissociation of the nautiloid pattern into loose networks of flattened and widened trabeculae (Fig. 26). Same alterations in pseudoreplicas (see GRÉGOIRE and LORENT, 1971, Fig. 5B)

TABLE

Material File number (in parentheses) Temperature (in °C) Exposure time Conditions of pyrolysis	Mineral composition of the samples : X-ray powder diffraction	Physical characteristics of the samples
(804) 5 hours Dry heating in sealed tubes.	Aragonite	See Part I, p. 42. Very brittle and cleavable. Burnishing of iridescence with metallic hue on the cleavage surfaces.
(1090) 5 hours Heating with distilled water in sealed tubes.	Aragonite	Moderately brittle and cleavable. Strongly iridescent on exposed surfaces. Light brown on the freshly cleaved surface Smell of burned horn during sample decalcification.
300 °C	300 °C	300 °C
(721-300, 904, 991) 5 hours Heating in open vessels.	Aragonite	Very brittle. Burnishing of iridescence on exposed surfaces. Surfaces of cleavage intensely iridescent with metallic hues (721-300, 991) or with fain pink bluish tints (904).

1 *(contd.)*

1. Surfaces of transverse fracture. Polished and etched surfaces of transverse section. 2. Surfaces of cleavage along the interlamellar planes, exposing the 001 facets of the tabular crystals of aragonite. Polished and etched surfaces of cleavage. 3. Alterations in the ultrastructure (trabeculae and fenestration) of the conchiolin matrix (see Part I, Table 1).
1. Original architecture preserved. Coalescence of crystal stacks into blocks. Pits and elevations on polished and etched cross sections of the crystals. 2. Parallel orientation of ridges and crystal seeds preserved on many 001 facets. In other areas, rarefaction of these structures. 3. See Part I, p. 42-43. Alteration of the nautiloid pattern into loose networks of flattened and widened trabeculae and their fragments. Vesicle-like rounded corpuscles (« knobs » : see GRÉGOIRE 1966a). Identical alterations in pseudoreplicas.
1. Coalescence of crystal stacks into blocks. 3. Flattening, widening and coalescence of the trabeculae slightly more developed than in the dry heated control (804) (Fig. 27).
300 °C
1. Original architecture altered as in the (721-225-21) (225 °C, 21 days) sample : inflation, fragmentation of individual crystals into small blocks. Protrusion, on the etched surfaces of transverse polished sections of the tabular crystals, of polygonal crystals appearing in the form of pits in the replicas (see discussion). Coalescence of crystal stacks into blocks. 2. Mosaic of polygonal surfaces on to which crystal seeds appear clustered in the region of the central elevations. Etching reveals in the replicas of the same surfaces polygonal (hexagonal) openings (See Fig. 56). 3. See Part I, p. 26-27. The study of an additional material (Fig. 28) revealed in the conchiolin matrices : 1. networks of trabeculae in which the nautiloid pattern has been preserved in certain areas, with fragmentation of the cylindrical trabeculae into nodules and twisted rods; 2. loose networks of flattened trabeculae and their fragments; 3. as reported in Part I, dislocation of the trabeculae into rounded corpuscles with or without dispersion; 4. fenestrate membranes. Identical alterations in pseudoreplicas.

TABLE

Material File number (in parentheses) Temperature (in °C) Exposure time Conditions of pyrolysis	Mineral composition of the samples : X-ray powder diffraction	Physical characteristics of the samples
(782) 5 hours Dry heating in sealed tubes.	Aragonite	Decrease in hardness. Parts of fragments cleaved into booklets o silvery-brown, iridescent or lustreless mine ral sheets.
(992) 5 hours Heating with sea water in sealed tubes.	Aragonite	Strong smell of H2S, burned horn and ta on breaking tubes. Hard or moderately brittle. Wet fragments, smoke-brown with intens metallic green hues. Smell of tar during sample decalcification.
(976); 1013; 1087) 5 hours Heating with distilled water in sealed tubes.	Aragonite	Pungent smell of burned horn on breakin tubes. Hard (976) or moderately brittle, cleaved i part (1013). (976) : wet fragments, pin chalky, slightly iridescent, with green an pink hues on exposed surfaces, more irides cent on surfaces of fresh fracture. Sample resembles mother-of-pearl of man Cretaceous fossils. (1013) : wet fragments, brown with iridescen spots and dark green metallic tints. Inne regions pale brown.

1 *(contd.)*

1. Surfaces of transverse fracture.
Polished and etched surfaces of transverse section.

2. Surfaces of cleavage along the interlamellar planes, exposing the 001 facets of the tabular crystals of aragonite.
Polished and etched surfaces of cleavage.

3. Alterations in the ultrastructure (trabeculae and fenestration) of the conchiolin matrix (see Part I, Table 1).

---

1. Lamellation preserved. Original architecture altered by coalescence of crystal stacks. Groups of these fused stacks form free foliate aggregates differently oriented.

2. The surfaces of cleavage appear in the form of polygonal flaggings fragmented in part into smaller units. Long parallel ridges, disposed in herring-bone in certain crystals extend throughout the surfaces and have replaced the crystal seeds and small ridges seen in the preceding stages. Square etch pits.

3. As in the samples heated to 300 °C in open vessels, the nautiloid pattern has been preserved in a few fragments (Fig. 29). Among the alterations described in Part I, p. 45 and Fig. 51, flattening and coalescence of the trabeculae into fenestrate membranes are predominant. The altered matrices form mosaics of polygonal areas in which the membranes of coalescence appear at the margins and are attached to the remnants in the form of cords of the intercrystalline matrix. Identical changes in pseudoreplicas.

---

1. Cleavage of the sample into parallel mineral sheets, frequently of the same thickness. Lamellar stratification preserved in scattered areas.
Alteration in original architecture consists predominantly of coalescence of parts of lamellae, including crystal columns, into foliate aggregates.

3. Rigid, mahogany-brown particles.
Nautiloid pattern recognizable in fragments of matrices (Fig. 30). As in the sample heated dry (782), flattening of the trabeculae into angulate structures and coalescence into fenestrate membranes. Dislocation into corpuscles.

---

1. The alterations in the original microstructure consist of coalescence of contiguous crystals or columns of crystals (Figs. 35, 36, 39). Groups of columns form foliate aggregates (Fig. 34). The grade of alteration differs greatly in contiguous areas of some samples : Fig. 37 shows a preserved brickwork texture in contiguity to foliate aggregates oriented at random.

2. Mosaics of polygonal crystal surfaces with parallel, straight, smooth ridges on the 001 facets, differently oriented in adjacent crystals. Scattered fragmentation of peripheral parts of the crystals.

3. Rigid brown particles.
Alterations as in samples heated dry (782) and with sea water (992), namely flattening (Fig. 31) and coalescence of the trabeculae into fenestrate membranes, and dislocation into corpuscles.

TABLE

Material File number (in parentheses) Temperature (in °C) Exposure time Conditions of pyrolysis	Mineral composition of the samples : X-ray powder diffraction	Physical characteristics of the samples
(986) 21 days Heating with sea water in sealed tubes.	Aragonite	On breaking tubes, pungent smell of tar and of burned horn. Very brittle. Breaks without cleavage. Wet brown-black fragments. Smell of burned horn and of petroleum during sample decalcification.
325 - 375 °C	325 - 375 °C	325 - 375 °C
(1041) 325 °C 5 hours Heating in open vessels.	Aragonite	Very brittle. Sample, cleaved into booklets of mineral sheets. Burnished iridescence with intense metallic hues.
(1044) (1088) 325 °C 5 hours Heating with distilled water in sealed tubes. Compare with (1041).	Calcite and traces of Aragonite (1044) Aragonite (1088)	On breaking tubes, pungent smell of tar and of burned horn. Transient smell of H2S. Moderately brittle. Break without cleavage Wet fragments, iridescent, black-brown on exposed surfaces, light pink-brown on surfaces of fresh cleavage. Pungent smell of petroleum during sample decalcification.

1 *(contd.)*

1. Surfaces of transverse fracture.
Polished and etched surfaces of transverse section.

2. Surfaces of cleavage along the interlamellar planes, exposing the 001 facets of the tabular crystals of aragonite.
Polished and etched surfaces of cleavage.

3. Alterations in the ultrastructure (trabeculae and fenestration) of the conchiolin matrix (see Part I, Table 1).

---

1 and 2. Alterations as in (992) (sea water, 5 hours) and (976, 1013, 1087) (distilled water, 5 hours) Foliate aggregates (Fig. 38).

3. Scum of black-brown particles floating on the supernate.
No appreciable difference with material heated dry for shorter periods of time (782).
Loose networks of flattened trabeculae and membranes (Figs. 32 and 33) forming a flagging of polygonal areas delimited by thickenings corresponding to the intercrystalline matrix (See GREGOIRE and VOSS-FOUCART, 1970, Fig. 16; GRÉGOIRE and LORENT, 1971, Fig. 8A).

325-375 °C

---

1. Original architecture preserved (Fig. 48).
Beginning of coalescence of crystal stacks.

2. Polygonal flagging preserved. Elongate polygonal or rounded crystal seeds in parallel or random orientation dispersed on the 001 facets of the tabular crystals, and clustered in the central elevations areas. Etching of the 001 facets reveals polyhedral intracrystalline structures.

3. Dark, mahogany-brown shreds.
In parts of the matrix, subdivided into polygonal areas delimited by intercrystalline cords, flattening (Fig. 44), and coalescence of the trabeculae into fenestrate membranes.
Disintegration of the trabeculae into corpuscles in other parts of the matrix (Fig. 45).

---

1. Columnar and lamellar stratifications altered by inflation and coalescence of groups of crystals (Fig. 49). Foliate aggregates of fused parallel fragments of lamellae (Fig. 50).

2. Fragmentation of the mosaic of polygonal crystal surfaces into smaller elements. Coalescence of other crystals. Decoration patterns on the 001 facets. On the cleavage surfaces, the foliate aggregates visible on the surfaces of transverse fracture appear in the form of differently oriented bundles of parallel, elongated crystals (Figs. 51 and 52).

3. Dark, mahogany — brown shreds.
Flattening and coalescence of the trabeculae into fenestrate membranes forming polygonal mosaics delimited by intercrystalline cords. Fragments of this material (Fig. 47). The openings in fenestration appear encircled by ring-shaped pads (Fig. 46).

TABLE

Material File number (in parentheses) Temperature (in °C) Exposure time Conditions of pyrolysis	Mineral composition of the samples : X-ray powder diffraction	Physical characteristics of the samples
(1042) 350 °C 5 hours Heating in open vessels.	Aragonite	Very brittle, cleaved into booklets of mineral sheets. Glistening, dark-grey fragments with intense metallic tints. Smell of tar and of petroleum during decalcification.
(1045) 350 °C 5 hours Heating with distilled water in sealed tubes. Compare with (1042)	Calcite	Pungent smell of tar and transient smell of H2S on breaking tubes. Brittle. Slightly wet. Some fragments still compact, other fragments cleaved into parallel minerals sheets. Exposed surfaces black-brown. Surfaces of fresh fracture or cleavage light chocolate-brown.
(1043) 375 °C 5 hours Heating in open vessels.	Calcite	Extremely brittle, cleaved into booklets of grey-violet mineral sheets with intense metallic hues.
(1046) (1089) 375 °C 5 hours Heating with distilled water in sealed tubes. Compare with (1043).	Calcite	Persisting smell of burned horn and tar, and transient smell of H2S on breaking tubes. Brittle, cleaved in part. Lustreless. Exposed surfaces of wet fragments black-brown. Surfaces of fresh cleavage light chocolate-brown.

1 *(contd.)*

1. Surfaces of transverse fracture. Polished and etched surfaces of transverse section. 2. Surfaces of cleavage along the interlamellar planes, exposing the 001 facets of the tabular crystals of aragonite. Polished and etched surfaces of cleavage. 3. Alterations in the ultrastructure (trabeculae and fenestration) of the conchiolin matrix (see Part I, Table 1).
1. Microstructure preserved (Fig. 53). Coalescence of groups of crystals. 2. Many crystal seeds on the mosaics of polygonal surfaces appear in the form of rounded or subhedral polygonal corpuscles scattered at random or clustered in the central elevation areas (Fig. 55). Etch elevations (Fig. 54) and etch pits on the tabular crystal surfaces. 3. Bright, mahogany-brown particles. Networks of flattened trabeculae. Disintegration into corpuscles.
1. Foliate aggregates in which the original lamellation is still distinguishable. Coalescence of crystals in the columns (Fig. 57). 2. Fragmentation of the polygonal crystal surfaces with or without separation into smaller rounded elements (Fig. 60). Coarser crystals with a different structure are scattered in the mosaic formed by these crystals (Fig. 58). 3. Dark-brown particles. Flattened trabeculae forming loose networks of angulate structures, fused into membranes (Fig. 59) and fragmented into rounded corpuscles. See also GRÉGOIRE and LORENT, 1971, Fig. 5D.
1. Original architecture preserved in certain parts of the samples. Coalescence of crystals in the columnar stacks (Fig. 66). Foliate aggregates (Fig. 68). 2. Fragmentation of the polygonal crystal surfaces into mosaics of smaller, domeshaped surfaces (Fig. 67) or into free tablets with contorted and indented outlines. 3. Black-brown or bright, mahogany-brown particles. Loose networks of flattened trabeculae. Perforated membranes Disintegration into rounded corpuscles with or without dispersion (Fig. 61).
1. Original microtexture preserved in certain areas with fragmentation, irregular inflation (Fig. 70) and coalescence of crystals (Fig. 69). 2. Coalescence and fragmentation of groups of crystals. Islands of recrystallization in the form of elusters of acicular (Fig. 71) and of coarse polyhedral, subhedral or euhedral (Fig. 72) crystals emerging from the mosaics of smaller crystals. 3. Black-brown particles. In the interlamellar matrices forming polygonal areas delimited by intercrystalline cords (Figs. 63, 64 and 65), flattening of the trabeculae into angulate structures and coalescence into membranes, with variously shaped fenestration (Figs. 62, 63 and 65). Dislocation into corpuscles (See also GRÉGOIRE and VOSS-FOUCART, 1970, Fig. 16 and GRÉGOIRE and LORENT 1971, Figs. 4B and 5B).

TABLE

Material File number (in parentheses) Temperature (in °C) Exposure time Conditions of pyrolysis	Mineral composition of the samples : X-ray powder diffraction	Physical characteristics of the samples
400 °C	400 °C	400 °C
(721-400) 5 hours Heating in open vessels.	Calcite	Very brittle. Fragments cleaved into booklet of iridescent, steel-coloured sheets, wit faint metallic hues.
(811) Preheating (20 to 400 °C) : 15 minutes. 400 °C : 30 minutes. Dry heating in sealed tubes.	Calcite	Brittle. Fragments cleaved into booklets c grey-brown or slate-coloured, glistenin sheets.
(812) Preheating (20 to 400° C) : 15 minutes. 400 °C : 60 minutes. Dry heating in sealed tubes.	Calcite	Alterations as in (811). Faint metallic hues.

1 *(contd.)*

1. Surfaces of transverse fracture. Polished and etched surfaces of transverse section. 2. Surfaces of cleavage along the interlamellar planes, exposing the 001 facets of the tabular crystals of aragonite. Polished and etched surfaces of cleavage. 3. Alterations in the ultrastructure (trabeculae and fenestration) of the conchiolin matrix (see Part I, Table 1).
400 °C
1. Original architecture preserved in certain areas. Inflation of individual crystals. Coalescence of portions of lamellae. 2. Mosaics or irregularly polygonal crystal surfaces (15-900 microns) in the process of fragmentation into smaller, dome-shaped elements, bulging on the 001 facets (Fig. 81). Needle-shaped structures erected on the surfaces. 3. See Part 1, p. 30-31. Disintegration of the trabeculae into rounded corpuscles. In pseudoreplicas of the matrix, these corpuscles appear still assembled in ribbon-shaped structures forming loose networks (Fig. 79).
1. Foliate aggregates. 2. Changes as in (721-400) (5 hours, open vessels). Fragmentation of large crystal surfaces into smaller elements (Fig. 82). 3. See Part 1, p. 44-45. Flattened trabeculae fused into membranes.
1. Lamellar stratification recognizable in certain areas. Foliate aggregates. 2. Mosaics of rounded crystal surfaces of different sizes, shapes and orientations. Coarse subhedral crystals scattered among the other elements. The foliate aggregates appear in the form of differently oriented bundles of parallel elongated crystals. Fig. 83 shows a crystal arrangement resembling an enfacial junction (BATHURST, 1964). 3. See Part I. p. 44-45. Changes as in (811 : 30 minutes).

TABLE

Material File number (in parentheses) Temperature (in °C) Exposure time Conditions of pyrolysis	Mineral composition of the samples : X-ray powder diffraction	Physical characteristics of the samples
(783) 5 hours Dry heating in sealed tubes.	Calcite	Brittle, as (811) and (812). Fragments cleaved into lustreless, grey-black sheets, with traces of iridescence.
(975 - 993) 5 hours Heating with sea water in sealed tubes. Compare with (783).	Calcite	Pungent persisting smell of tar and of burned horn, transient smell of H2S on breaking tubes. Moderately brittle. Easily cleavable. Still compact grey-brown (975) or black-brown (993) fragments. Smell of tar and of petroleum during sample decalcification.
(879) 21 days Dry heating in sealed tubes.	Calcite	Fragments cleaved into booklets of dark-grey slate-coloured, faintly iridescent or lustreless sheets.
500 °C	500 °C	500 °C
(771) Explosion after 5 minutes, during preheating to 500 °C in dry argon atmosphere.	Aragonite	Beginning of cleavage of the samples. Bronze-coloured fragments, iridescent with intense metallic hues.

1 *(contd.)*

1. Surfaces of transverse fracture.
Polished and etched surfaces of transverse section.

2. Surfaces of cleavage along the interlamellar planes, exposing the 001 facets of the tabular crystals of aragonite.
Polished and etched surfaces of cleavage.

3. Alterations in the ultrastructure (trabeculae and fenestration) of the conchiolin matrix (see Part I, Table 1).

---

1. and 2. Changes as in (812) (60 minutes).

3. See Part I, p. 44-45.
Dark-brown and black particles.
Changes as in (811 and 812) (30 and 60 minutes). Dislocation into spheroidal corpuscles.

---

1. Foliate aggregates (Figs. 84 and 85).

2. Changes as in (812) (60 minutes, dry).
Needle-like structures erected on the cleavage surfaces.

3. Black-brown and brown particles.
Alterations as in (783) (5 hours, dry). Flattening and dislocation of the trabeculae into angulate, twisted structures, cords, corpuscles (Fig. 80), enclosed in polygonal areas delimited by intercrystalline cords: These alterations resemble those described in the Jurassic ammonite *Harpoceras mulgravium* : see GRÉGOIRE, 1966, Fig. 40).

---

1. Changes as in the samples heated for 60 minutes (812) and for 5 hours (783). Foliate aggregates. Etch pits and etch elevations.

2. Changes as in (812). Fragmentation or large polygonal tabular crystal surfaces into mosaics of smaller rounded elements.

3. See Part I, p. 46-47.
Alterations as in (811 : 30 minutes dry), (812 : 60 minutes dry), (975 and 993 : 5 hours, sea water).

---

500 °C

---

1. Brickwork architecture preserved (Fig. 92). Scattered fragmentation and dislocation of individual crystals. Coalescence and fragmentation of groups of lamellae.

2. Mosaics of crystal tabular surfaces. Rounded crystal seeds and smaller unidentified hemispheral elevations. Square and polygonal etch pits and elevations (Fig. 94).

3. See Part. I, p. 46-47, and GRÉGOIRE and LORENT, Fig. 6A. In pseudoreplicas, on etched cleavage surfaces, the conchiolin matrices appear in the form of loose networks of flat membraneous trabeculae (Figs. 88 and 91). Dislocation into corpuscles.

TABLE

Material File number (in parentheses) Temperature (in °C) Exposure time Conditions of pyrolysis	Mineral composition of the samples : X-ray powder diffraction	Physical characteristics of the samples
(721 - 500 - 10) Preheating (20° to 500 °C) : 2 minutes 30 seconds. 500 °C : 10 minutes. Heating in open vessels.	Calcite	Very brittle. Fragments cleaved into booklet of slate- or silver-coloured, faintly irides cent or lustreless sheets.
(721-500; 905) 5 hours Heating in open vessels.	Calcite	Very brittle. Cleaved into booklets of mineral glistening silver-grey or lustreless sheets with traces of iridescence.
(780) 5 hours. Dry heating in sealed tubes.	Calcite	Brittle. Fragments cleaved into booklets o grey-black and slate-coloured sheets, with traces of iridescence.
(979) (994) 5 hours Heating with sea water in sealed tubes. Compare with (780).	Calcite	Transient smell of H2S, pungent, persisting smell of tar and burned horn on breaking tubes. Moderately brittle, still compact or cleaved in part. Wet fragments, steel-black with bluish hues on exposed surfaces, light slate-grey or surfaces of fresh cleavage.

1 *(contd.)*

1. Surfaces of transverse fracture.
Polished and etched surfaces of transverse section.

2. Surfaces of cleavage along the interlamellar planes, exposing the 001 facets of the tabular crystals of aragonite.
Polished and etched surfaces of cleavage.

3. Alterations in the ultrastructure (trabeculae and fenestration) of the conchiolin matrix (see Part I, Table 1).

---

1. Foliate aggregates.

2. Dislocation of irregularly polygonal crystal surfaces into mosaics of smaller elements (See 721-500-3 : Fig. 100). In other areas, large dome-shaped crystals, rod- and needle-like structures (Fig. 96) stand out in relief on the cleavage surfaces.

3. See Part I, p. 30-31.
A few networks of flattened trabeculae. Disintegration into spheroidal corpuscles.

---

1. Original architecture preserved in parts of the samples (Figs. 93 and 95), with disjunction of the crystals (see GRÉGOIRE & al., 1969, Fig. 9). Square etch-pits and notches in the crystals.
In other areas, foliate aggregates and mosaics of polyhedral blocks with parallel cleavage striation (Fig. 102).

2. Changes as in (721-500-10) (10 minutes, Fig. 100) including needle- and girdle-like crystals (Fig. 97).

3. See Part I, p. 32-33.
Dark-brown and black shreds and particles. Predominant alteration consisting of disintegration of the trabeculae into rounded corpuscles.

---

1. Traces of lamellation, altered by inflation, fragmentation and coalescence of the original crystals. Foliate aggregates.

2. Mosaics of rounded crystal surfaces. Scattered coarse polyhedral crystals.

3. See Part I, p. 48-49.
Black particles.
Networks of flattened trabeculae, fused into fenestrate membranes (holes encircled by bulging pads), enclosed in polygonal areas delimited by intercrystalline cords.

---

1. Foliate aggregates showing signs of disintegration into rounded smaller blocks composed of agglutinated, inflated anhedral crystals (Figs. 98 and 99).

3. Dark-grey or brown particles.
(979). Dislocation of the matrices into dispersed fragments of cylindrical or ribbon-like trabeculae, twisted rods, cords, nodules, rounded corpuscles.
Organic ghosts of needle-like structures.
(994) : Loose networks of flattened trabeculae, fused into continuous (Fig. 89) or fenestrate membranes (ring-shaped pads around the openings (See 1014 : Fig. 90).

TABLE

Material File number (in parentheses) Temperature (in °C) Exposure time Conditions of pyrolysis	Mineral composition of the samples : X-ray powder diffraction	Physical characteristics of the samples
(1014) 5 hours Heating with distilled water in sealed tubes. Compare with (780).	Calcite	Transient smell of H2S and of burned hor on breaking tubes. Brittle. Wet fragments black-brown or steel-coloure with bluish iridescence.
600 °C	600 °C	600 °C
(813) Preheating (20 °C to 600 °C) : 15 minutes. 600 °C : 5 minutes. Dry heating in sealed tubes.	Calcite	See Part. I, p. 48.
(814) Preheating (20 °C to 600 °C) : 15 minutes. 600 °C : 30 minutes. Dry heating in sealed tubes.	Calcite	See Part. I, p. 50.
(815) Preheating (20 °C to 600 °C) : 15 minutes. 600 °C : 60 minutes. Dry heating in sealed tubes.	Calcite	See Part. I, p. 50.

1 *(contd.)*

1. Surfaces of transverse fracture. Polished and etched surfaces of transverse section. 2. Surfaces of cleavage along the interlamellar planes, exposing the 001 facets of the tabular crystals of aragonite. Polished and etched surfaces of cleavage. 3. Alterations in the ultrastructure (trabeculae and fenestration) of the conchiolin matrix (see Part I, Table 1).
1. Lamellar stratification recognizable in certain areas. Foliate aggregates. 3. Scum of black-brown particles, floating on the supernate. Alterations as in (994) : (Sea water) (Fig. 90).
600 °C
1. Lamellar stratification still recognizable, altered by inflation, fragmentation and coalescence of crystals in the columns and in parts of lamellae. 2. Fragmentation of polygonal surfaces into smaller elements. 3. See Part I, p. 48-49. Coalescence of networks of flattened trabeculae into fenestrate membranes with ring-shaped pads encircling the openings (see below, 779, 5 hours, Fig. 106). Same alterations in pseudoreplicas. Organic ghosts of needle-like crystals.
1. Foliate aggregates. 2. Mosaics of small, rounded, anhedral, bulging crystal surfaces. Scattered, small euhedral crystals (Fig. 108). 3. See Part I, p. 50-51. Changes as in (813) (5 minutes).
1. Foliate aggregates. 2. Changes as in (814). Tabular facets of large crystals with traces of fragmentation into smaller elements (Fig. 109). 3. See Part I, p. 50-51. Changes as in (813) (5 minutes) and (814) (30 minutes).

TABLE

Material File number (in parentheses) Temperature (in °C) Exposure time Conditions of pyrolysis	Mineral composition of the samples : X-ray powder diffraction	Physical characteristics of the samples
(779) 5 hours Dry heating in sealed tubes.	Calcite	On breaking tubes, transient smell of H2 and persisting ammoniacal smell. Very brittle. Fragments split into booklets o glistening grey-black sheets, with intens violet metallic hues.
(977; 995) 5 hours Heating with sea water in sealed tubes. Compare with (779).	Calcite	On breaking tubes, intense transient smell o H2 S and persisting smell of tar. Moderately brittle, not cleaved. Wet, glis tening grey-black or dull, ash-grey frag ments. Faintly violet iridescence on sur faces of fresh cleavage. Smell of naphtalene during sample decalc fication.
700 °C	700 °C	700 °C
(806) Preheating (20° C to 700 °C) : 15 minutes. 700 °C : 10 minutes. Heating in open vessels.	Calcite	Brittle. Fragments split into booklets of ash grey, lustreless sheets.

1 *(contd.)*

1. Surfaces of transverse fracture.
   Polished and etched surfaces of transverse section.
2. Surfaces of cleavage along the interlamellar planes, exposing the 001 facets of the tabular crystals of aragonite.
   Polished and etched surfaces of cleavage.
3. Alterations in the ultrastructure (trabeculae and fenestration) of the conchiolin matrix (see Part I, Table 1).

1. Alterations as in (813) (5 minutes). Foliate aggregates.
2. Mosaics of tabular surfaces of polygonal crystals, agglutinated into sheets (Fig. 111).
3. See Part I, p. 50-51.
   Scum of biuret-positive black particles.
   Changes as in (813) (5 minutes), (814) (30 minutes) and (815) (60 minutes).
   Flattened trabeculae forming loose networks within polygonal areas (Fig. 107).

1. Foliate aggregates (977). In (995), in comparison with the 400 °C and 500 °C stages, the structure of the foliate aggregates seems to have changed : the agglutinated parallel fragments of lamellae which compose these aggregates have been replaced by mosaics of rounded polyhedral crystals resembling those depicted below in the 700 °C and 800 °C stages.
2. Mosaics of crystals of different sizes and shapes (977) (995). In parts of the cleavage surfaces, small rounded crystals observed in the precedings stages seem to have fused into coarser crystalline elements (Fig. 110). These elements appear in the form of anhedral or subhedral polyhedral structures with dome-shaped bulging surfaces. Abundant protrusion of rod- and needle-shaped structures (Fig. 103).
3. Scum of rigid, curled, dark-brown or black biuret-positive shreds.
   Networks of flattened trabeculae (995); fragmentation into rounded corpuscles (977).
   Organic remnants of needle-shaped expansions (Fig. 103) appear in the form of elongate collapsed, membraneous tubes perforated by rectangular, triangular, lozenge-shaped fenestration (Figs. 104 and 105), disposed in a regular array.

700 °C

1. Mosaics of tightly interlocked polyhedral blocks.
2. Mosaics of coarse polyhedral crystals with dome-shaped bulging facets.
3. See Part I, p. 34-35.
   Fragments of flattened trabeculae and spheroidal corpuscles.

TABLE

Material File number (in parentheses) Temperature (in °C) Exposure time Conditions of pyrolysis	Mineral composition of the samples : X-ray powder diffraction	Physical characteristics of the samples
(807) Preheating (20 °C to 700 °C) : 15 minutes. 700 °C : 60 minutes. Heating in open vessels.	Calcite	Ash-grey powdery substance.
721 - 700 (906) 5 hours Heating in open vessels	Traces of Calcite Ca (OH)2 (Portlandite)	Very brittle. Fragments split into paper-whi sheets with grey spots and disintegrate into white powder.
(778) 5 hours Dry heating in sealed tubes.	Calcite	Transient smell of H2 S and persisting sme of NH 3 on breaking tubes. Brittle. Samples split into lustreless, grey black sheets.
(981-996) 5 hours Heating with sea water in sealed tubes. (1015) 5 hours Heating with distilled water in sealed tubes. Compare with (778).	Calcite	Intense, transient smell of H2S, NH 3 and ta on breaking tubes. Very brittle. Wet samples not split, brea without cleavage, appear in the form lustreless, grey or snow-white (with gr spots) slabs.

1 *(contd.)*

1. Surfaces of transverse fracture. Polished and etched surfaces of transverse section. 2. Surfaces of cleavage along the interlamellar planes, exposing the 001 facets of the tabular crystals of aragonite. Polished and etched surfaces of cleavage. 3. Alterations in the ultrastructure (trabeculae and fenestration) of the conchiolin matrix (see Part I, Table 1).
1. Changes as in (806) : Mosaics of interlocked, anhedral or subhedral crystals (Figs. 116 and 117). 2. Changes as in (806) (clusters of small, sharp-edged crystals). 3. See Part I, p. 34-35.
3. See Part I, p. 34-35. Spheroidal corpuscles, debris of membranes and of flattened trabeculae.
1. Mosaics of tightly interlocked, coarse polyhedral blocks of different sizes. In scattered regions of the samples, persistance of traces of the brickwork architecture. 2. Mosaics of large, rounded or ovoid crystals with dome-shaped facets bulging on the cleavage surfaces. Abundant protrusion of rod- or needle-shaped crystals from the lateral surfaces of the mineral sheets. 3. See Part I, p. 50-51. Loose networks of considerably flattened trabeculae fused into fenestrate membranes and broken into angulate blades and corpuscles. Organic ghosts of the needle-shaped crystals.
1. Mosaics of tightly or loosely interlocked polyhedral, anhedral or subhedral crystals (Figs. 118 to 123). 2. Mosaics of crystals of large size, with dome-shaped facets bulging on to the cleavage surfaces (996) (Fig. 112 : TEM; Figs. 119 and 123 : SEM). 3. Rigid, white, biuret-positive pellicles and flakes. The remnants of the conchiolin matrices (Figs. 113, 114, 115) consist of a large variety of soft and rigid structures : bars, filaments, parallel, straight strips, corpuscles, membranes, crossed by straight opaque parallel ridges, with a polygonal fenestration disposed in a regular array. These different structures form frequently polygonal assemblages (see below, 978). Organic residues of needle-shaped crystals.

TABLE

Material File number (in parentheses) Temperature (in °C) Exposure time Conditions of pyrolysis	Mineral composition of the samples : X-ray powder diffraction	Physical characteristics of the samples
800 °C	800 °C	800 °C
(816) Preheating : 15 minutes. 800 °C : 5 minutes. Dry heating in sealed tubes.	Calcite	Very brittle. Samples split into booklets o grey-black, pulverulent sheets, with scatte red, intensely iridescent areas.
(808) Preheating : 15 minutes. 800 °C : 10 minutes. Heating in open vessels.	Calcite	Grey-white powder with traces of lamella tion.
(817) Preheating : 15 minutes. 800 °C : 30 minutes. Dry heating in sealed tubes.	Calcite	Very brittle. Samples split into lustreless dark-grey and black pulverulent sheets.
(818) Preheating : 15 minutes. 800 °C : 60 minutes. Dry heating in sealed tubes.	Calcite	Very brittle. Samples split into lustreless, grey black, powdery sheets.

1 *(contd.)*

1. Surfaces of transverse fracture. Polished and etched surfaces of transverse section. 2. Surfaces of cleavage along the interlamellar planes, exposing the 001 facets of the tabular crystals of aragonite. Polished and etched surfaces of cleavage. 3. Alterations in the ultrastructure (trabeculae and fenestration) of the conchiolin matrix (see Part I, Table 1).
800 °C
1. Mosaics of interlocked, polyhedral, anhedral or subhedral crystals (see Figs. 116-123). 2. Mosaics of crystals of large size, with bulging dome-shaped surfaces surrounded by clusters of small euhedral crystals. Protrusion of needle-like structures. 3. See Part I, p. 52-53. Loose network of flattened trabeculae and fenestrate membranes, enclosed in polygonal areas delimited by intercrystalline cords.
1. and 2. Mosaics of oval, rounded or polyhedral corpuscles. 3. See Part I, p. 36-37. Disintegration into corpuscles. Coalescence into granular membranes.
1. Mosaics of tightly or loosely interlocked polyhedral, anhedral or subhedral, crystals (Figs. 128 and 130). Small euhedral crystals disposed along the margins of these crystals (Fig. 127). 2. Mosaics of polygonal, dome-shaped facets of large crystals bulging on the surfaces of cleavage. Protruding needle-like structures. 3. See in Part I, p. 52-53, especially Figs. 79 and 80. Predominantly fenestrate membranes. Networks of trabeculae encircling the small crystals at the margins of the coarse crystals (Fig. 127). Organic ghosts of needle-like crystals.
1. and 2. Changes as in (817) (30 minutes) (see Figs. 116-123). 3. See Part I, p. 52-53. Polygonal structures, with euhedral, frequently hexagonal outlines, contain loose networks of cylindrical or flattened trabeculae fused into membranes or disintegrated into corpuscles (see below, 978, 5 hours, Figs. 124, 125 and 126).

TABLE

Material File number (in parentheses) Temperature (in °C) Exposure time	Mineral composition of the samples : X-ray powder diffraction	Physical characteristics of the samples
(775 - 776) 5 hours Dry heating in sealed tubes.	Calcite	Smell of H2S on breaking tubes. Ash-grey, powdery substance marbled wit scattered black spots.
(978) 5 hours Heating with sea water in sealed tubes. Cooling in the oven (800 °C to 20 °C) : 18 hours 30 minutes. (1019) 5 hours Heating with distilled water in sealed tubes. Compare with (775, 776).	Calcite	Transient smell of H2S and of NH3 o breaking tubes. Extremely brittle. Samples split into booklet of mineral sheets. Snow-white powdery slabs.
900 °C	900 °C	900 °C
(1000; 880; 805; 889). Preheating : 30 minutes. 900 °C : 5 hours. Dry heating in sealed tubes.	Calcite	Brittle. Cleaved into glistening, snow-whit flakes and white powder.

1 *(contd.)*

1. Surfaces of transverse fracture. Polished and etched surfaces of transverse section. 2. Surfaces of cleavage along the interlamellar planes, exposing the 001 facets of the tabular crystals of aragonite. Polished and etched surfaces of cleavage. 3. Alterations in the ultrastructure (trabeculae and fenestration) of the conchiolin matrix (see Part I, Table 1).
3. See in Part I, p. 54-55 and Figs. 82-85. Changes as in (818) (60 minutes).
1. Mosaics of coarse, rounded, polyhedral crystals. 2. Mosaics of bulging facets of coarse polyhedral crystals (Fig. 129). 3. Rigid, biuret-positive, white shreds. Alterations as in (818) (60 minutes, dry) and in (775-776) (5 hours) (Figs. 124, 125, 126. Organic ghosts of needle-like structures.
900 °C
1. and 2. Mosaics of coarse polyhedral crystals differing in part in their structure from those depicted in the 600 °C, 700 °C and 800 °C stages : increase in the number of facets, traces of fusion with contiguous crystals, perforation pits, decoration patterns on the facets (Figs. 131, 132, 133). 3. See Part I, p. 54-55 and Figs. 86-95. Alterations as in (818) (800 °C, 60 minutes). Straight parallel dense cords cross the membranes Absence of crystalline material in several of these polygonal structures, controlled by electron diffraction. Organic ghosts of needle-like crystals.

TABLE

Material File number (in parentheses) Temperature (in °C) Exposure time	Mineral composition of the samples X-ray powder diffraction	Physical characteristics of the samples
(985) Preheating : 30 minutes. 900 °C : 5 hours. Heating with sea water in sealed tubes. Cooling in the oven (900 °C to 20 °C) : 18 hours 30 minutes. (1020) Preheating : 30 minutes. 900 °C : 5 hours. Heating with distilled water in sealed tubes.	Calcite	Pungent, transient smell of H2S and of NH on breaking tubes. Samples remnants in the form of a wet white, glistening substance with a crystal line appearance (985) or of snow-white lustreless slabs (1020).

1 *(contd. and end)*

1. Surfaces of transverse fracture. Polished and etched surfaces of transverse section. 2. Surfaces of cleavage along the interlamellar planes, exposing the 001 facets of the tabular crystals of aragonite. Polished and etched surfaces of cleavage. 3. Alterations in the ultrastructure (trabeculae and fenestration) of the conchiolin matrix (see Part I, Table 1).	1. and 2. Mosaics of coarse polyhedral crystals. 3. White, biuret-positive shreds. As in the material heated dry (1000, 880, 805) (5 hours), rigid, flat, fenestrate membranes with polygonal outlines, enclosing various dense elements (straight cords, corpuscles) disposed in regular arrays.

TABLE 2

Similarities between the changes produced experimentally in the microtexture of mother-of-pearl of the modern *Nautilus* and diagenetic changes in microtexture of fossil mother-of-pearl.

Pyrolysed mother-of-pearl of modern *Nautilus* shell.	Changes in microtexture of mother-of-pearl.	Mother-of-pearl of ammonites and fossil nautiloids.
A. Aragonitic columnar texture. Aragonitic-calcitic (scattered islands of recrystallisation) and calcitic samples (with islands of preserved original architecture).		
Samples boiled, heated in open vessels, and dry and wet in sealed tubes in the temperature range of 150 °C - 275 °C for 5 hours. (Figs. 2, 4, 5) (Aragonite).	Preservation of the brickwork architecture with no distinct or little alteration.	*Wellerites mohri* (Pennsylvanian, Fig. 7). *Leioceras opalinum* (Jurassic, Fig. 3). *Eutrephoceras* sp. (Cretaceous, Fig. 11). *Baculites ovatus* (Cretaceous, Fig. 12). *Acanthohoplites* sp. (Cretaceous, Fig. 14). (All aragonitic).
Aragonitic and calcitic samples heated in the range of 300 °C - 500 °C for 5 hours. Fig. 70 (calcite). Fig. 68 (calcite). Fig. 102 (calcite).	Fragmentation of individual crystals. Coalescence of fragments of adjacent lamellae and of columns of crystals into foliate aggregates, transformed into islands of polyhedral crystals scattered in the brickwall architecture.	*Baculites claviformis* (Cretaceous, Figs 9 and 10). (Aragonite). *Placenticeras* sp. Cretaceous, Fig. 41 (Aragonite) (See also Grégoire, 1966a, Figs. 47 and 48 in Pennsylvanian samples). *Ammonites lineatus penicillatus* (Jurassic, Figs. 40, 42, 101) (Aragonite and calcite). *Psiloceras planorbis* (Jurassic, Fig. 43). (Aragonite).
Figs 54 and 56 (Aragonite).	Polygonal structures on the etched 001 facets of tabular crystals.	*Eutrephoceras balcombensis* (Middle Miocene, not shown) (Aragonite).
B. Samples integrally or predominantly recrystallized into calcite.		
Samples heated in the range of 300 °C (aragonite) and 600 °C (calcite). Fig. 38 (aragonite). Fig. 68 (calcite). Fig. 84-85 (calcite). Figs 98-99 (calcite).	Cleavage of the samples into parallel mineral sheets, former original sublayers of nacre, and composed of foliate aggregates or lamellated blocks differently oriented. Relics of the original mineral architecture (traces of columnar pattern of lamellation) scattered among mosaics of coarse polyhedral crystals.	*Ludwigia murchisonae* (Jurassic, Figs. 73, 74 and 75) (Calcite). *Hildoceras* sp. (Jurassic, Fig. 76) (Calcite). *Domatoceras* sp. (Permian, Fig. 78) (Calcite). See Grégoire, 1966a : *Isorthoceras sociale* (Ordovician, Figs 52 and 53).
Persistance of aragonitic microareas with brickwall texture in a sample heated in open vessels at 500 °C for 5 hours. Figs 93, 95, 95a.		Persistance of original aragonite in Paleozoic mollusc shells. (Stehli, 1956; Hallam and O'Hara, 1962; Grandjean, et al., 1964).

EXPLANATION OF FIGURES

PLATE I

Fig. 1

Nautilus pompilius LINNÉ (control)

Surface of transverse fracture of the nacreous layer (Aragonite). Direct replica.
Brickwork architecture. Interlamellar matrices on the 001 facets of the tabular crystals (thickness : about 400 millimicrons) and intercrystalline matrices appear in the form of networks of contorted trabeculae.
TEM. × 24 000.

Fig. 2

Nautilus pompilius LINNÉ (801)

Sample of nacre heated to 150 °C for 5 hours in a sealed tube (Aragonite).
Surface of transverse fracture. Direct replica.
Compare with Fig. 1. This picture does not reveal any distinct change in the organic and mineral components (crystal thickness : about 400 millimicrons).
TEM. × 36 000.

Fig. 3

Leioceras (Harpoceras) opalinum REINECKE (966)

Middle Jurassic. Upper Aalenian, Goslar, Harz, Germany (Aragonite).
Surface of transverse fracture of the shell wall showing the nacre crystals stacked into parallel columns.
SEM (STEREOSCAN) × 1.300.

PLATE II

Nautilus pompilius LINNÉ (886-3)

Mother-of-pearl of the shell wall boiled for 42 hours in sea mud and sea water and kept for 42 months in the same environment at 10-20 °C (Aragonite).

Figs. 4 and 5

Surfaces of transverse fracture. Direct replicas.
Brickwork microtexture. No distinct change appears in the organic (horizontal interlamellar and vertical intercrystalline conchiolin) and in the main architectural features of the mineral components (crystal thickness : 400-500 millimicrons). Possible changes (inflation, fragmentation ?) in the crystalline subunits, in the superficial layers of the aragonite crystals (Fig. 4).
TEM. × 36 000.

Fig. 6

In the same sample, cleavage of the nacre along the interlamellar planes, showing fragments of five superposed lamellae with rounded crystal seeds (100-200 millimicrons) standing out in relief on the 001 facets of the crystals. These seeds are especially gathered in the centre of the facets.
TEM. × 10 000.

PLATE III

Fig. 7.

Wellerites mohri PLUMMER & SCOTT (ammonoid) (769). Pennsylvanian, Buckhorn asphalt, Sulfur, Oklahoma, U. S. A. Specimen given by Prof. William M. FURNISH and Prof. Brian F. GLENISTER (S. U. I. 8891) (Aragonite and calcite).

Surface of transverse fracture of the shell wall. Direct replica. The organic (substantial, horizontal, interlamellar and vertical, intercrystalline conchiolin matrices) and mineral components (columns of tabular crystals, 300-400 millimicrons thick) have been integrally preserved in this specimen buried in asphalt. The aspect of the field does not distinctly differ from that of a surface of transverse fracture in the shell wall of the modern *Nautilus*.

TEM. × 36 000.

PLATES IV and V

Nacreous layers of the shell wall in 6 different fossil cephalopods. Surfaces of transverse fracture. Direct replicas. TEM.

Fig. 8.

Placenticeras sp. (ammonoid) (1006) Cretaceous, U. S. A. Specimen given by Dr. Norman F. SOHL. (Aragonite).
× 30 000.

Figs. 9 and 10

Baculites claviformis STEPHENSON (ammonoid) (393-998) Cretaceous, Senonian, Coon Creek Member, Ripley Formation, near Enville-Adamsville, Mc Nairy Co, Tennessee, U. S. A. Specimen given by Dr Norman SOHL (U. S. G. S. 25 406) (Aragonite).
Fig. 9 : × 36 000; Fig. 10 : × 30 000.

Fig. 11

Eutrephoceras sp. (nautiloid) (999). Cretaceous, Eutaw Formation, Menabites, Alabama, U. S. A. Specimen given by Dr Norman F. SOHL (U. S. G. S. 27 065) (Aragonite).
× 27 000.

Fig. 12

Baculites ovatus SAY (ammonoid) (356) Cretaceous, Senonian, Pierre Shale of Montana Group, Colorado Springs, Colorado, U. S. A. Specimen given by Prof. William M. FURNISH (Aragonite).
× 25 000.

Fig. 13

Ammonites lineatus penicillatus (785), Jurassic, Brauner Jura, Gammelshausen bei Boll, Württemberg, Germany. Specimen given by Prof. O. H. SCHINDEWOLF and by Dr. Fr. WESTPHAL (Aragonite and calcite).
× 24 000.

Fig. 14

Acanthohoplites sp. (?) (Ammonoid) (499). Cretaceous, Gault, Folkestone, England (Aragonite).
× 36 000.

Figs. 8 to 14 show various aspects of the mineral microtexture in five aragonitic (GRANDJEAN & al., 1964) and one aragonitic and calcitic (785) nacreous layers of the shell wall. Approximate thickness of the aragonite crystals : 300 (Figs. 8, 9, 13 and 14), 270 (Fig. 10), 300-600 (Fig. 11) and 600 millimicrons (Fig. 12).

In the fields shown in Figs. 11 and 12, the brickwork texture appears unchanged. Fig. 8 (above, left), Fig. 13 (above and centre left) and Fig. 14 (centre right) show various grades of discontinuity in portions of the interlamellar matrices, which suggests that adjacent crystals are in contact or are fused by coalescence.

Fragmentation of the crystals into globular or ovoid elements appears in Figs. 9 and 10. Note, in Fig. 13, the preserved interlamellar conchiolin sheet on the 001 facet of a tabular crystal.

PLATE VI

Figs. 15 to 17.

Nautilus pompilius LINNÉ (1047)

Fig. 15

Surface of fracture and of cleavage along the interlamellar planes obtained by lateral percussion parallel to the lamellation of the nacreous layer of the shell wall. Direct replica. Rows of rod-like ridges with the same parallel orientation in seven consecutive lamellae (001 facets of the tabular aragonite crystals) emerge on the terraces produced by the cleavage. In other fields (not shown) of the sample, orientation differs in adjacent crystals or lamellae. The grey amorphous slopes between the terraces are regions of transverse or oblique fracture of the crystals. The surfaces of fracture are subconchoidal and do not show any visible subdivision.

TEM × 24 000.

Figs. 16 and 17

In another field of the same sample, the ridges, mixed with seeds which protrude on the 001 facets of the aragonite crystals, especially in the areas of central elevation (Fig. 16) present the aspect of imbricate or of overlapping scales (Fig. 17). The white shreds in the grooves between the ridges might be intracrystalline conchiolin emerging at the surface.

TEM, Fig. 16 : × 10 000; Fig. 17 : 60 000.

PLATE VII

Figs. 18, 20 and 21

Surfaces of cleavage of mother-of-pearl along the interlamellar planes in shells of fossil cephalopods. Direct replicas. TEM.

Fig. 18

Leioceras opalinum REINECKE (ammonoid) (362-7). Jurassic, Upper Aalenian, Opalinus-Ton, Ziegelei Osterfeld, Goslar, Harz, Germany, Specimen given by Dr P. L. MAUBEUGE (Aragonite : GRANDJEAN et al., 1964).

× 9 000.

Fig. 19

Unidentified nautiloid (orthocone) (420-9). Pennsylvanian, Kendrick Shale, COW Creek, Kentucky, U. S. A. Specimen given by Prof. F. G. STEHLI (Aragonite and principal ray of calcite, 3.03 Å, very week : GRANDJEAN et al., 1964).

Surface of cleavage of the innermost portion of the nacreous layer near a septal junction. A column involving about 18 stacked crystals, is seen obliquely.

× 10 000.

Fig. 20

Placenticeras sp. (ammonoid) (1006). Cretaceous, Eutaw Formation, Menabites, Alabama, U. S. A. Specimen given by Dr Norman F. SOHL (Aragonite).
× 9000.

Fig. 21

Placenticeras sp. (ammonoid) (386) Cretaceous. Coffee Sand, Ratliff, Lee Co., Mississippi, U. S. A. Specimen given by Dr Norman F. SOHL (U. S. G. S. 17809) (Aragonite : GRANDJEAN et al., 1964).
× 9000.
In the samples shown in Figs. 18-21, the aspects of the flaggings of polygonal surfaces do not differ from those of the modern *Nautilus*. Crystal seeds are irregularly scattered on the 001 facets of the crystals. In Fig. 20, note the parallel triangular dimples on the surfaces of some crystals. Figs. 18, 20 and 21 : 9000; Fig. 19 : × 10 000.

PLATE VIII

Nautilus pompilius LINNÉ

Fig. 22

Nacreous layer of the shellwall heated in open vessels to 225 °C for 10 minutes (721-225-10) (Aragonite).
Surface of cleavage of mother-of-pearl along the interlamellar planes, parallel to the 001 facets of the aragonite crystals. The elongate oval structures, scattered in small groups of parallel elements (see right bottom portion of the field) are probably emerging ridges shown in the normal nacre in Figs. 15, 16 and 17. Rounded elements standing out in high relief (centre left, top right: asterisk) are probably crystal seeds. Comparison with the corresponding structures in control samples suggests that the pyrolytic changes might consist of inflation and coalescence of the seeds into clusters in some areas and disappearance in other regions.
TEM × 18 000.

Fig. 23

Nautilus pompilius LINNÉ

Mother-of-pearl heated in open vessels at 225 °C for 21 days (721-225-21). (Aragonite).
Cleavage of mother-of-pearl parallel to the 001 facets of the aragonite crystals. Direct replica. The exposed lamella covered by microcrystals, is incomplete, on the left half portion of the picture. The gap in this lamella exposes the surface of the preceding lamella, on which single or agglutinated microcrystals are scattered.
TEM × 48 000.

Nautilus pompilius LINNÉ

Fig. 24

Nacreous layer of the shell wall heated in open vessels at 225 °C for 21 days (721-225-21 E) (Aragonite).
Polished and etched (EDTA : 40 seconds) transverse section. Direct replica. Brickwork texture preserved. The interlamellar and intercrystalline matrices of conchiolin appear in the form of white cords. A moderate loosening of the lamellar cohesion without intervention of artifacts of replication (mechanical dislocation) is possible. Lateral coalescence of crystals from the same lamella into large tablets seems to appear in this field. Notches, square, polygonal or irregular etch-pits or etch-elevations are visible on the surfaces of transverse section of several crystals (thickness : 160-300 millimicrons).
TEM. × 36 000.

PLATE IX

Nautilus pompilius LINNÉ

Fig. 25

Nacreous layer of the shell wall heated dry in a sealed tube under argon atmosphere at 225 °C for 21 days (770). (Aragonite.)
Residues of decalcification. Nautiloid pattern recognizable in parts of the samples. Flattening, coalescence into membranes (top right) and disintegration (bottom right and left) of the trabeculae are seen. Rounded corpuscles scattered on these trabeculae are in part remains of the original protuberances.
Shadowed with platinum. TEM × 42 000.

Fig. 26

Nacreous layer of the shell wall heated in open vessels to 275 °C for 5 hours (721-275). (Aragonite).
Residues of decalcification. Nautiloid pattern recognizable. Flattening, coalescence into membranes and disintegration of the trabeculae (corpuscles) characterize the changes in the conchiolin matrices.
Shadowed with platinum. TEM × 48 000.

Fig. 27

Nacreous layer of the shell wall heated with distilled water in a sealed tube at 275 °C for 5 hours (1090). (Aragonite).
Residues of decalcification. Considerable flattening and coalescence of the trabeculae. This sample heated wet differs only by the grade in intensity from the changes in samples heated dry under the same other conditions of time and temperature (see Part I, Fig. 50).
Shadowed with platinum. TEM × 48 000.

PLATE X

Nautilus pompilius LINNÉ

Fig. 28

Nacreous layer of the shell wall heated in open vessels to 300 °C for 5 hours (904). (Aragonite).
Residues of decalcification. Dislocation of the interlamellar matrices into twisted, knobby or moderately flattened fragments of trabeculae with bulging scattered protuberances. Disintegration of these fragments into clustered rounded corpuscles (see Part I, Fig. 21). The dark, condensed, knobby trabeculae could proceed from a « central elevation area » in the interlamellar matrices.
Shadowed with platinum. TEM × 48 000.

Fig. 29

Nacreous layer of the shell wall heated dry in a sealed tube at 300 °C for 5 hours (782). (Aragonite).
Residues of decalcification. Nautiloid pattern recognizable. Flattening, coalescence (membranes) and disintegration of the trabeculae. Hemispheral protuberances are still visible on the flattened trabeculae. Other aspects of the changes are shown in Part I, Figs. 51, 52 and 53.
Shadowed with platinum. TEM × 30 000.

Fig. 30

Nacreous layer of the shell wall heated with sea water in a sealed tube at 300 °C for 5 hours (992). (Aragonite).

Residues of decalcification. Nautiloid pattern recognizable. Flattening, coalescence and moderate disintegration of the trabeculae into pebble-shaped corpuscles.

Shadowed with platinum. TEM × 48 000.

PLATE XI

Nautilus pompilius LINNÉ

Fig. 31

Nacreous layer of the shell wall heated with distilled water in a sealed tube at 300 °C for 5 hours (976). (Aragonite).

Residues of decalcification. Nautiloid pattern destroyed in this area of the preparation. Fragments of cylindrical or flattened trabeculae and of membranes of coalescence. (wedge-shaped, angulate blades and rods, corpuscles).

Shadowed with platinum. TEM × 48 000.

Figs 32 and 33

Nacreous layer of the shell wall heated with sea water in sealed tubes at 300 °C for 21 days (986). (Aragonite).

Fig. 32. Nacre polished and etched in tangential orientation, parallel to the lamellae.

Double stage replica, showing pseudoreplicas of networks of conchiolin matrices in the form of considerably flattened trabeculae, fused into membranes, enclosed in polygonal areas (crystal imprints) surrounded by remnants of intercrystalline matrices (black ribbons).

Fig. 33. Residues of decalcification. Except for a more important dislocation into corpuscles produced in the suspensions of the brittle organic material, the changes (flattening of the trabeculae and coalescence into membranes) are identical to those observed in pseudoreplicas of the same material (Fig. 32).

Shadowed with platinum. TEM × 48 000.

PLATE XII

Nautilus pompilius LINNÉ

Figs 34 - 37

Nacreous layer of the shell wall heated with distiller water in sealed tubes at 300 °C for 5 hours (1013). (Aragonite).

Transverse fracture of the shell wall. The changes produced by pyrolysis in the stacks of crystals disposed in parallel columns (Fig. 35) consist of inflation and coalescence into blocks composed of two or more superposed crystals (Fig. 36).

Fig. 34 shows the beginning of formation of four foliate aggregates, 28-35 microns in height, located in the mineral sheet at the left of Fig. 37 (asterisk). These aggregates were formed by fragmentation of the sample and separation of groups of parallel columns of crystals. Displacement of the two inferior groups has changed their orientation regarding the two upper groups.

Fig. 37. Great differences in the reaction of the nacre to pyrolysis were frequently observed in closely adjacent regions of a sample : in one (right hand side) of three parallel mineral sheets of cleavage with straight boundaries spontaneously developed during pyrolysis, the original texture (lamellation) is shown in close contiguity to foliate aggregates forming mosaics of blocks in the same sheet.

SEM (STEREOSCAN). Fig. 34 : × 1 440; Fig. 35 : × 1 500; Fig. 36 : × 2 400; Fig. 37 : × 288.

PLATE XIII

Nautilus pompilius LINNÉ

Fig. 38

Sample heated with sea water in a sealed tube at 300 °C for 21 days (986). (Aragonite).

Transverse fracture. This field shows parts of three mineral sheets composed of mosaics of foliate aggregates. These aggregates differently oriented, consist of agglutinated parallel fragments of lamellae which give them a highly stratified appearance. The pits (in black) scattered all over the aggregates are the traces of the intercrystalline spaces in the lamellae.

SEM (STEREOSCAN) × 935.

Fig. 39

Sample heated with distilled water in a sealed tube at 300 °C for 5 hours (976). (Aragonite).

Transverse fracture of the shell wall. Direct replica. The picture shows various grades of coalescence in groups of contiguous crystals in the same column and in the same lamella (lateral coalescence). The holes visible on the surfaces of transverse section of the fused crystals are the remnants of the original interlamellar and intercrystalline spaces. In the regions of crystal coalescence, the organic structures are no more visible.

TEM Fig. 41 : × 18 000.

PLATE XIV

Figs 40 and 42

Ammonites lineatus penicillatus (785). Middle Jurassic, Brauner Jura, Gammelshausen bei Boll, Württemberg, Germany. Specimens given by Prof. O. H. SCHINDEWOLF, Prof. Ad. SEILACHER and Dr Fr. WESTPHAL. (Aragonite and calcite).

Transverse fracture of the shell wall. Direct replicas.

Fig. 40. This picture shows different grades of transformation by coalescence and recrystallization of original columnar stacks of aragonite crystals into columns of blocks involving varying numbers of superposed crystals. In the two columns running obliquely from top left to bottom right of the picture, irregular crystals with subhedral facets are fused fragments of superposed crystals. In the centre right of the picture, below a single tabular crystal, four crystals fused together form a block in which the interlamellar spaces are still faintly visible. Stacks of original aragonite crystals in the process of coalescence are shown in the bottom right region of the picture (asterisk).

TEM × 12 000.

Fig. 42. In this region, the original columns of crystals have been transformed into parallel rows of polyhedral subhedral or euhedral crystals (1-3 microns) with plane facets, seen running obliquely from left to right of the picture.

TEM × 9 000.

Fig. 41

Placenticeras sp. (ammonoid). Cretaceous, Coffee Sand, Mississippi. Specimen supplied by Dr Norman F. SOHL (U. S. G. S. 17809 & 25483) (1006) (Aragonite).

Transverse fracture of the shell wall. Direct replica. In this field columns of tabular crystals, 0.20-0.25 microns thick, have fused by coalescence into superposed blocks.

TEM × 24 000.

PLATE XV

Fig. 43

Psiloceras planorbis (J. de C. SOWERBY) (Ammonoid). Jurassic, Lower Lias, Planorbis zone range. Hettangian, Probably from Watchet, Somerset coast, England (988). (Aragonite).

Transverse fracture of the nacreous layer of the shell wall. The picture shows different stages in the process of coalescence and recrystallization of the original tabular crystals of aragonite. The original texture is recognizable in some areas (bottom left). Top right : about ten stacked crystals have completely fused into an anhedral-subhedral block (2.4 microns) in which all trace of the original lamellation has disappeared. On the left part of the flat subhedral facet visible on the surface of this block, thin parallel lines suggest the presence in this block of a system of cleavage unrelated to the original crystalline orientation. Centre left : another block (1.7 microns) formed similarly by fusion of several crystals presents also cleavage lines. Bottom centre : in the right portion of this block six or seven superposed crystals are still visible. In the left portion of the same block, these crystals have fused into a polyhedral, subhedral structure. Bottom right : no trace of the original lamellation remains in this polyhedral, subhedral or euhedral structure.

TEM × 21 000.

PLATE XVI

Nautilus pompilius LINNÉ

Figs 44 and 45

Samples of nacre heated in open vessels at 325 °C for 5 hours (1041) (Aragonite).

Residues of decalcification. Two aspects of the pyrolysed conchiolin matrices are seen : fragments of flattened trabeculae and of membranes formed by coalescence of the trabeculae (Fig. 44), general disintegration into corpuscles of small size (Fig. 45).

Shadowed with platinum. TEM. Fig. 44 : × 48 000; Fig. 45 : × 48 000.

Figs 46 and 47

Sample of nacre heated with distilled water in sealed tubes at 325 °C for 5 hours (1044) (calcite).

Residues of decalcification. Fig. 46 shows a portion of the interlamellar conchiolin matrices composed of polygonal areas, which outline the original mosaic of tabular crystals of aragonite. Within these areas, the pyrolysed conchiolin matrices consist of membranes and of fragments of contorted wedge-shaped, angulate, flat ribbons formed by fragmentation of the flattened and fused original trabeculae. Fig. 47 is a picture at higher magnification of the membranes and of their fragments, which seem to have a thin laminated structure visible at their broken edges.

Shadowed with platinum. TEM. Fig. 46 : × 18 000; Fig. 47 : × 48 000.

PLATE XVII

Nautilus pompilius LINNÉ

Fig. 48

Samples heated in open vessels at 325 °C for 5 hours (1041). (Aragonite).

Transverse fracture. Columns of crystals.

SEM (STEREOSCAN) (20 KV) × 2550.

Figs 49, 50, 51 and 52

Samples heated with distilled water in sealed tubes at 325 °C for 5 hours (1044). (Calcite).

In Fig. 49, except for changes in scattered crystals (inflation, coalescence into blocks, fragmentation) the texture does not greatly differ from that shown in Fig. 48.
SEM (STEREOSCAN) (20kV) × 2600.

Fig. 50. shows foliate aggregates differently oriented, composed of inflated, superposed, parallel fragments of lamellae (size of the central spheroidal aggregate : 47 microns). Bottom right : in a fragment of lamella seen in tangential orientation, pits are the relics of the intercrystalline spaces between fused crystals.
SEM (STEREOSCAN) (15 kV) × 1370.

Figs. 51 and 52

Surfaces of cleavage of the nacre along the interlamellar planes (001 facets of the original tabular crystals of aragonite). The mosaic of polygonal tabular surfaces has disappeared and has been replaced by another mosaic of interlocked, smooth-edged, irregularly rounded or elongate structures, some grouped into bundles. Rounded or polygonal patterns of decoration are scattered on these surfaces.
TEM. Fig. 51 : × 6000; Fig. 52 : × 11400.

PLATE XVIII

Nautilus pompilius LINNÉ

Figs 53, 54, 55 and 56

Samples heated in open vessels to 350 °C for 5 hours (1042). (Aragonite).

Fig. 53. Transverse fracture. Original microtexture. Parallel columns of crystals.
SEM (STEREOSCAN); × 2600.

Fig. 54. Cleavage of the sample along the lamellar planes followed by etching (EDTA, ph 4.0, 54 minutes). Direct replica. Square or polygonal elevations stand out in relief on to the surfaces of a tabular crystal still included in the polygonal flagging. Parallel ridges are faintly visible on the background.
TEM. × 15 000.

Fig. 55. Surface of cleavage of the sample along an interlamellar plane. Direct replica. Rounded microcrystals (50-200 millimicrons) appear on the crystal surface and are especially clustered in the « areas of the central elevations ».
TEM × 30 000.

Fig. 56. Large, rounded, polygonal, tabular crystals (3-5 microns) have been detached from a surface of cleavage of the nacreous layer etched by EDTA (pH 4.0, 54 minutes). Direct replica. The crystals appear perforated by polygonal holes. Identical changes were observed (unpublished) on the 001 crystal facets, on tangential cleavage surfaces, in an australian specimen of the Miocene nautiloid. *Eutrephoceras balcombensis*. Free black shreds (asterisks) anchored to the edges of perforations are the covers of protruding structures detached during preparation of the replicas and leaving perforations (artifacts).
TEM. × 15 000.

PLATE XIX

Nautilus pompilius LINNÉ

Samples heated with distilled water in sealed tubes at 350 °C for 5 hours (1045). (Calcite).

Fig. 57. In this surface of transverse fracture, the pyrolytic changes in the brickwork texture consist of fragmentation and inflation of crystals, coalescence of columns of crystals involving varying numbers of superposed elements, and of formation of foliate aggregates (top right, bottom centre).

SEM (STEREOSCAN); (20 kV) × 3 100.

Fig. 58. Direct replica of a surface of cleavage parallel to the lamellation. A large subhedral crystal or a group of agglutinated crystals associated into a complex polyhedral structure appear in the mosaic of smaller crystals developed by transformation (possibly fragmentation) of the original tabular crystals.

TEM : × 14 000.

Fig. 59. Residues of decalcification of the nacreous layer. Fragments of membranes formed by coalescence of flattened trabeculae.
TEM. × 48 000.

Fig. 60.

Surface of cleavage along the interlamellar planes. Direct replica. The picture shows the changes in the original mosaics of tabular crystals. These changes consist probably of fragmentation into smaller crystalline elements, and of coalescence of these elements into this loose mosaic of groups of fused crystals.

TEM × 8000.

PLATE XX

Nautilus pompilius LINNÉ

Fig. 61

Sample heated in open vessels at 375 °C for 5 hours (1043). (Calcite).
The changes in the brown conchiolin shreds left by decalcification of the sample consist predominantly of disintegration of the trabeculae of the matrices into pebble-shaped corpuscles.
Shadowed with platinum. TEM × 48 000.

Fig. 62

Sample heated with distilled water in a sealed tube at 375 °C for 5 hours (1046). (Calcite).
One of the aspects (see Figs. 63, 64 and 65) of the interlamellar conchiolin remnants of decalcification, in the form of a loose network of flattened trabeculae. The broad, irregularly rounded or oval openings in the considerably widened original fenestration are surrounded by thickenings in the form of cylindrical pads.
The conchiolin fragment shown in this field could be a portion of the interlamellar matrices located in the « central elevations areas ».
TEM × 48 000.

PLATE XXI

Nautilus pompilius LINNÉ

Figs 63, 64 and 65

Sample heated with distilled water in sealed tubes at 375 °C for 5 hours (1046). (Calcite).
Residues of decalcification. In Fig. 63, intercrystalline conchiolin in the form of opaque cords delimits five polygonal areas (crystal imprints) in which the interlamellar conchilin matrices have been transformed into membranes. In these membranes, the relics of the original fenestration appear in the form of rounded or oval holes encircled by ring-shaped, thick pads (Figs. 63 and 65).
Fig. 64. Fragments of a continuous membrane adhering to the periphery of a polygonal area, delimited by opaque cords (intercrystalline conchiolin). The central portion of this area corresponding to the « areas of central elevations » is empty.
Shadowed with platinum : TEM. Fig. 63 : 11 400; Fig. 64 : × 18 000; Fig. 65 : × 48 000.

PLATE XXII

Nautilus pompilius LINNÉ

Figs 66, 67 and 68

Sample heated in open vessels at 375 °C for 5 hours (1043). (Calcite).
Fig. 66 : Transverse fracture. Lamellation preserved. Changes (local inflation, coalescence, fragmentation) appear in scattered groups of crystals.
SEM (STEREOSCAN) (20 kV) × 2700.

Figs 67 and 68

Surfaces of cleavage and of fracture exposing several lamellae. In these lamellae, the original tabular crystals of aragonite seem to have been fragmented into mosaics of smaller, tightly interlocked crystals. Fig. 68 is a TEM micrograph of a foliate aggregate composed of about five agglutinated fragments of lamellae, which display the same mosaics of interlocked crystals as those shown in Fig. 67. Compare with the foliate aggregates shown in SEM (Figs. 38, 50, 84, 85, 98.) Fig. 67 : 8000; Fig. 68 : × 21 000.

PLATE XXIII

Nautilus pompilius LINNÉ

Figs 69, 70, 71 and 72

Sample heated with distilled water in sealed tubes at 375 °C for 5 hours (1046). (Calcite).
Fig. 69. Transverse fracture. The lamellation and the columnar stacking of crystals are preserved. Efflorescences of diverging blades (top) developed on the rough surface of the sample.
SEM (STEREOSCAN). × 2700.
Fig. 70. Transverse fracture. Direct replica. Fragmentation and inflation of superposed crystals belonging to four consecutive lamellae.
TEM. × 20 000.
Figs. 71 and 72. Cleavage along the interlamellar planes. On the surface of the lamellae, scattered groups of polyhedral, subhedral and euhedral crystals (Figs. 72) and elongate acicular parallel blades (Fig. 71) were found in the mosaics of flat crystals.
TEM × 8 000.

PLATE XXIV

Figs 73, 74 and 75

Ludwigia murchisonae (ammonite) (836) Lower Jurassic, Lias, Lower Oolith, Dorset, England (Calcite).
Surfaces of transverse fracture of the recrystallized nacreous layer of the shell wall. The textures shown in three differents fields consist of mosaics of interlocked blocks with parallel cleavage striations, differing in orientation in the contiguous blocks. The arrangement of these blocks resemble that of the foliate aggregates obtained experimentally (compare with Figs. 38, 50, 84, 85). In the inferior left portion of Fig. 75, a surface of cleavage viewed tangentially exhibits the same perforations as those representing the relics of intercrystalline spaces in experimental material. See Fig. 50).
SEM (STEREOSCAN), Fig. 73 : × 1088; Fig. 74 : × 700; Fig. 75 : × 670.

PLATE XXV

Fig. 76

Hildoceras sp. (ammonoid) (1008). Jurassic, Lower Lias, Lyme Regis, Dorset, England. (Calcite).

Transverse fracture of the recrystallized nacreous layer of the shell wall composed of blocks, displaying parallel lamellation, differently oriented in contiguous blocks.
SEM (STEREOSCAN) (20 kV) × 500.

Figs 77 and 78

Domatoceras or *Stearoceras* sp. (nautiloid) (422). Permian, San Andres Limestone. Rio Penasco River, East of Alamogordo, New Mexico, U. S. A. (Calcite).
Recrystallized nacreous layer of the shell wall. Transverse fracture. Direct replica.
Fig. 77. A thin lamellation, differently oriented in contiguous structures, appears in the blocks forming the mosaic of recrystallization.
Fig. 78. The three parallel linear shallow grooves and ridges which run obliquely across the field without interruption through crystals could be the traces of planes of cleavage into mineral sheets similar to those developed spontaneously in the experimental material (see Figs. 84, 85, 98 and 99). As in the foliate aggregates obtained experimentally, the material within the limits of these parallel lines consists of groups of parallel mineral sheets forming crystalline blocks differently oriented.
SEM (STEREOSCAN) Fig. 77 : × 1400; Fig. 78 : × 1920.

PLATE XXVI

Nautilus pompilius LINNÉ

Figs 79 and 81

Samples heated in open vessels at 400 °C for 5 hours (721-400-2) (Calcite).
Fig. 79. Double-stage replica of a polished and etched surface of cleavage along the interlamellar planes. In agreement with the results obtained by other methods (see Part I, Fig. 22), the pseudoreplicas of the remnants of the conchiolin interlamellar matrices consist of rounded corpuscles of varying sizes produced by fragmentation of the trabeculae. In this field, the debris seem to be preserved in three strips corresponding to widened trabeculae, and not to have been dispersed at random as in Fig. 22, Part I.
TEM × 48 000.
Fig. 81. This direct replica of an unetched surface of cleavage along the interlamellar planes suggests the fragmentation without dislocation of the original polygonal tabular crystals (surrounded by thin black shreds on the picture) into mosaics or tightly interlocked smaller crystals.
TEM × 6000.

Fig. 80

Samples heated with sea water in sealed tubes at 400 °C for 5 hours (975). (Calcite).
Conchiolin residues of decalcified samples in the form of angulate blades, fragments of membranes, and corpuscles.
Comparison with samples heated dry (see Part I; Figs. 55 and 56) does not reveal any distinct difference between dry and wet heating as regards the changes in the organic matrices in sealed tubes. On the other hand, comparison of Figs. 79 and 80 confirms former observations that pyrolysis of nacre in open vessels alters the conchiolin matrices differently than dry and wet heating in sealed tubes.
Shadowed with platinum. TEM × 48 000.

Figs 82 and 83

Samples heated dry in sealed tubes at 400 °C for 30 minutes (Fig. 82) and 60 minutes (Fig. 83).
Direct replica of surfaces of cleavage along the lamellation. The original polygonal surfaces of the lamellar planes have been replaced by mosaics of small crystals (Fig. 82), of bundles or rows, differently oriented, of parallel crystals, fragments of crystals, or by single elongated crystals (Fig. 83). An arrangement resembling an enfacial junction

(BATHURST, 1964), a texture rarely found in the materials recrystallized in situ, is shown in the centre of Fig. 83.

TEM. Fig. 82 : × 6000; Fig. 83 : × 12 000.

PLATE XXVII

Nautilus pompilius LINNÉ

Figs 84 and 85

Samples heated with sea water in sealed tubes at 400 °C for 5 hours (975) (Calcite). Transverse fracture. Mosaics of foliate aggregates disposed at random within three mineral sheets of cleavage are shown. The components of these foliate aggregates seem to be inflated and more loosely agglutinated than in similar preparations of the material pyrolysed at 300 °C (See Fig. 37). The traces, in the form of holes, of the original intercrystalline spaces in the lamellae, enlarged during the first steps of pyrolysis, are especially well visible in this preparation.

SEM (STEREOSCAN) (20 kV). Fig. 84 : × 2240; Fig. 85 : × 2128.

PLATE XXVIII

Fig. 86

Nautilus pompilius LINNÉ

Sample heated dry under argon atmosphere in a sealed tube. Explosion of the tube after 5 minutes during preheating to 500 °C (771) Aragonite).

Double-stage replica of a fragment polished along the lamellation and etched (EDTA, pH 7.5, 11 minutes). The interlamellar conchiolin matrices are shown in the form of pseudoreplicas. The pyrolytic changes in the structure of these matrices in two polygonal areas (crystal imprints) consist of loosening of the network, flattening, widening and coalescence of the trabeculae with preservation of a part of the fenestration (See also Fig. 88).

Shadowed with platinum. TEM. × 24 000.

Fig. 87

Collignoniceras sp. (433). Cretaceous, Gulfian, Blue Hills Shale Member, Carlile Shale, Smith Co, Kansas (Kansas Geological Survey, 10540). Specimen supplied by Prof. Raymond C. MOORE. (Aragonite : GRANDJEAN et al., 1964).

Nacreous layer of the shell wall. Same method of preparation as in Fig. 86.

The changes produced by diagenesis in the structure of the conchiolin matrices (seen in this preparation in the form of pseudoreplicas) consist of loosening of the network, flattening and coalescence of the trabeculae, persistance of fenestration) and are identical to those obtained experimentally (see Fig. 86).

TEM × 24 000.

PLATE XXIX

Nautilus pompilius LINNÉ

Figs 88 and 91

Sample heated dry in a sealed tube. Explosion after 5 minutes during preheating to 500 °C (771) (Aragonite).

Double-stage replica of a polished and etched (EDTA, pH 7.5, 11 minutes) tangential section of the nacreous layer of the shell wall. The pseudoreplicas of the pyrolysed

interlamellar conchiolin matrices appear in the form of loose networks of considerably flattened and widened trabeculae, enclosed within polygonal fields and located especially at their periphery. These polygonal fields are delimited by intercrystalline conchiolin in the form of white threads. As shown in Fig. 91, the « areas of central elevations » are empty (see also Fig. 86).

TEM. Fig. 88 : × 42 000; Fig. 91 : × 18 000.

Fig. 89

Samples heated with sea water in sealed tubes at 500 °C for 5 hours (994) (Calcite). One of the aspects of the alterations in the conchiolin remnants in the form of substantial membranes surrounded by debris of the intercrystalline conchiolin.

Shadowed with platinum. TEM. × 36000.

Fig. 90

Samples heated with distilled water in sealed tubes at 500 °C for 5 hours (1014). Calcite).

Conchiolin remnants of decalcification in the form of fenestrate membranes. Identical structures with openings surrounded by thickenings in the form of pads were observed previously in the samples heated dry in sealed tubes at 800 °C (see Part I, Figs. 78, 79, 80, 85).

Shadowed with platinum. TEM × 48000.

PLATE XXX

Nautilus pompilius LINNÉ

Fig. 92

Sample heated dry in sealed tubes. Explosion after 5 minutes during preheating to 500 °C (771). (Aragonite).

Direct replica of polished and etched (EDTA, pH 7.5, 60 seconds) transverse sections of the nacreous layer of the shell wall. Brickwork microtexture preserved (300 millimicrons thick crystals). The interlamellar conchiolin appears in the form of rounded flat nodules and fragments of ribbons (grey-white). Etch figures in crystals consist of rounded polygonal or square pits and notches (see discussion), similar to those recorded on the 001 facets of the crystals in other samples (see Figs. 24 and 56).

TEM. × 48 000.

PLATE XXXI

Nautilus pompilius LINNÉ

Figs 93, 95, 95a, 96 and 97

Samples heated in open vessels at 500 °C for 5 hours (721-500-3) (Figs. 93, 95 and 96) and for 10 minutes (preheating time : 2 minutes 30 seconds) (721-500-10) (Fig. 96). (Calcite).

Fig. 93. Direct replica of a transverse, polished and etched (EDTA, 60 seconds) section of the nacreous layer.

The brickwork texture has been exceptionally preserved in this region of the sample. Degradation in the conchiolin cement has produced dislocation into free crystals. These crystals have retained the aspect of the original tabular crystals. Similar gaps between the crystals have been observed by HUDSON (1968) in the Middle Jurassic *Mytilus (Praemytilus) strathairdensis*. The organic remnants appear in this field in the form of scarce white shreds in the interlamellar spaces (centre and bottom right). As in the sample heated in sealed tubes for 5 minutes (Fig. 92) square notches, pits and elevations appear on the surfaces of transverse fracture of the crystals (see also Figs. 24, 56 and 95).

Figs. 95 and 95a. show a crystal remained attached (pseudoreplica) to the replicas of two other crystals and its electron diffraction pattern (Aragonite and a very weak, unidentified ray).

TEM. Fig. 93 : × 48 000; Fig. 95 : × 40 000; Fig. 95a : × 20 000.

Fig. 97. Elongated, girdle- and needle-like crystals erected at different angles on the surfaces of spontaneous cleavage of the lamellae during pyrolysis. Similar structures developed in samples heated in open vessels at 500 °C for 10 minutes (Fig. 96).

SEM (STEREOSCAN) (20 kV) Fig. 97 : × 1500; Fig. 96 : × 1075.

Fig. 94

Sample heated dry in sealed tubes. Explosion after 5 minutes during preheating to 500 °C (771) (Aragonite).

Direct replica of a surface of tangential cleavage of the nacreous layer along the plane of lamellation. Etching with EDTA (pH. 7.5 for 17 minutes). Polygonal etch elevations stand out in relief on the 001 facets ot the aragonite crystals.

TEM × 10 000.

PLATE XXXII

Nautilus pompilius LINNÉ

Figs. 98 and 99

Samples heated with sea water in sealed tubes at 500 °C for 5 hours (979) (Calcite).

Transverse fracture. Mineral sheets of cleavage of varying thickness (5-8 microns in Fig. 99), produced spontaneously during pyrolysis, consist, as in the samples of the preceding stages, heated to lower temperature (Figs. 24, 38, 50, 84 and 85), of foliate aggregates, made up of agglutinated parallel fragments of lamellae differently oriented in the adjacent aggregates. In contrast with the similar structures in the samples of those stages, the crystals constituting the parallel lamellar sheets appear distinctly inflated into rounded elements and bulge over the surfaces. Holes separating these crystals are remains of the intercrystalline spaces. In Fig. 99, the lateral surfaces of cleavage appear in the form of pavements of cobblestones. The textures shown in Figs. 98 and 99 resemble that of lime after slagging in oxygen converters, as reported by OBST and al. (1969, Fig. 3b).

SEM (STEREOSCAN) (20 kV). Fig. 98 : × 2100; Fig. 99 : × 2700.

Fig. 100

Samples heated in open vessels at 500 °C for 5 hours (721-500-3) (Calcite).

Direct replica of cleavage surface along the lamellation displaying the TEM aspect of the surfaces of cleavage shown in SEM in Fig. 99. The original flagging of polygonal tabular crystals has been replaced by a mosaic of small, interlocked, irregularly rounded crystals. Traces of subdivision without dislocation appear on larger crystals scattered among the small elements. Comparison of Figs. 99 and 100 reveals that the crystals involved in the mosaic of flat surfaces shown in Fig. 100 are oriented at random.

TEM : × 6000.

PLATE XXXIII

Fig. 101

Ammonites lineatus penicillatus (785). Jurassic, Brauner Jura, Gammelshausen bei Boll, Württemberg. (Aragonite and calcite).

Surface of transverse fracture of the nacreous layer of the shell wall. Direct replica. A portion of the layer in which the original texture, observed in several other regions of the samples, (see Fig. 13), has been replaced by a mosaic of loosely interlocked, polyhedral subhedral crystals (1.5-4 microns) with one or several flat smooth polygonal facets. In this field, parallel cleavage striations have the same orientation in three contiguous crystals. Compare with Fig. 102.

TEM. × 15 000.

Nautilus pompilius LINNÉ

Fig. 102

Sample heated in an open vessel at 500 °C for 5 hours (721-500-3). (Calcite).

Direct replica of a polished and etched (EDTA, pH 7.5, 10 seconds) transverse section of the nacreous layer of the shell wall. As in the fossil sample shown in Fig. 101, the original mineral texture has been replaced by a mosaic of polyhedral crystals (3-4 microns) showing a parallel lamellation. In contrast with the preparation of Fig. 101, orientation of the parallel striations differs in some contiguous crystals.

TEM. × 18 000.

PLATE XXXIV

Nautilus pompilius LINNÉ

Figs 103, 104, 105

Samples heated with sea water in sealed tubes at 600 °C for 5 hours (995) (Calcite).

Fig. 103

Needle-shaped crystals resembling whiskers, pincushioned on the lateral surface of mineral sheets of cleavage.

SEM (STEREOSCAN) (20 kV). × 1420.

Figs 104 and 105

The organic ghosts left by decalcification of the needle-like structures shown in Fig. 103 appear after desiccation on the grids in the form of a double, fenestrate membrane resembling a collapsed sheath. The rectangular holes forming the fenestration are oriented in parallel rows. Some of these holes are surrounded, as shown in Fig. 105, by thickenings in the form of pads.

TEM. Fig. 104 : × 21 000; Fig. 105 (shadowed with platinum) : 72 000.

Figs 106 and 107

Samples heated dry in sealed tubes at 600 °C for 5 hours (779) (Calcite).

Fig. 106. Interlamellar conchiolin matrix from the decalcified sample, in the form of fenestrate membranes with pads surrounding the holes (see also Part I, Figs. 75, 76).

TEM. × 42 000.

Fig. 107. Double stage replica of a polished and etched (EDTA, pH. 7.5, 2 minutes) surface of cleavage along the lamellation.

Pseudoreplicas of interlamellar matrices form polygonal areas in which flattened trabeculae and membranes of coalescence have been broken into angulate blades and fragments of ribbons.

TEM. × 18 000.

PLATE XXXV

Nautilus pompilius LINNÉ

Samples heated dry in sealed tubes at 600 °C for 30 minutes (Fig. 108 : 814) for 60 minutes (Fig. 109 : 815), for 5 hours (Fig. 111 : 779), heated with sea water in sealed tubes at 600 °C for 5 hours (Fig. 110 : 995) and at 700 °C for 5 hours (Fig. 112 : 996). (Calcite).

Direct replicas (except Fig. 111) of tangential surfaces of cleavage of the nacre along the lamellation.

The original polygonal tabular crystal facets have been replaced, possibly by a process of fragmentation (Fig. 109) by mosaics of small, loosely interlocked crystals (Fig. 108)

or by mosaics of larger polyhedral, anhedral (Fig. 110) or bulging, dome-shaped crystals (Fig. 112). Small euhedral crystals differing by their aspect from the other elements are scattered among the other crystals of the mosaics (Fig. 108, centre).

Fig. 111 shows lateral surfaces of cleavage in which the lamellation has not disappeared. The mosaics of small crystals shown in Figs. 108 and 109 appear in this field agglutinated into large flat mineral sheets.

TEM. Figs. 108, 109, 110 and 112 : × 6000. SEM (STEREOSCAN). Fig. 111 : × 2050.

PLATE XXXVI

Nautilus pompilius LINNÉ

Figs 113, 114 and 115

Samples heated with sea water in sealed tubes at 700 °C for 5 hours (996, 981) (Calcite).

The remnants of the interlamellar conchiolin material left by decalcification consist of granular (Fig. 113) and of perforated membranes (Fig. 115) on which rows of dense corpuscles delimiting polygonal areas (crystals imprints) are remnants of intercrystalline conchiolin (Fig. 113).

Fig. 114 shows a conchiolin membrane on which rows of rounded corpuscles are aligned, forming parallel, straight cylindrical rod-like structures.

TEM. Fig. 113 : × 36 000; Fig. 114 : × 48 000; Fig. 115 : × 48 000.

PLATE XXXVII

Nautilus pompilius LINNÉ

Figs 116, 117 and 118

Samples heated in open vessels at 700 °C for 60 minutes (Figs. 116 and 117 : 807) and with sea water in sealed tubes for 5 hours (Fig. 118 : 996) (Calcite).

Surfaces of transverse fracture. The foliate aggregates observed in the material of the preceding stages heated at lower temperatures (300 °C — 600 °C) (Figs. 38, 50, 84 and 85) have been replaced by mosaics of tightly interlocked (except in the regions of accidental ejections during preparation of the samples), smooth-edged, polyhedral blocks (14-22 microns) characterized by a great number of contact surfaces (Fig. 118). Cleavage striations appearing on the surface of fracture of the coarse polyhedral structures (upper right hand corners of Figs. 116 and 117) reveal that these blocks are still composed of lamellae, as are the foliate aggregates from which they derived and that these lamellae have fused, probably by an increase in the process of coalescence and condensation with elevation in temperature. The smaller crystals result probably from fragmentation of foliate aggregates followed by a similar process of coalescence of their lamellar components. The changes in the mineral components do not distinctly differ in dry (Figs. 116 and 117) and wet (Fig. 118) heated samples.

SEM (STEREOSCAN) (20 kV) Fig. 116 : × 3600; Fig. 117 : × 1700; Fig. 118 : × 600.

PLATE XXXVIII

Nautilus pompilius LINNÉ

Figs 119 to 123

Samples heated with sea water in sealed tubes at 700 °C for 5 hours (996).

Surfaces of transverse fracture. In Fig. 119, a mineral sheet of cleavage appears to be composed of a mosaic, resembling the section of a coarse ragstone wall, of

smooth-edged, anhedral, interlocked, irregularly shaped crystals. On the lateral surfaces of cleavage of this sheet, resembling pavements of cobblestones (Figs. 119 and 123) anhedral crystals show dome-shaped, bulging facets (see Fig. 112 : TEM record). Similar mosaics in the form of pavements characterize the rocks which have been subjected to thermal stress (FISCHER & al., 1967). Each crystal shows several irregularly polygonal contact surfaces. These surfaces are concave or convex, and are perforated by hemispheric or elongated pits (Figs. 120, 121 and 122).

SEM (STEREOSCAN) (20 kV). Fig. 119 : × 827; Fig. 120 : × 850; Fig. 121 :× 1000; Fig. 122 : × 600; Fig. 123 : × 1000.

PLATE XXXIX

Nautilus pompilius LINNE

Figs 124, 125 and 126

Samples heated with sea water in sealed tubes at 800 °C for 5 hours (978) (Calcite).

The changes produced in the conchiolin matrices by heating of the samples with sea water did not differ from those obtained by dry pyrolysis (see in Part I, Figs. 78 to 85) : loose networks of flattened trabeculae (Figs. 124 and 125), rounded corpuscles agglutinated into membranes (Fig. 126). As shown in Figs. 124 and 125, these remnants of conchiolin form frequently assemblages with polygonal outlines, as if they were casts of the conchiolin matrices compressed between subhedral or euhedral facets of the polyhedral crystals shown in the plates XXXVII and XXXVIII.

TEM. Fig. 124 : × 24 000; Fig. 125 : 57 000; Fig. 126 : 48 000.

PLATE XL

Nautilus pompilius LINNE

Fig. 127

Sample heated dry in sealed tubes at 800 °C for 30 minutes (817) (Calcite).

Direct replica of a surface of transverse fracture of the nacreous layer.

Small euhedral crystals (700-1700 millimicrons) with cleavage patterns are scattered along the boundaries of large crystals (See Fig. 112). These crystals and other much smaller (50-300 millimicrons) pebble-shaped crystals are embedded in substantial amounts of organic substance (white) forming a loose network. Parallel oriented elongate seed-like elevations are scattered on the facets of the large crystals.

TEM. × 9000.

PLATE XLI

Figs 128 and 130

Sample heated dry in sealed tubes at 800 °C for 30 minutes (817) (Calcite).

Surface of transverse fracture of the nacreous layer. In this field, a spontaneous cleavage of the samples into eight parallel mineral sheets is shown. These sheets, resembling walls of ragstones, are composed of one or more layers of interlocked, polyhedral, subhedral crystals (about 20-25 microns in Fig. 128), with slightly convex and concave contact surfaces which also appear on the lateral cleavage surfaces of the sheets. In Fig. 130, conchiolin remnants assembled in structures with geometrical outlines shown in Figs. 124 and 125 are visible on the crystal facets exposed by transverse fracture of the mineral sheets (centre left).

Fig. 129

Samples heated with sea water in sealed tubes at 800 °C for 5 hours (978) (Calcite).

A mosaic of smooth-edged or rounded crystals with slightly convex and concave facets characterizes the cleavage surfaces in these samples. This aspect does not distinctly differ from that observed on the cleavage surfaces of the dry heated samples (Fig. 128).

SEM (STEREOSCAN) (20 kV); Fig. 128 : × 432; Fig. 129 : × 600; Fig. 130 : × 680.

PLATE XLII

Nautilus pompilius LINNÉ

Figs 131, 132 and 133

Samples heated dry in sealed tubes at 900 °C for 5 hours (805) (Calcite).

Surfaces of transverse fracture (Figs. 131 and 133) and of lateral cleavage (Fig. 132). As in the 800 °C samples, the fragments of nacre have been spontaneously cleaved during pyrolysis into mineral sheets composed of mosaics of interlocked crystals. In contrast with the alterations observed in the 800 °C samples (Plate XLI), several crystals show signs of coalescence. Their exposed facets, on which decoration patterns are visible, are flat, perforated by deep hemispheral holes, several of them located at the intersection of the crystal facets. In Fig. 132, the polyhedral crystals shown in Figs. 131 and 133 appear on the cleavage surfaces in the form of mosaics of flat polygonal areas. Two elongate rounded tablets (right portion of the picture) are probably fused crystals.

SEM (STEREOSCAN) (20 kV), Fig. 131 : × 388; Fig. 132 : × 250; Fig. 133 : × 620.

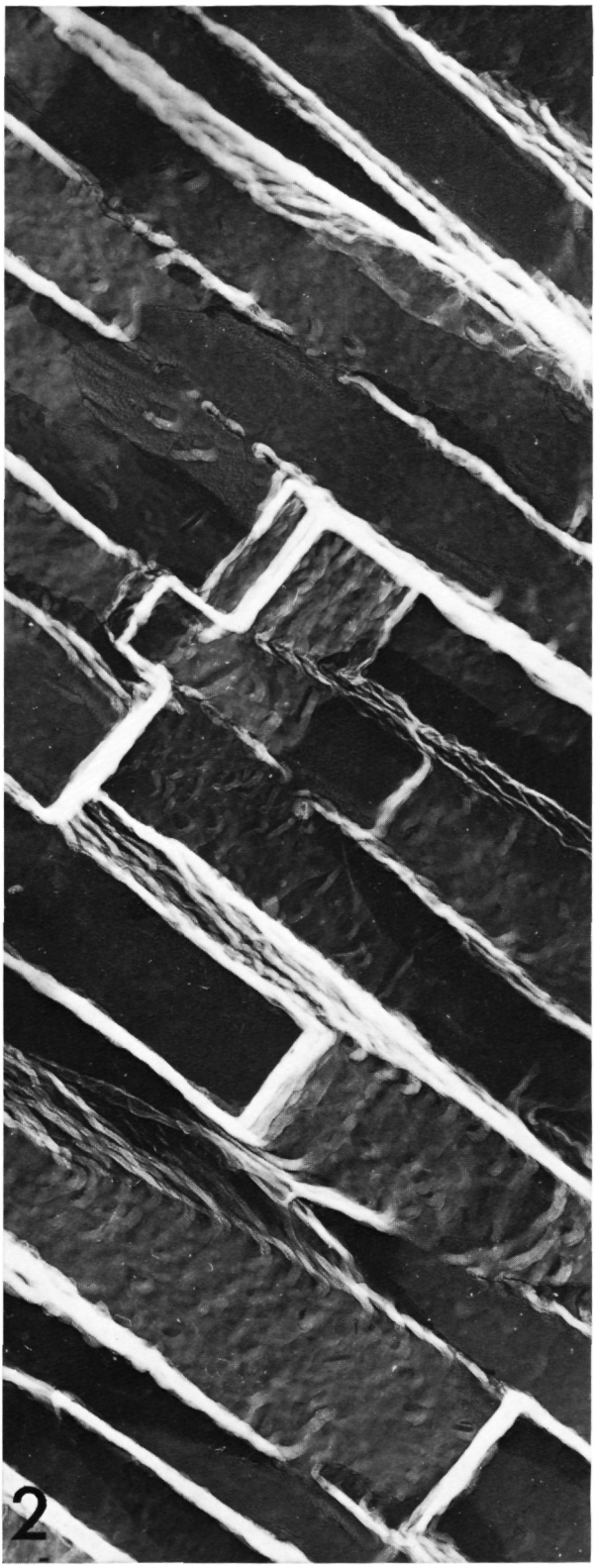

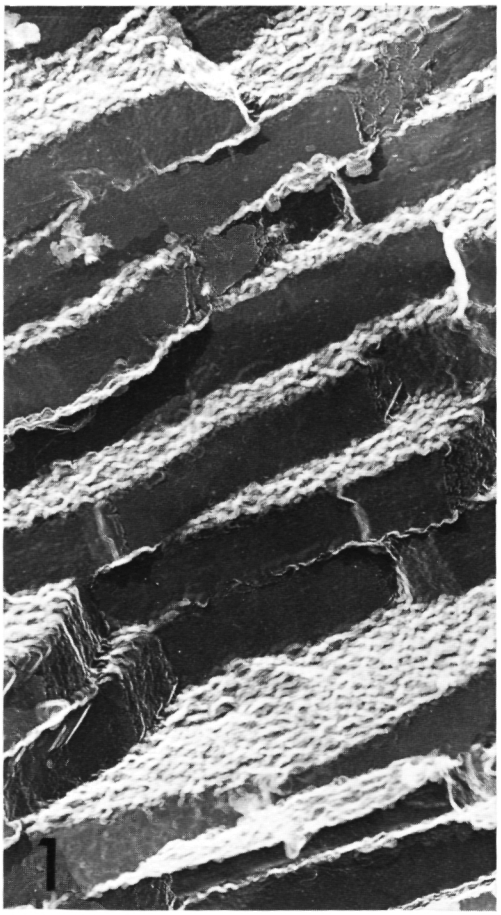

Ch. GREGOIRE. — Experimental alteration of the Nautilus shell.

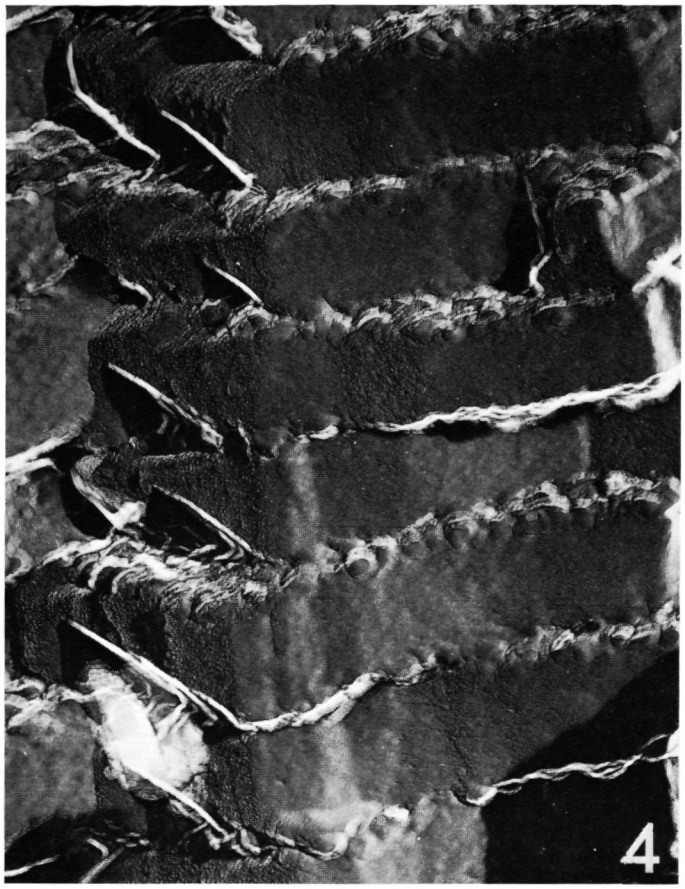

Ch. GREGOIRE. — Experimental alteration of the Nautilus shell.

Ch. GREGOIRE. — Experimental alteration of the Nautilus shell.

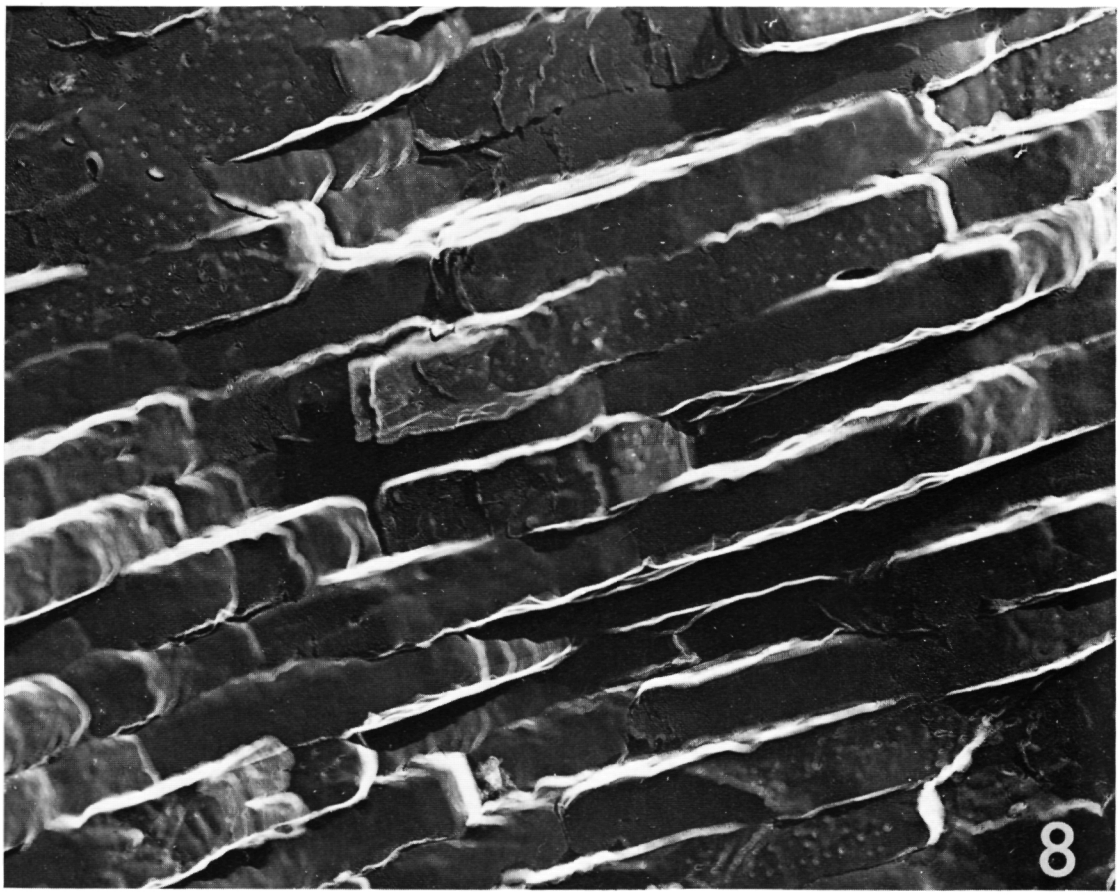

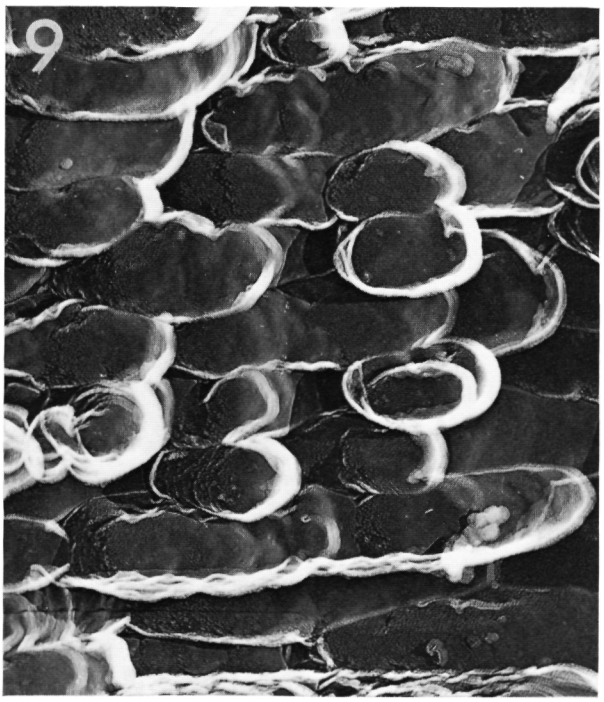

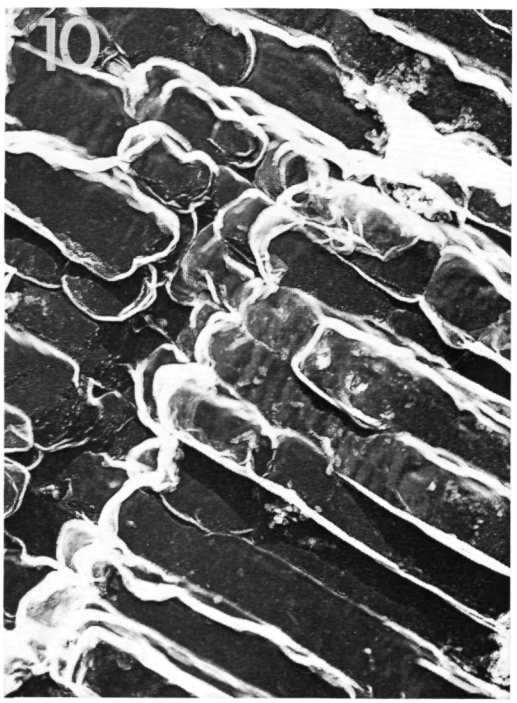

Ch. GREGOIRE. — Experimental alteration of the Nautilus shell.

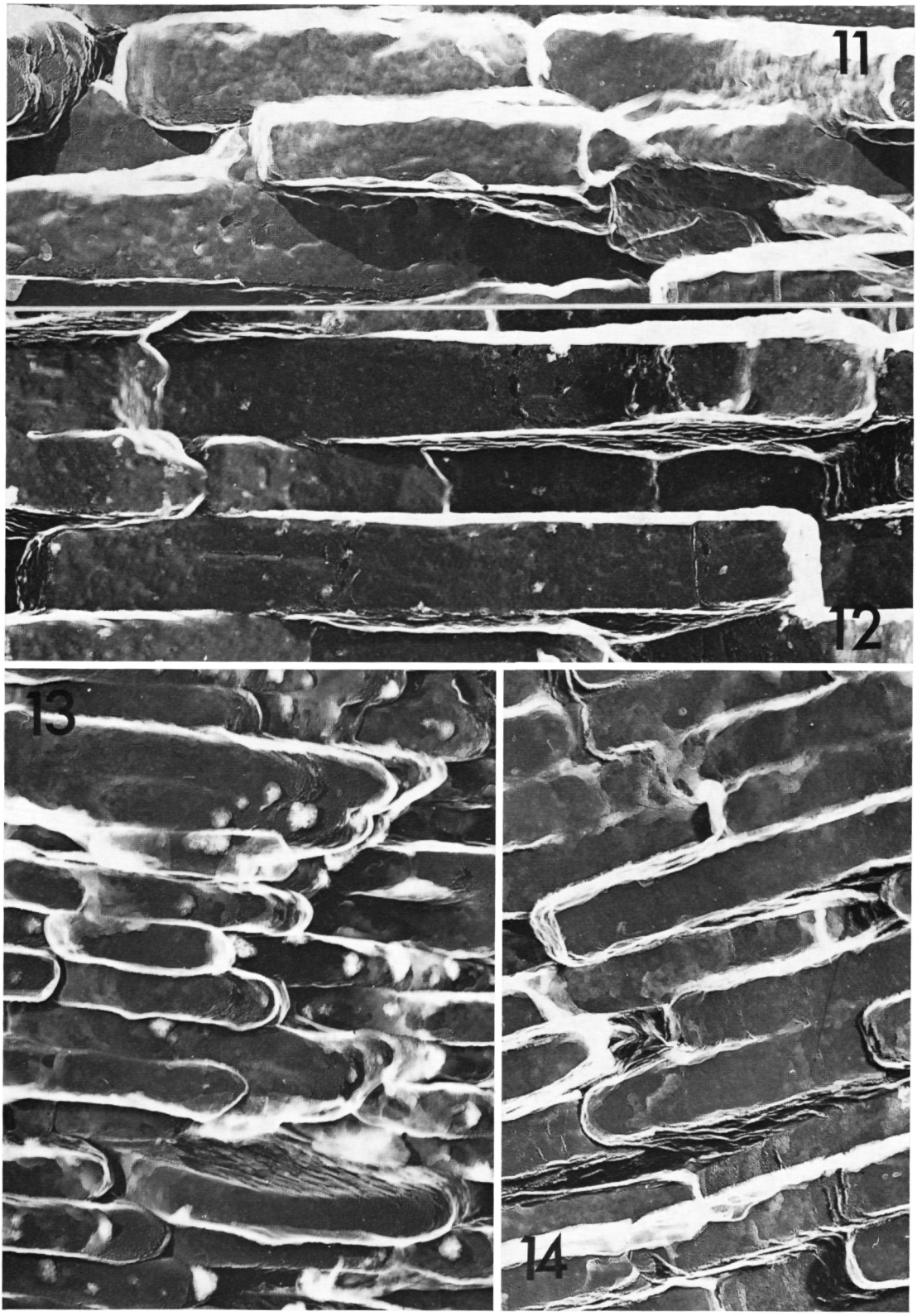

Ch. GREGOIRE. — Experimental alteration of the Nautilus shell.

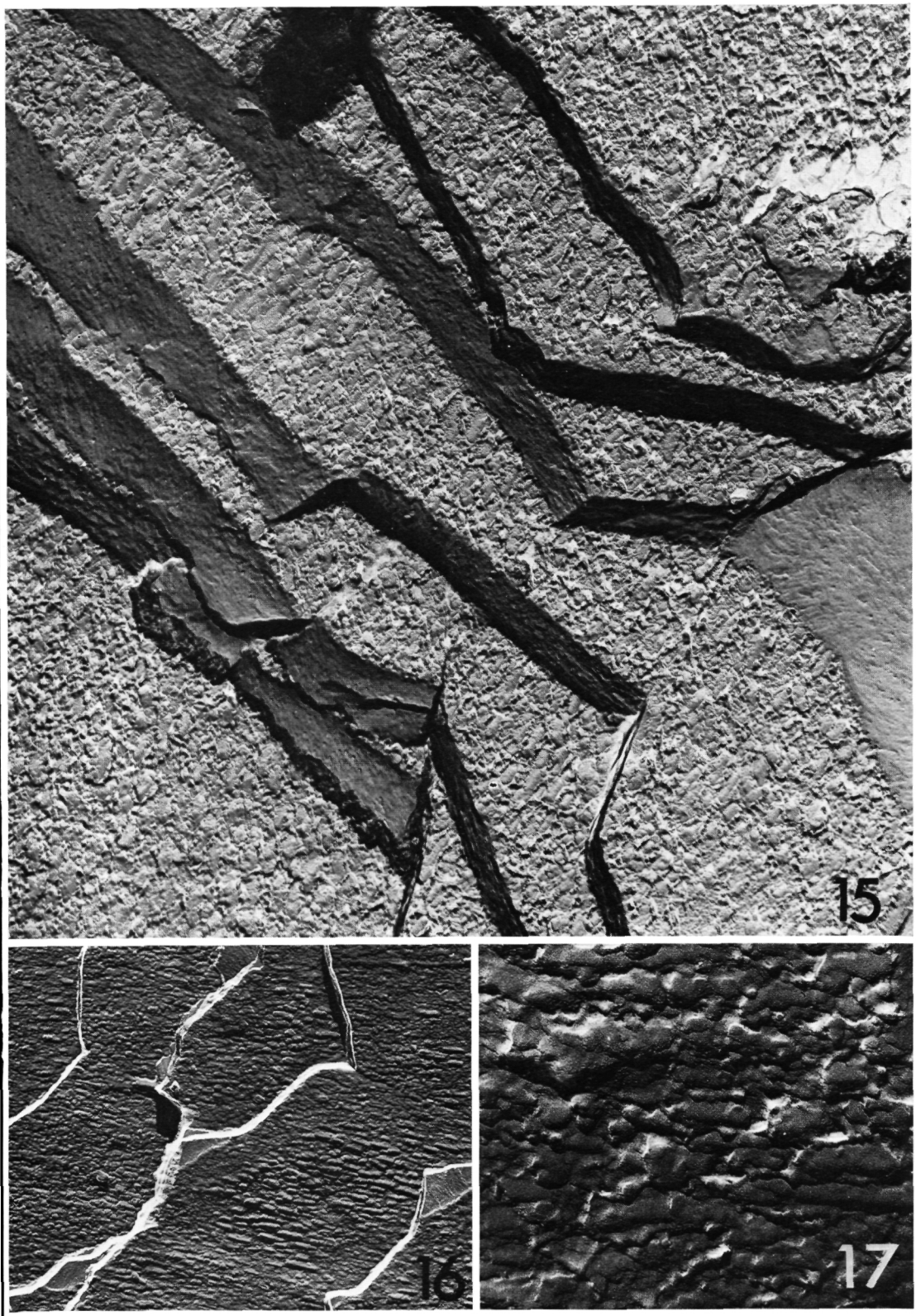

Ch. GREGOIRE. — Experimental alteration of the Nautilus shell.

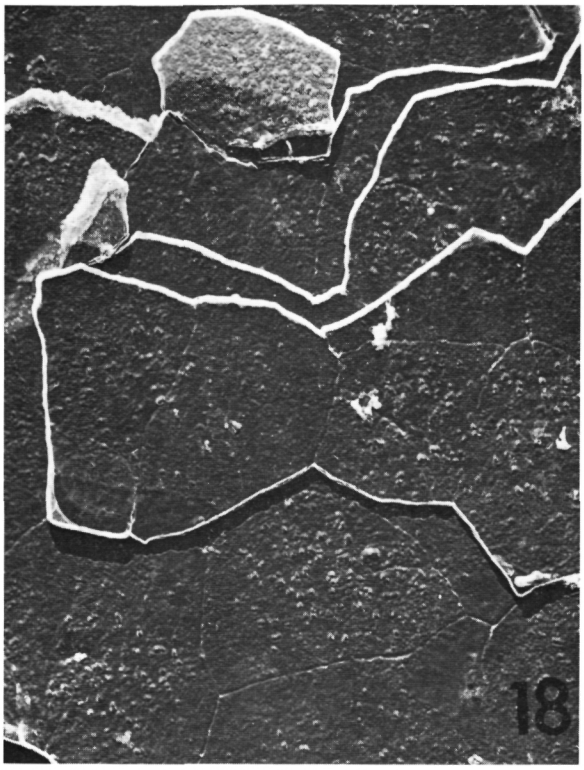

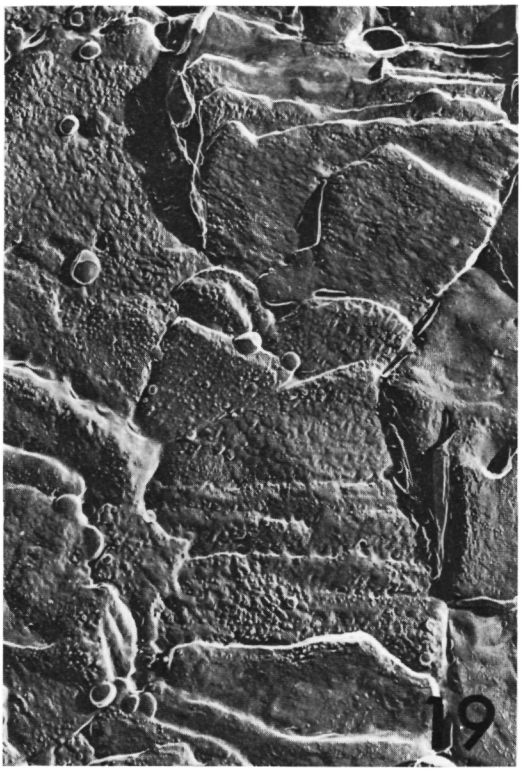

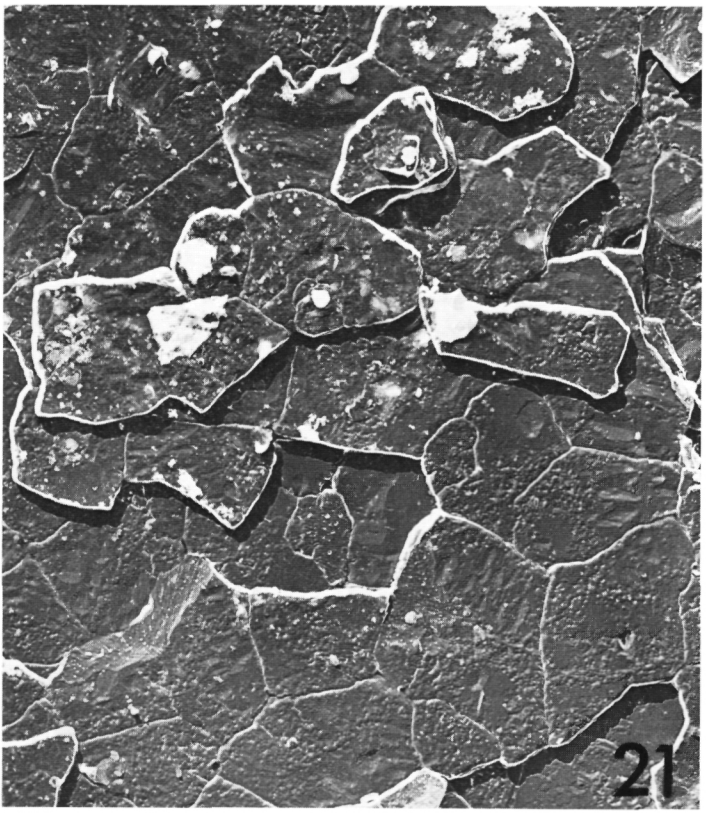

Ch. GREGOIRE. — Experimental alteration of the Nautilus shell.

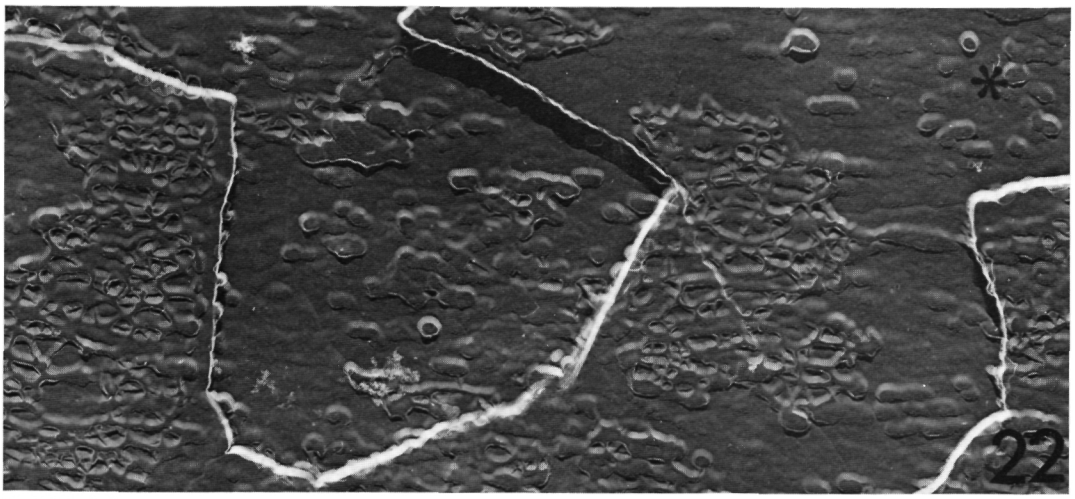

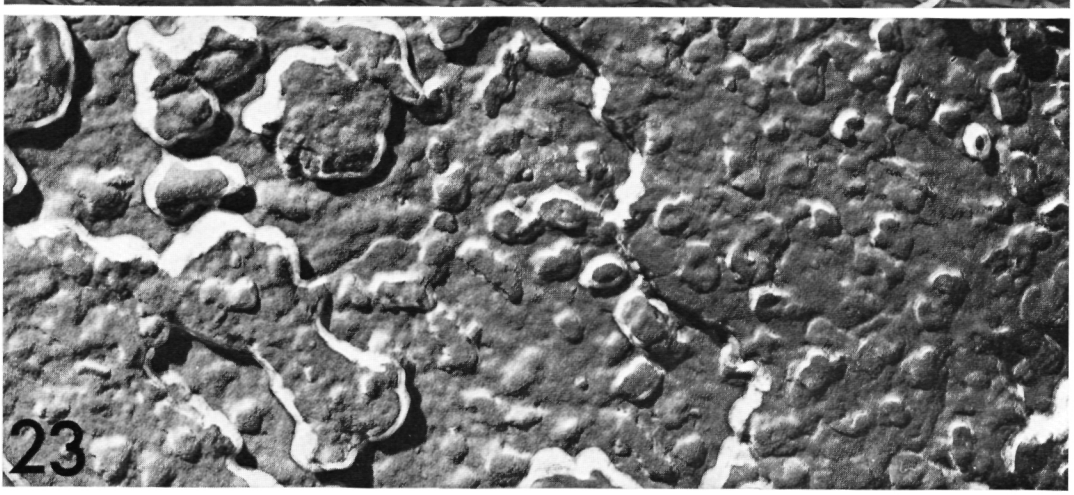

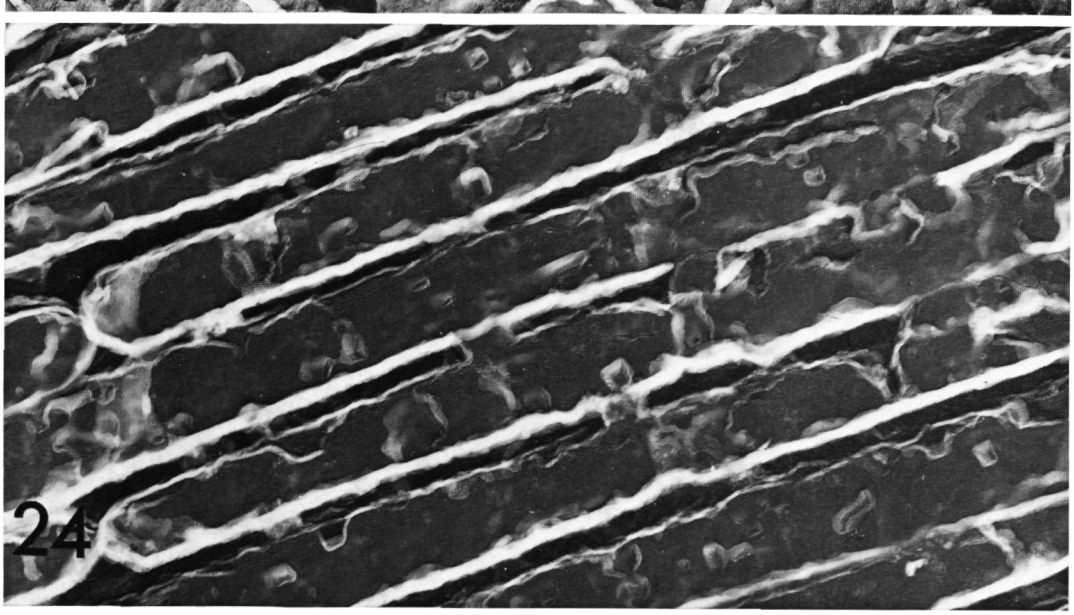

Ch. GREGOIRE. — Experimental alteration of the Nautilus shell.

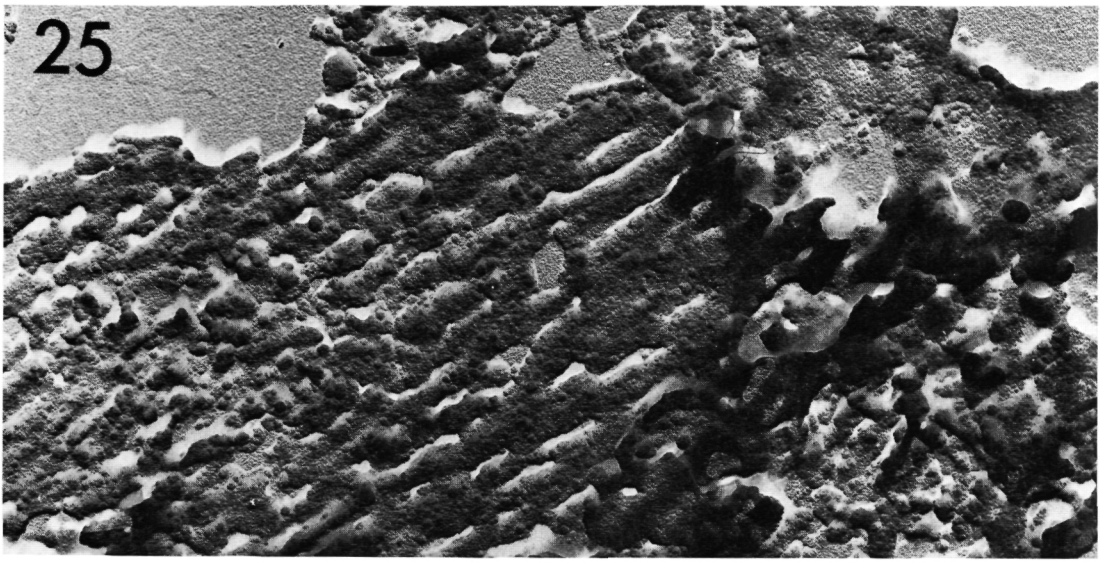

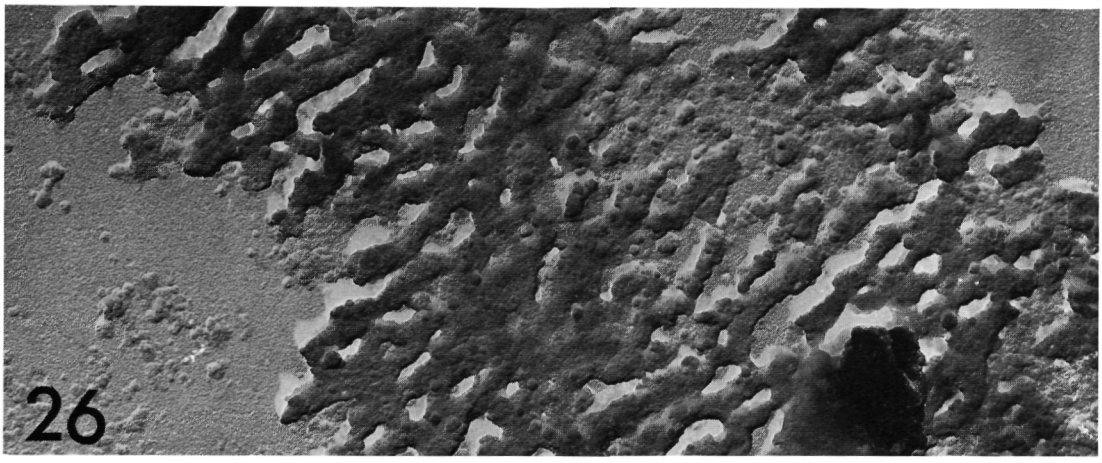

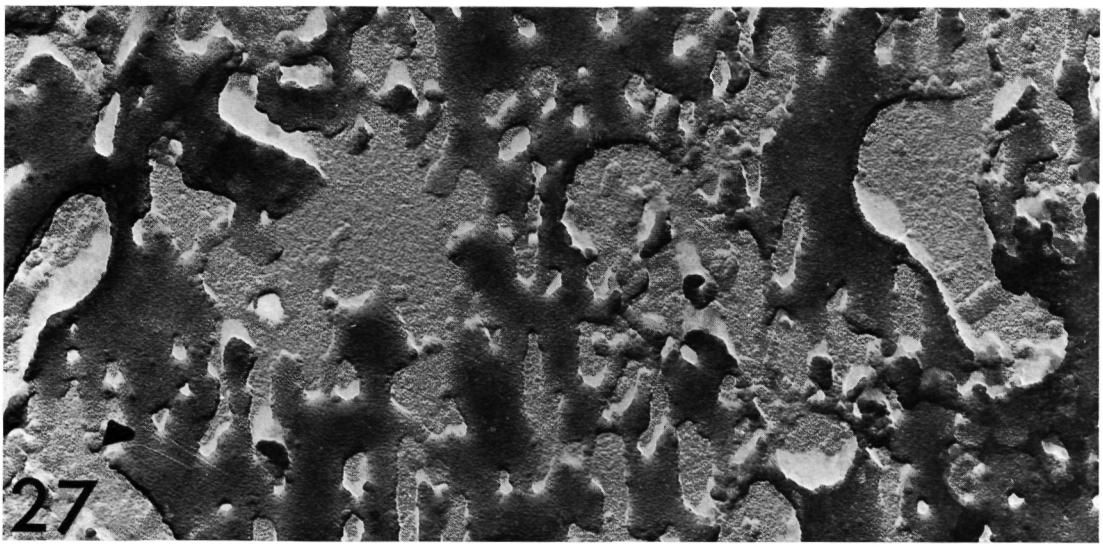

Ch. GREGOIRE. — Experimental alteration of the Nautilus shell.

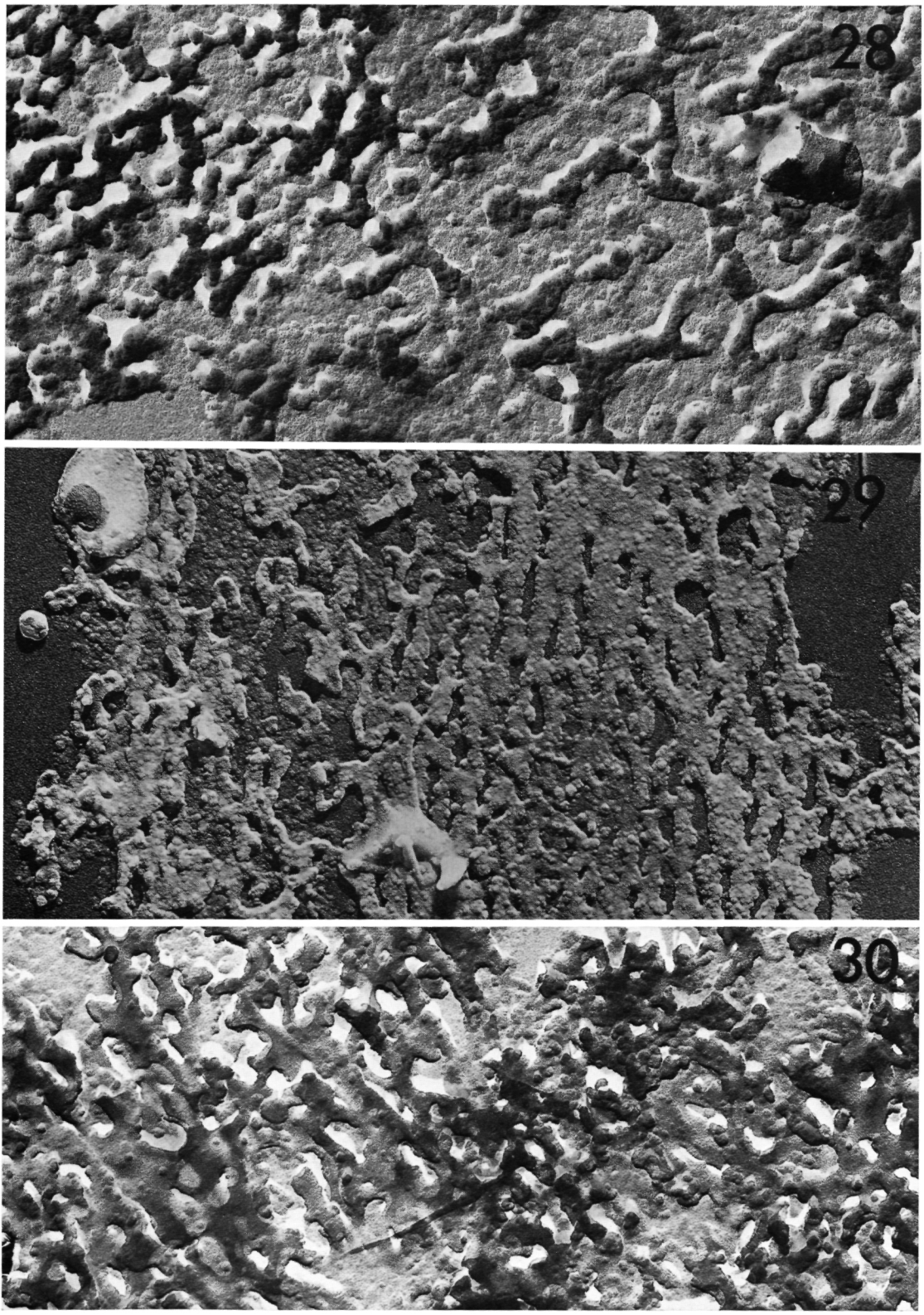

Ch. GREGOIRE. — Experimental alteration of the Nautilus shell.

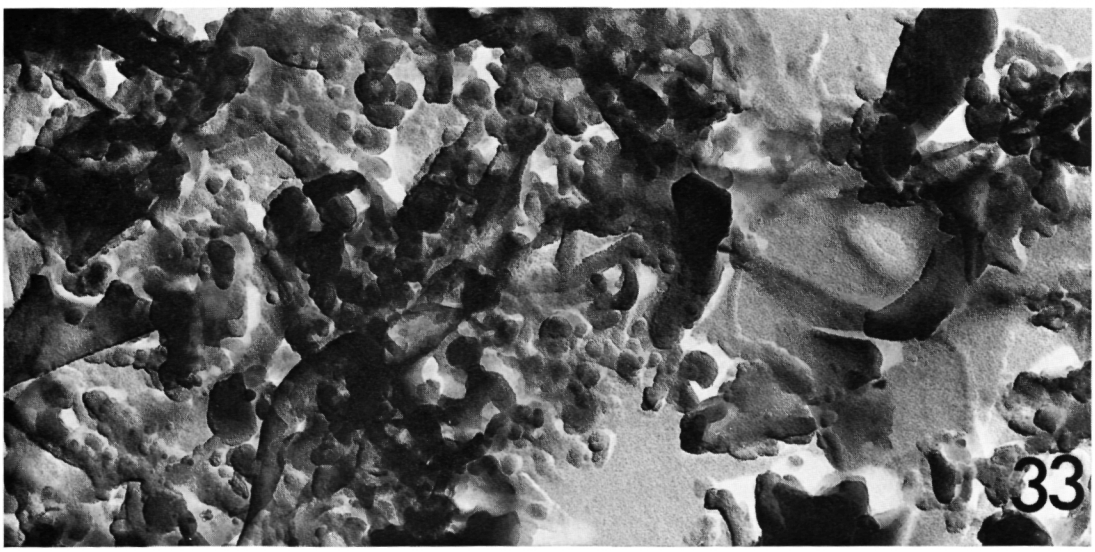

Ch. GREGOIRE. — Experimental alteration of the Nautilus shell.

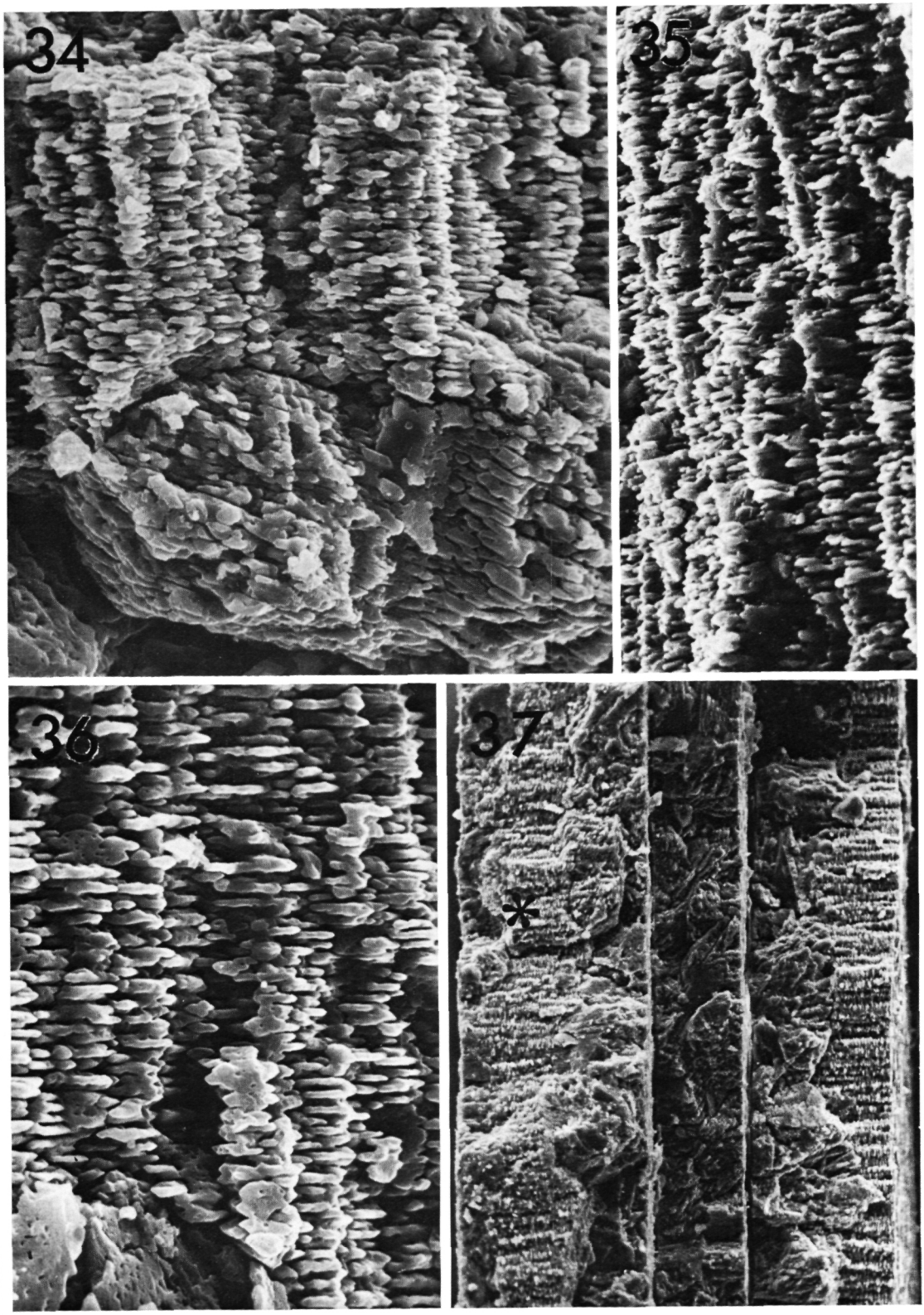

Ch. GREGOIRE. — Experimental alteration of the Nautilus shell.

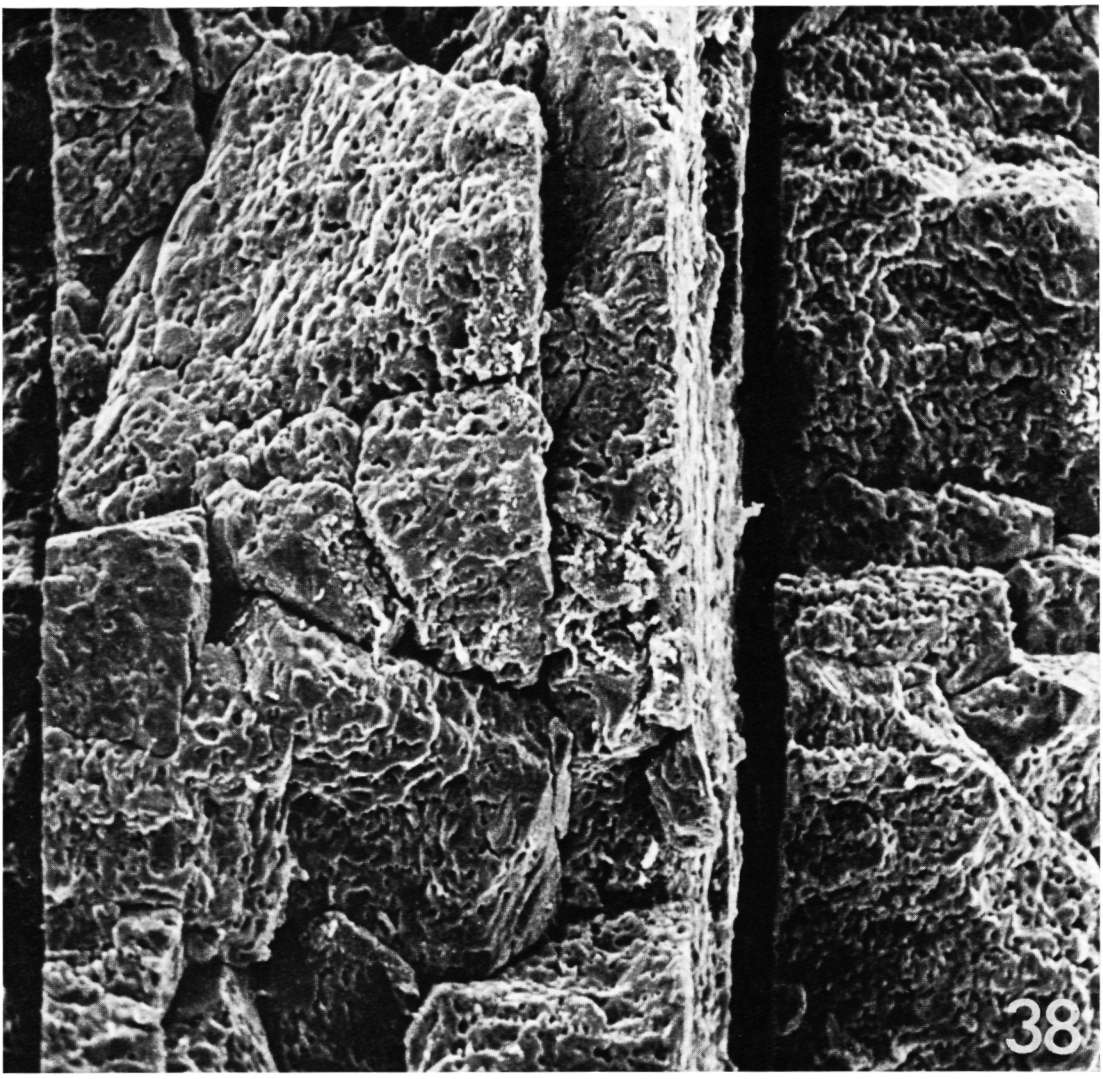

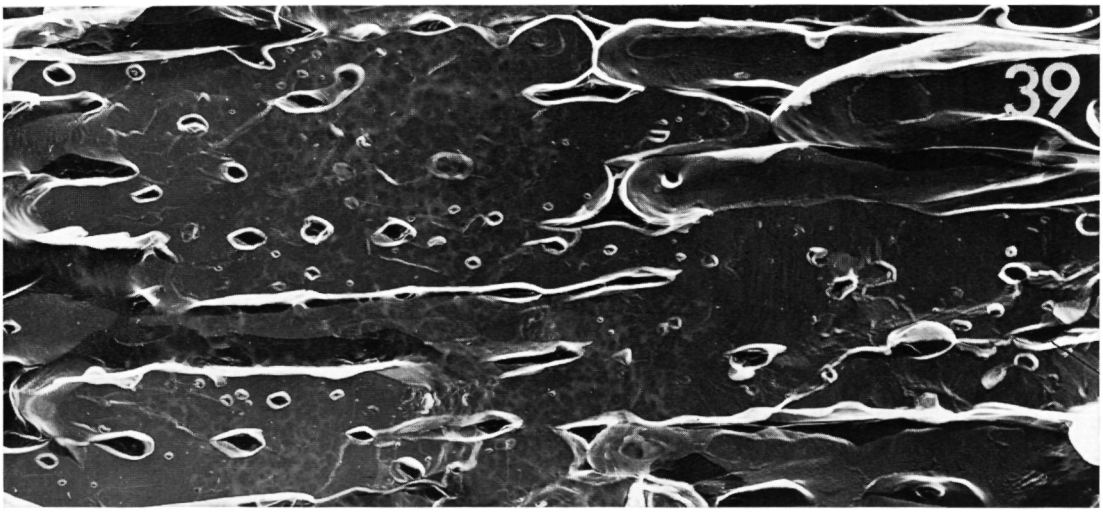

Ch. GREGOIRE. — Experimental alteration of the Nautilus shell.

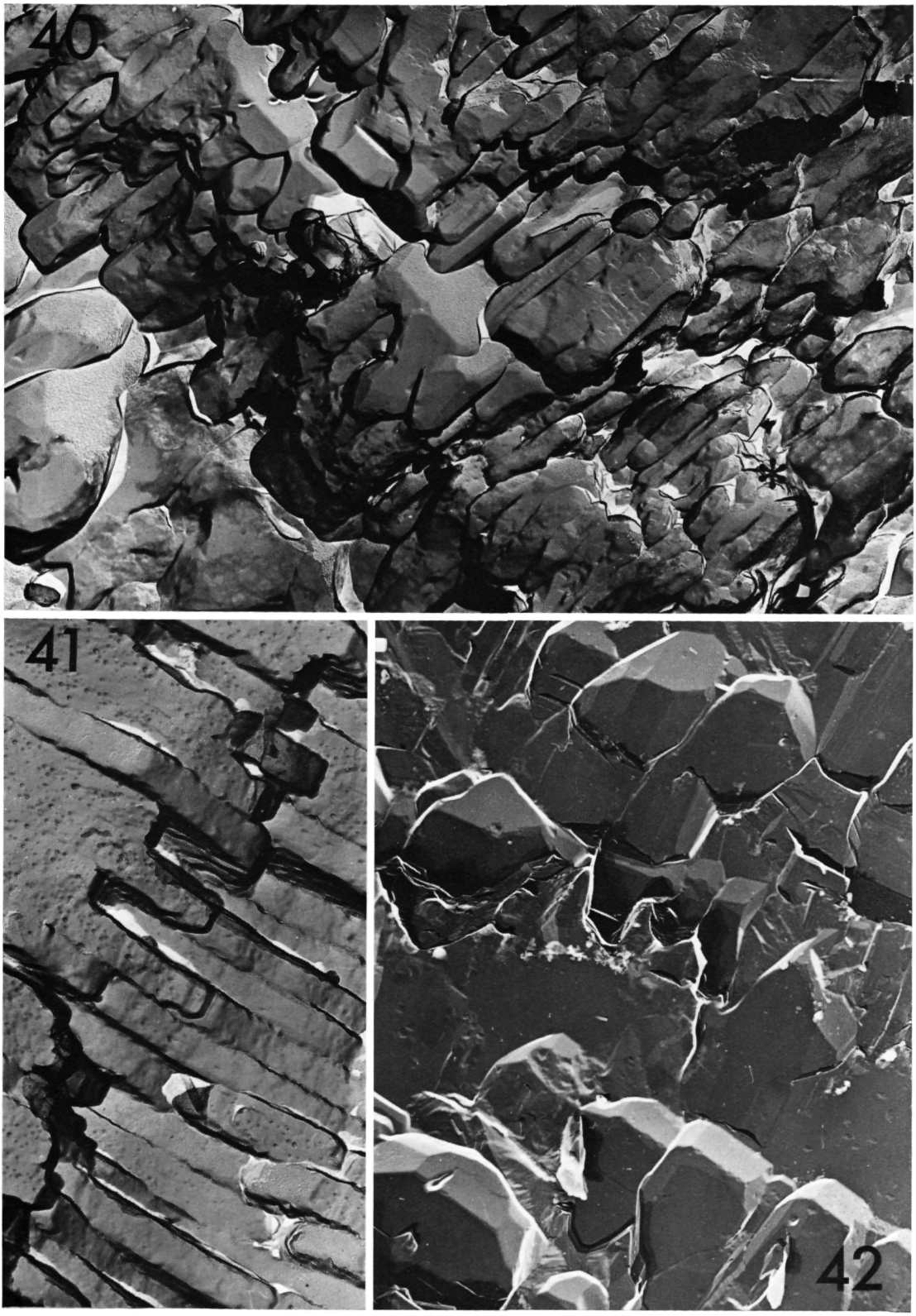

Ch. GREGOIRE. — Experimental alteration of the Nautilus shell.

Ch. GREGOIRE. — Experimental alteration of the Nautilus shell.

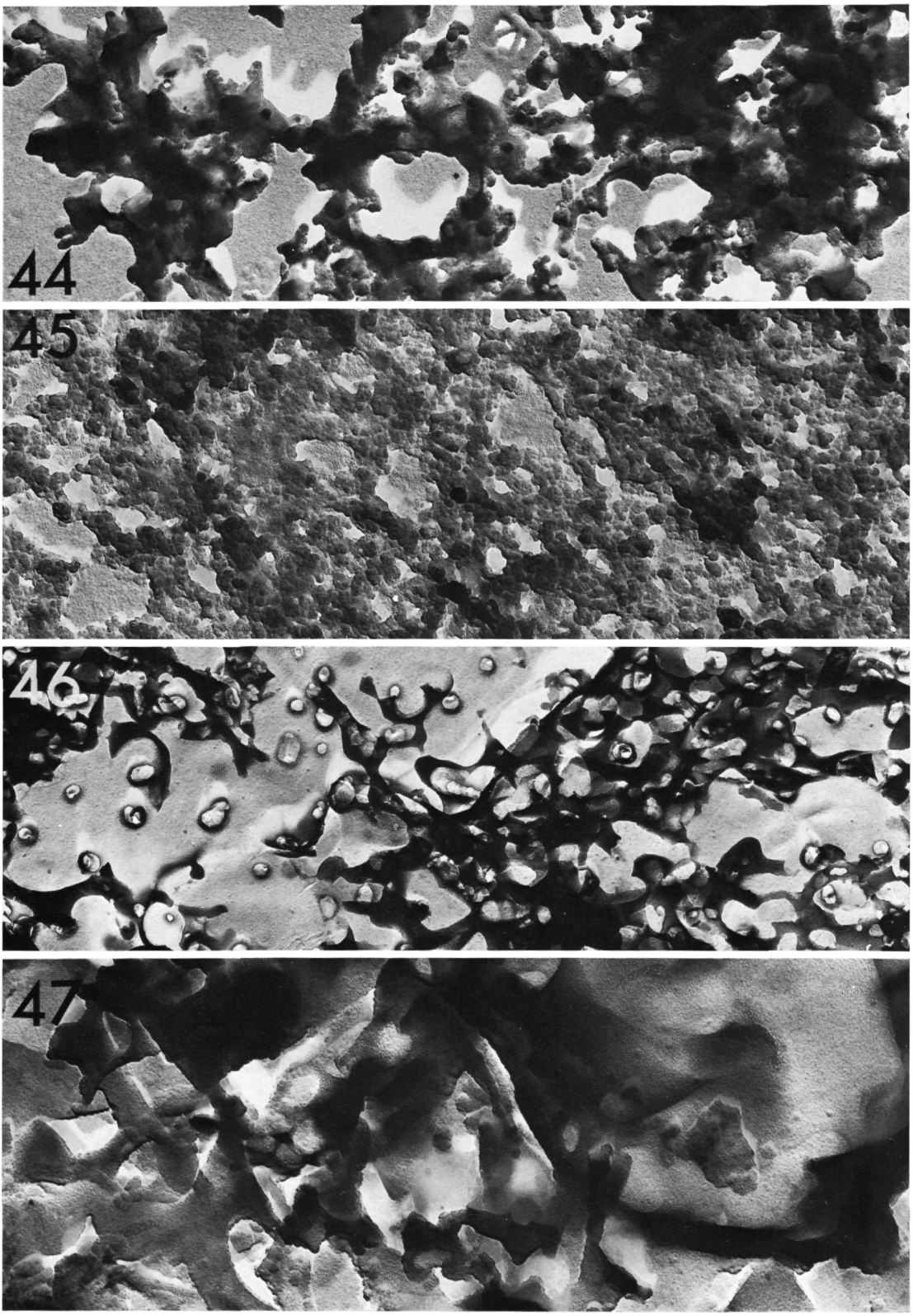

Ch. GREGOIRE. — Experimental alteration of the Nautilus shell.

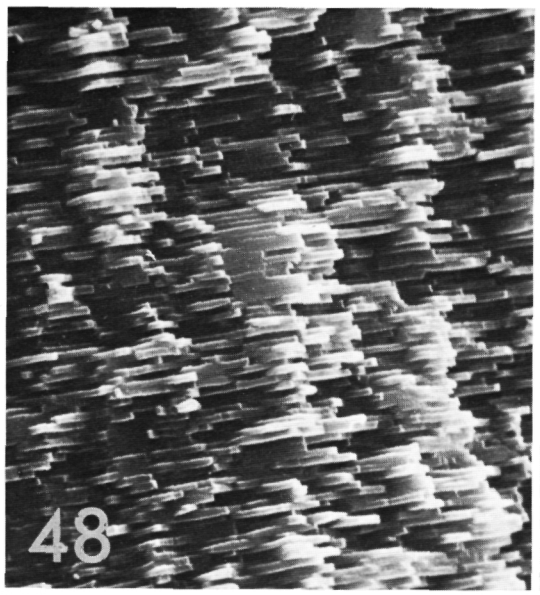

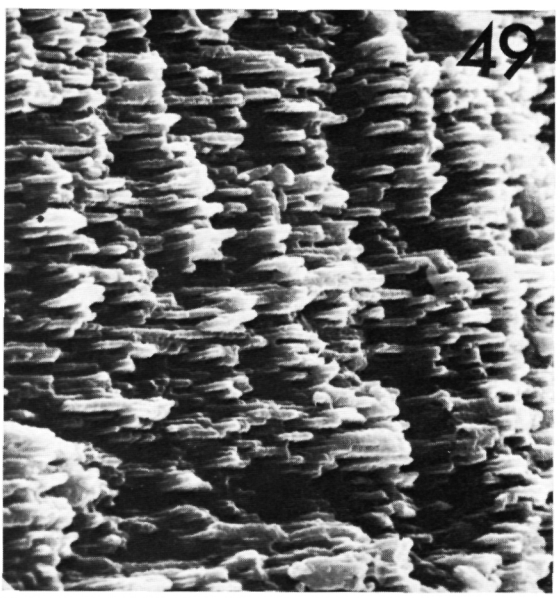

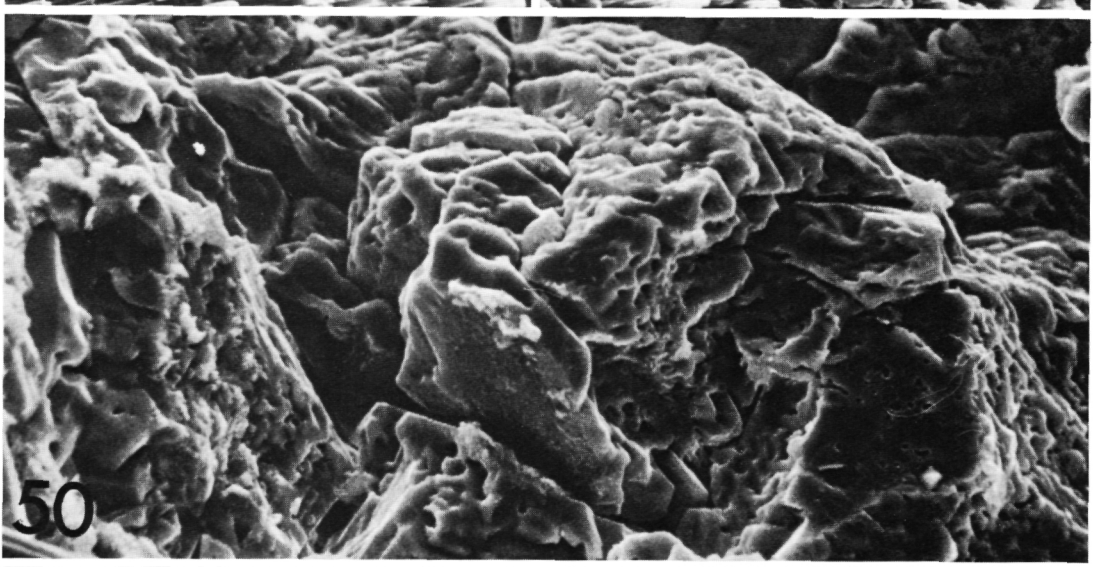

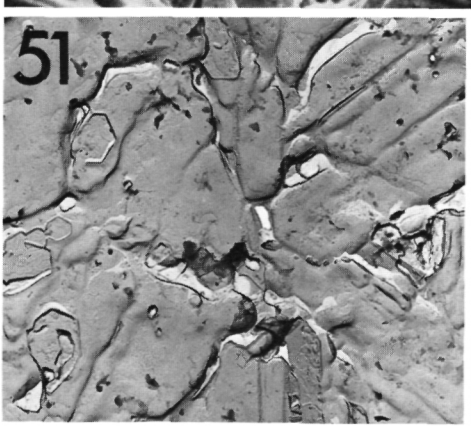

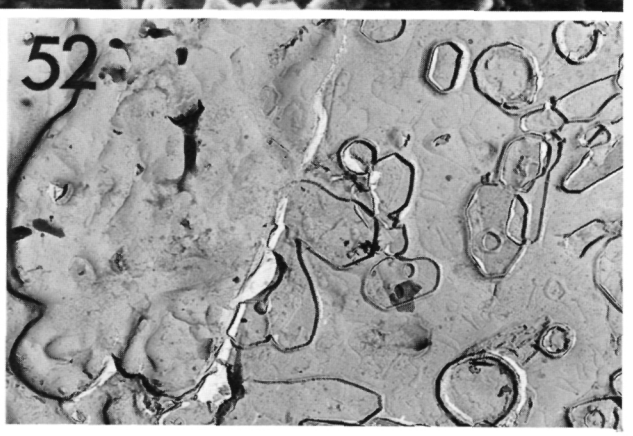

Ch. GREGOIRE. — Experimental alteration of the Nautilus shell.

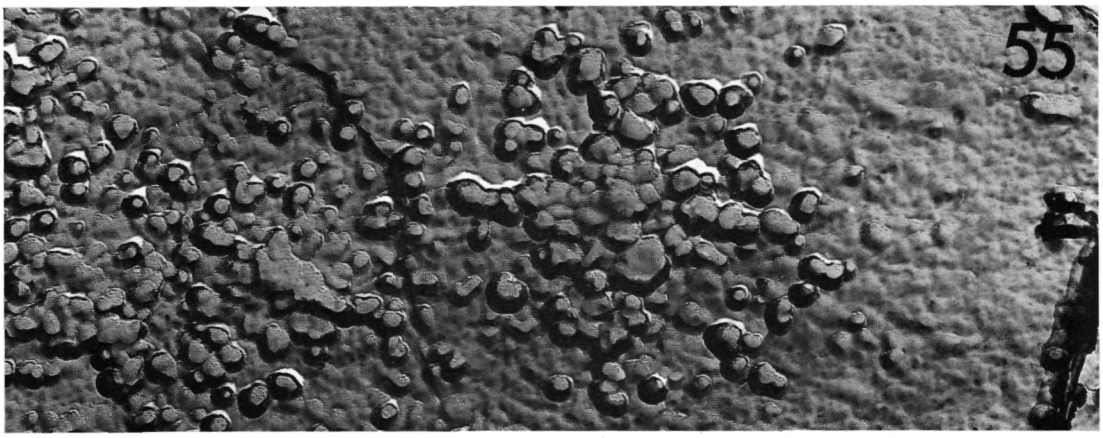

Ch. GREGOIRE. — Experimental alteration of the Nautilus shell.

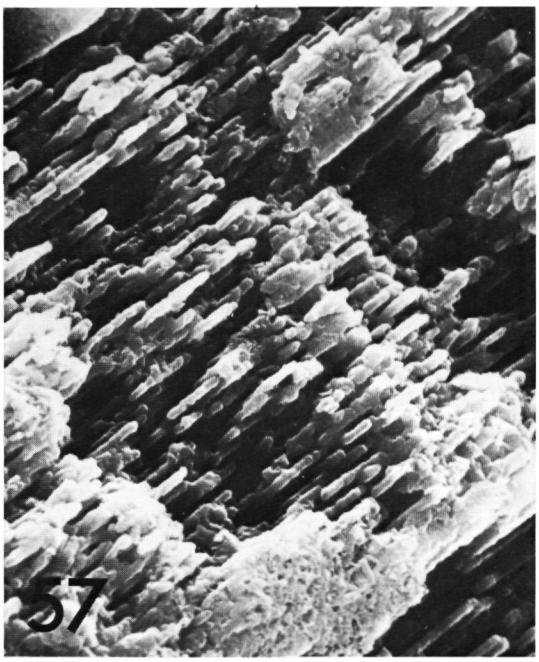

Ch. GREGOIRE. — Experimental alteration of the Nautilus shell.

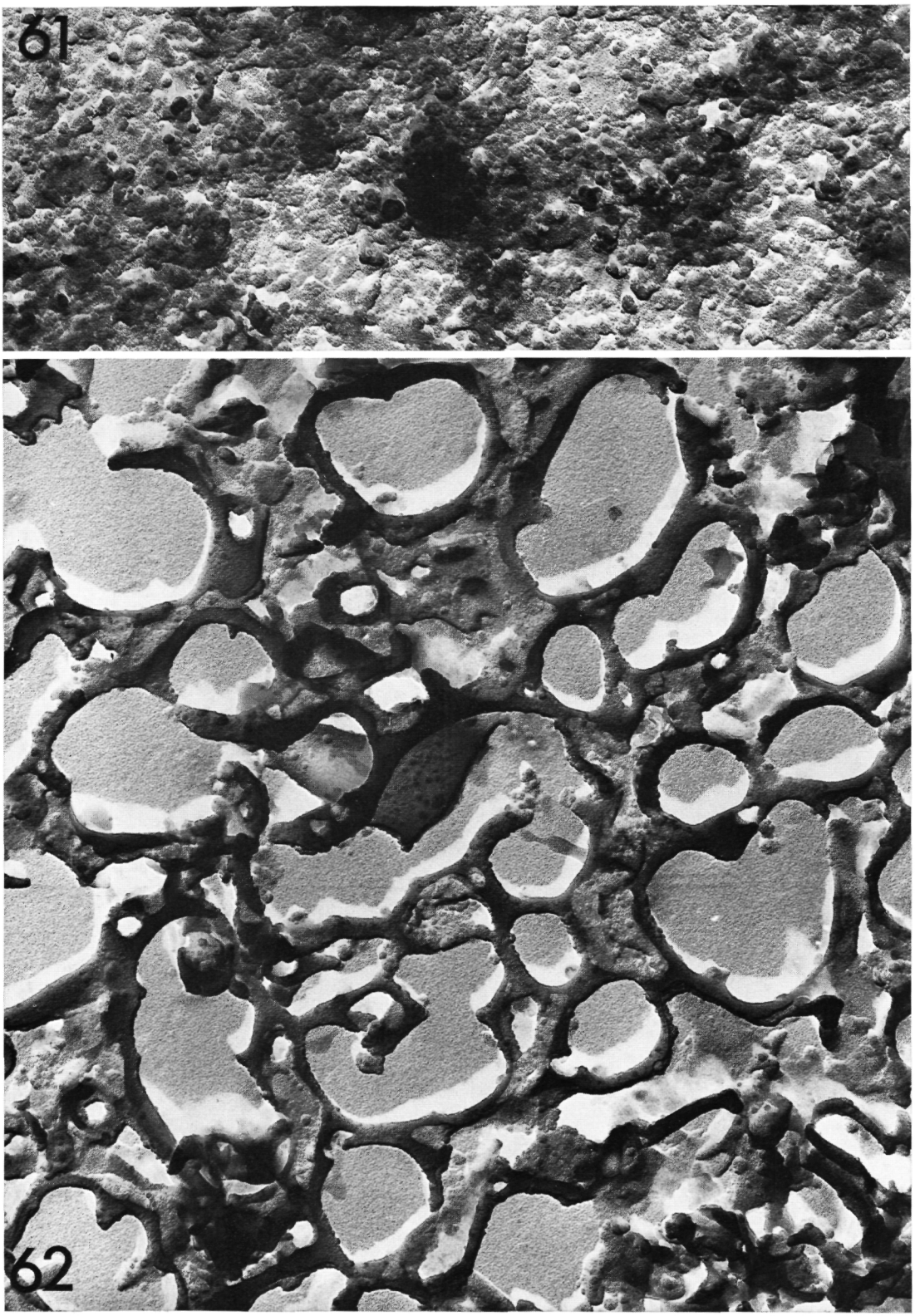

Ch. GREGOIRE. — Experimental alteration of the Nautilus shell.

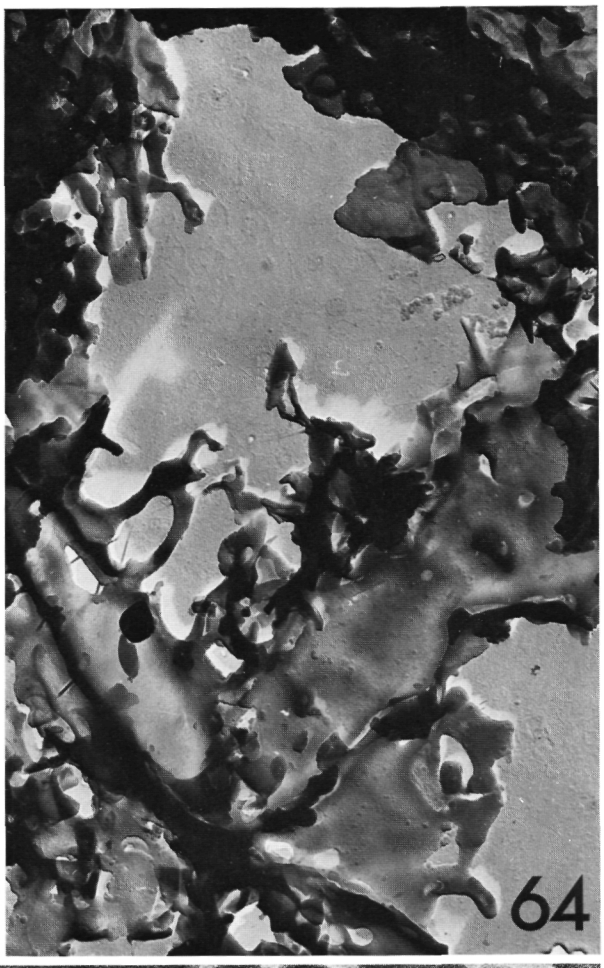

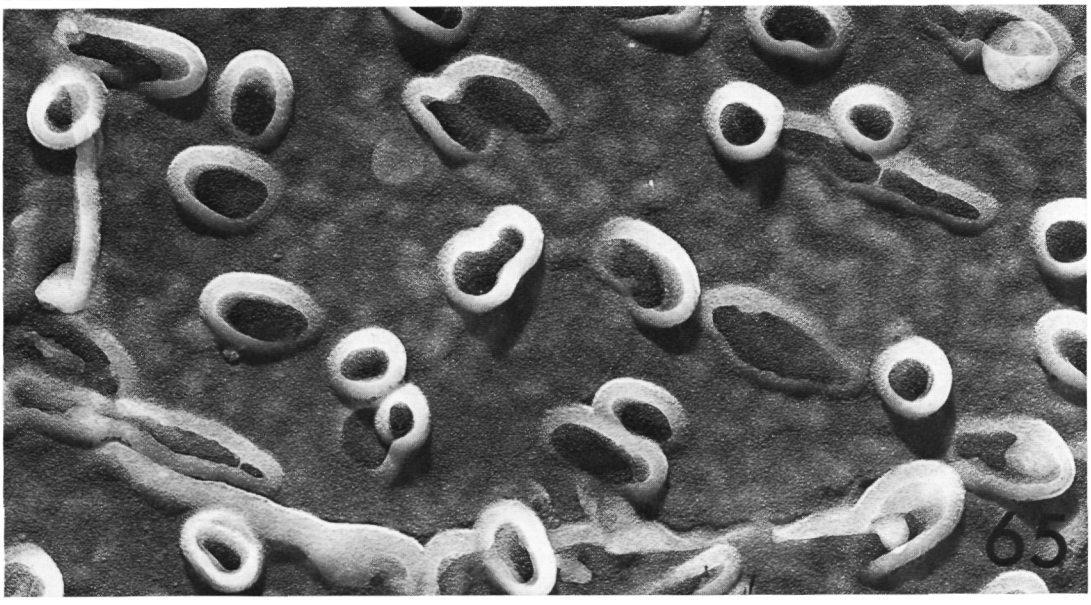

Ch. GREGOIRE. — Experimental alteration of the Nautilus shell.

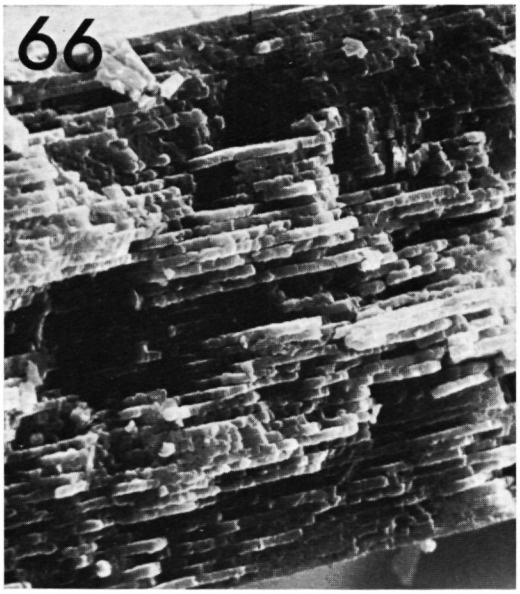

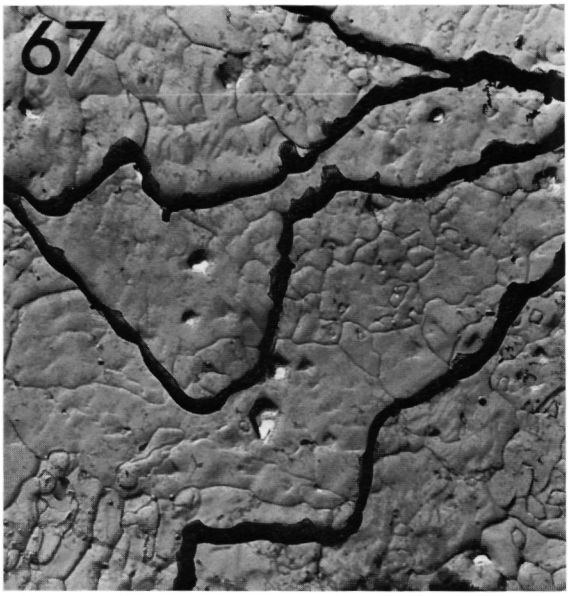

Ch. GREGOIRE. — Experimental alteration of the Nautilus shell.

Ch. GREGOIRE. — Experimental alteration of the Nautilus shell.

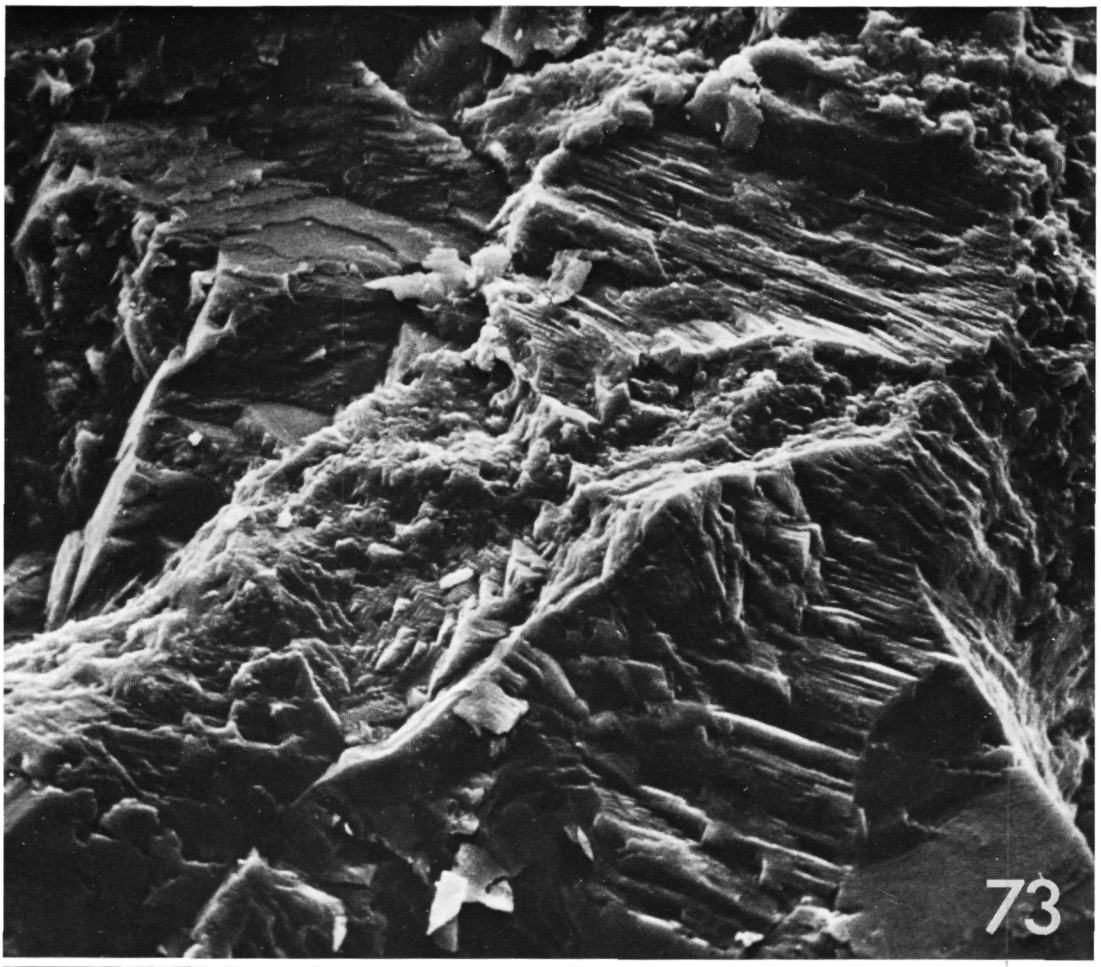

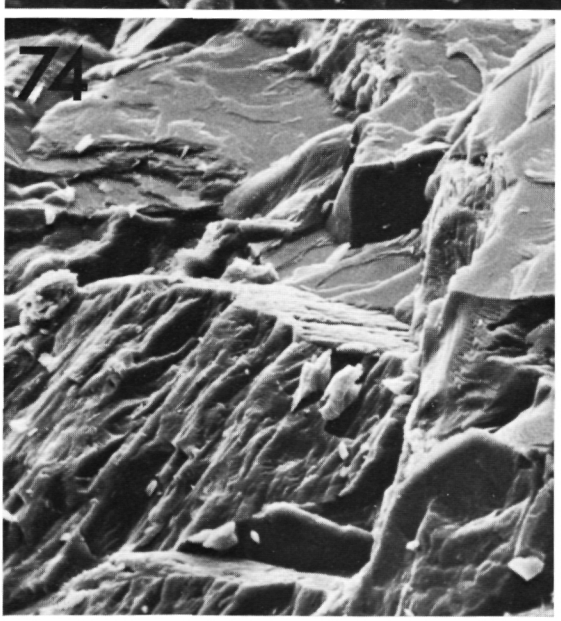

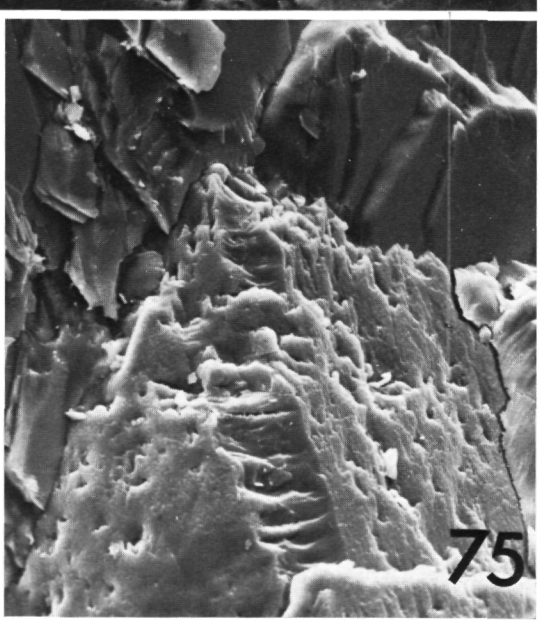

Ch. GREGOIRE. — Experimental alteration of the Nautilus shell.

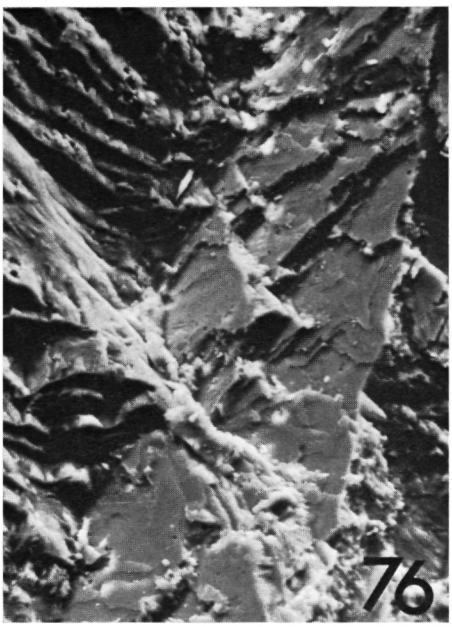

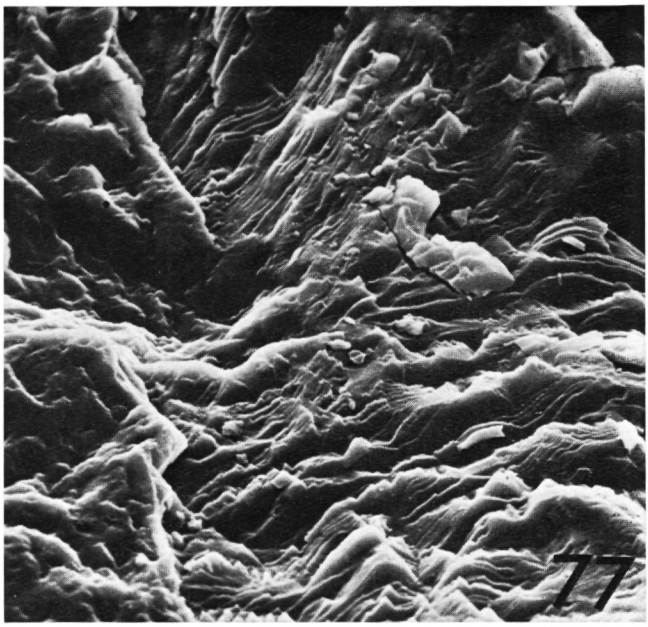

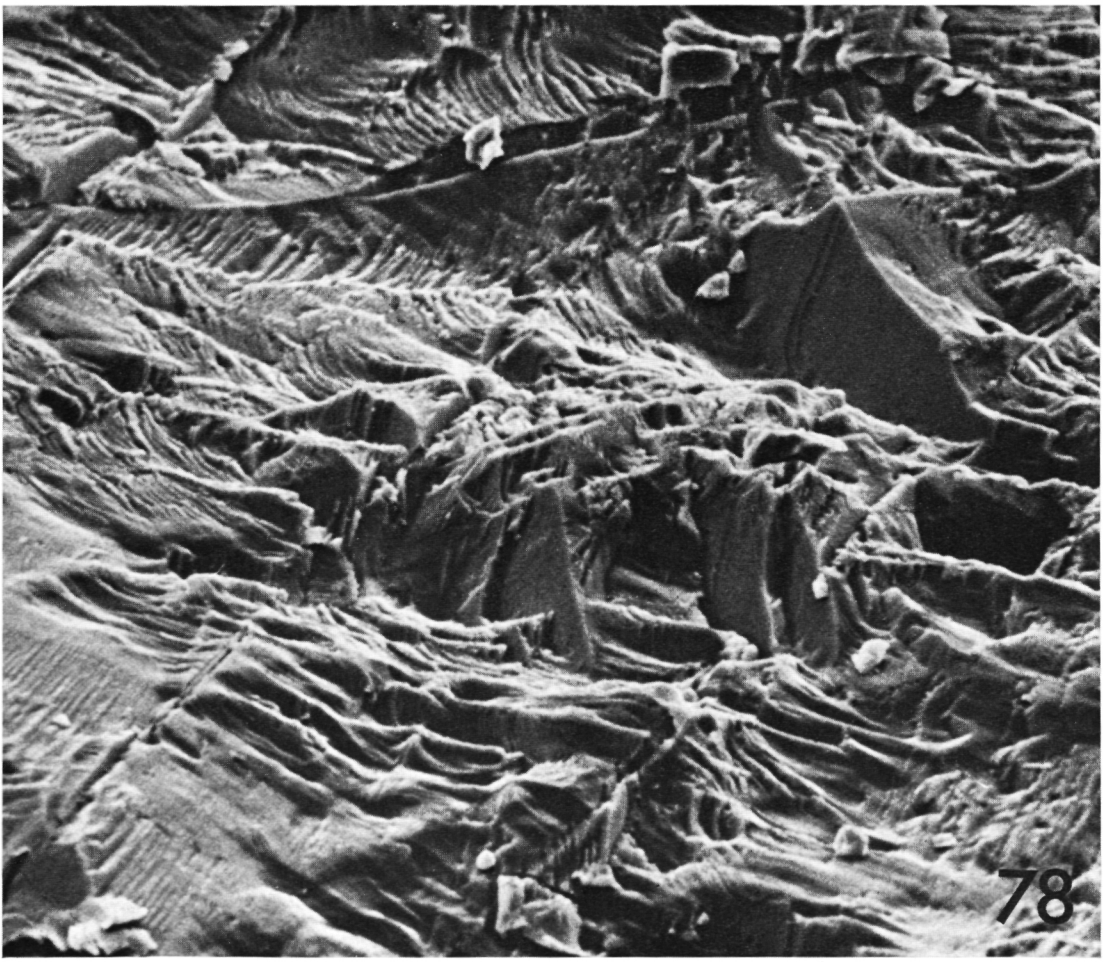

Ch. GREGOIRE. — Experimental alteration of the Nautilus shell.

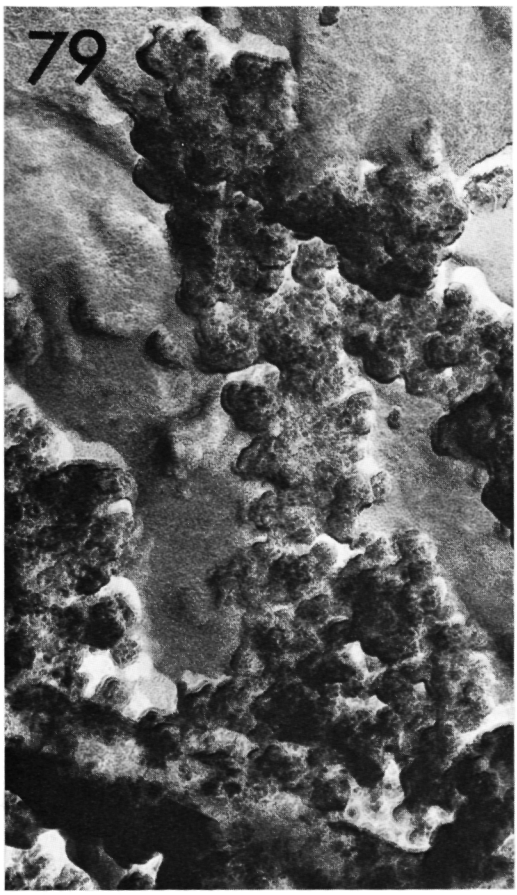

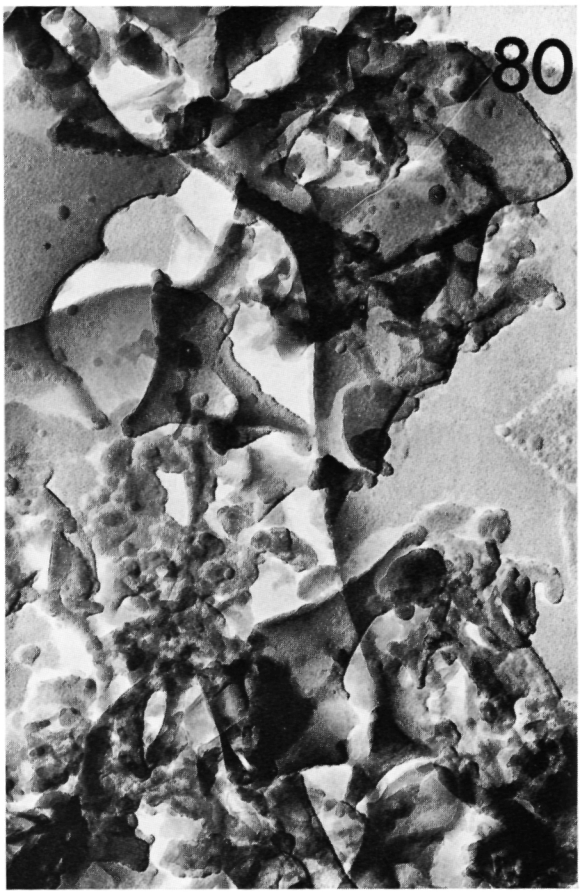

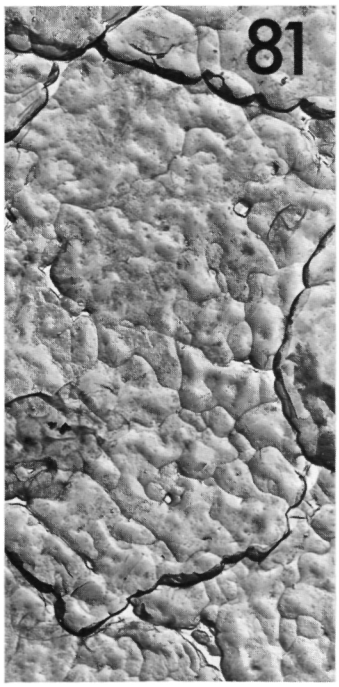

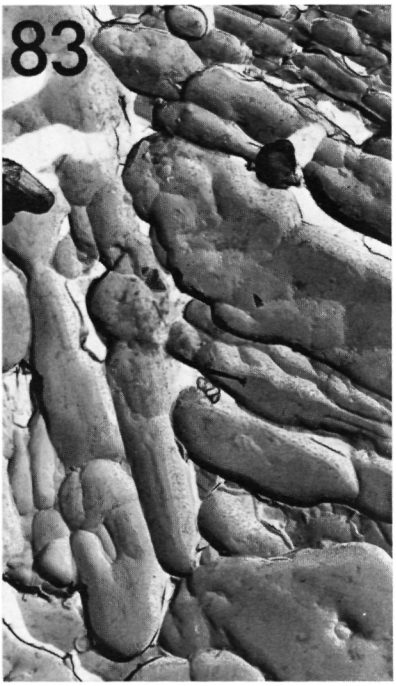

Ch. GREGOIRE. — Experimental alteration of the Nautilus shell.

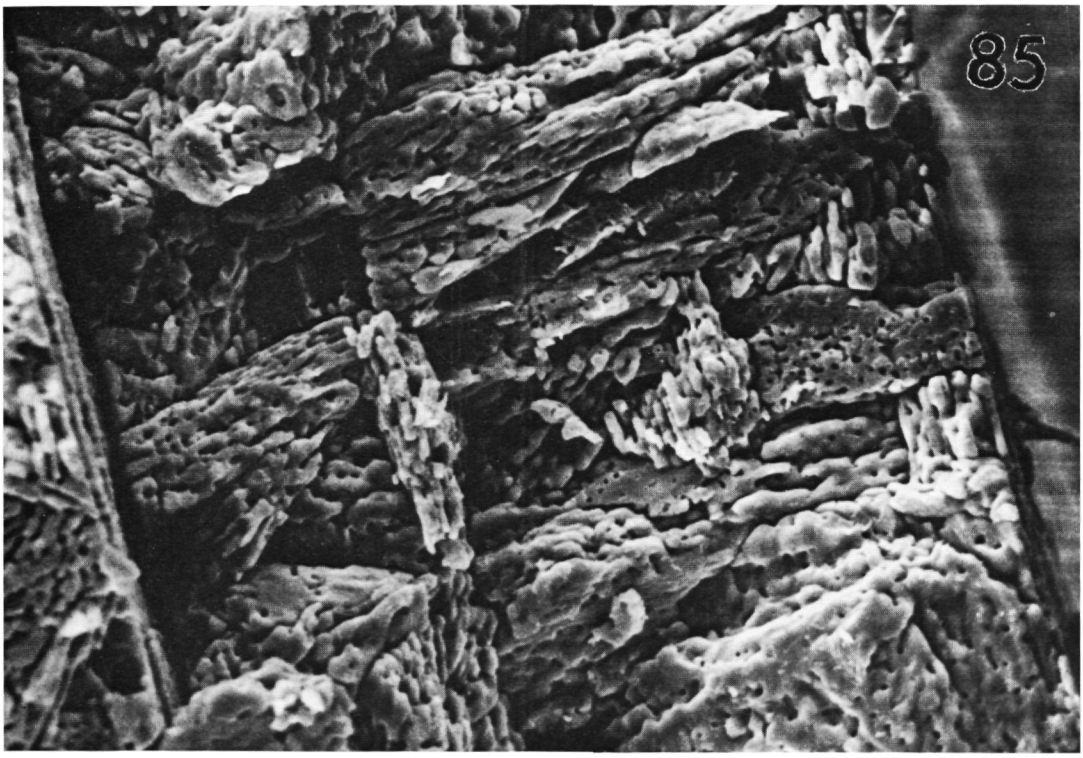

Ch. GREGOIRE. — Experimental alteration of the Nautilus shell.

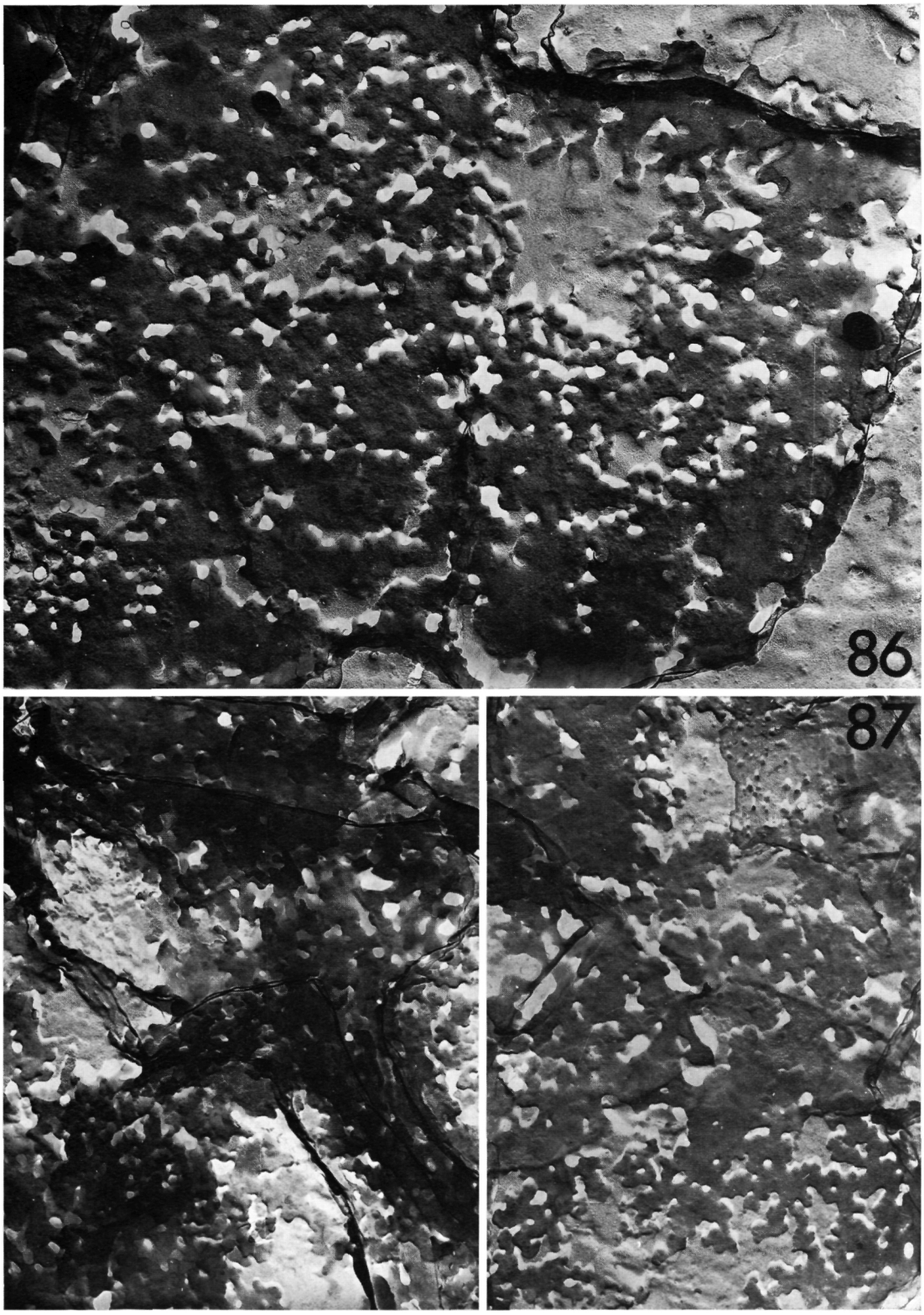

Ch. GREGOIRE. — Experimental alteration of the Nautilus shell.

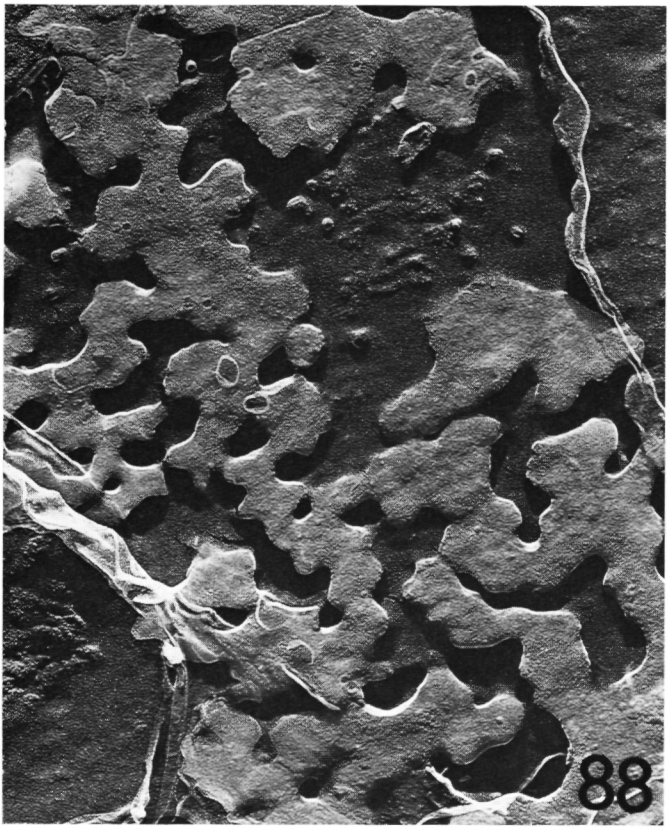

Ch. GREGOIRE. — Experimental alteration of the Nautilus shell.

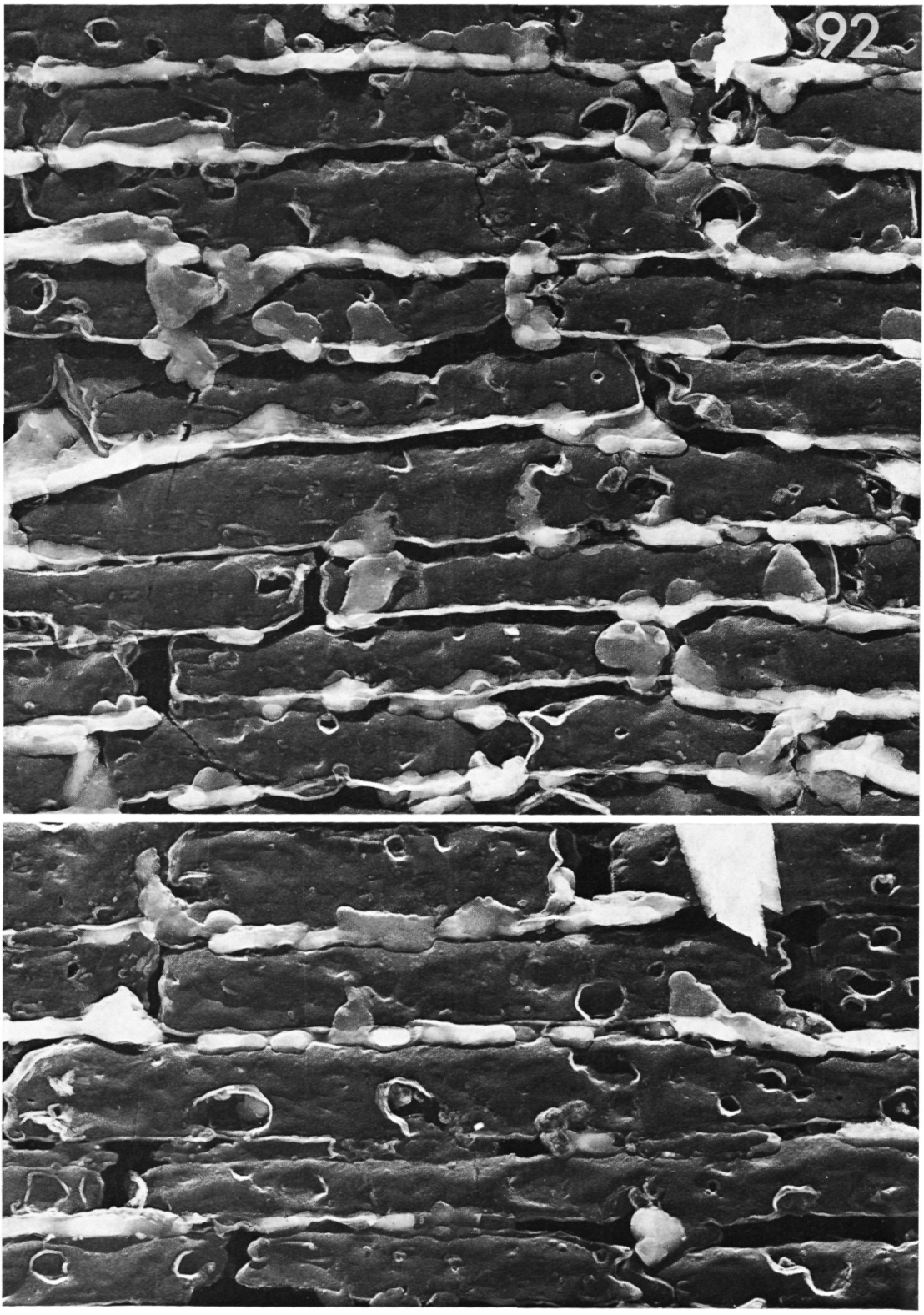

Ch. GREGOIRE. — Experimental alteration of the Nautilus shell.

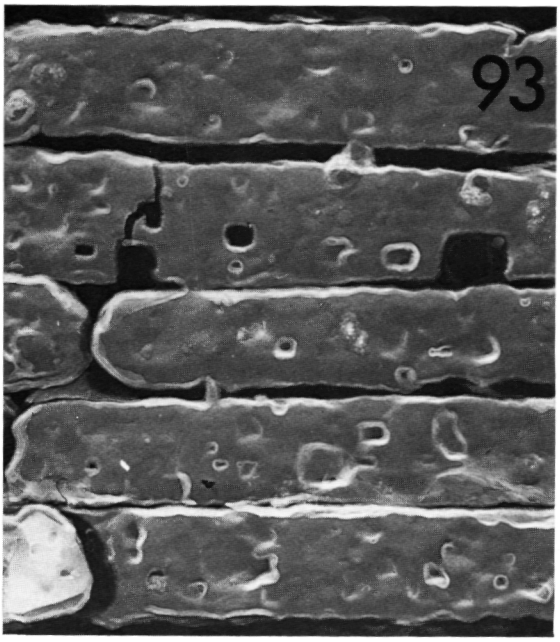

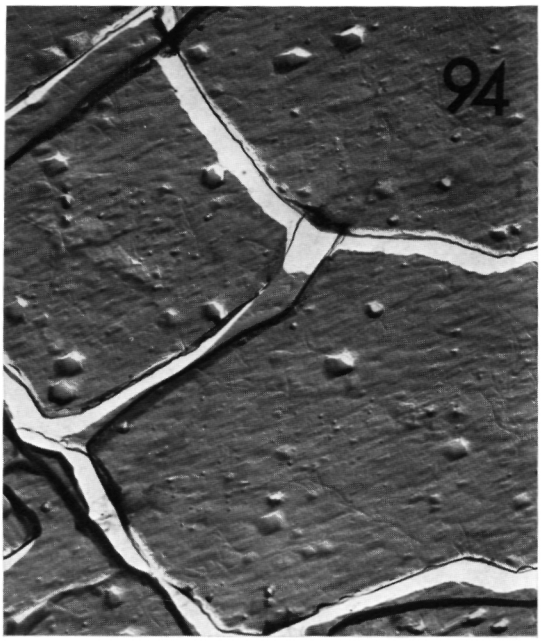

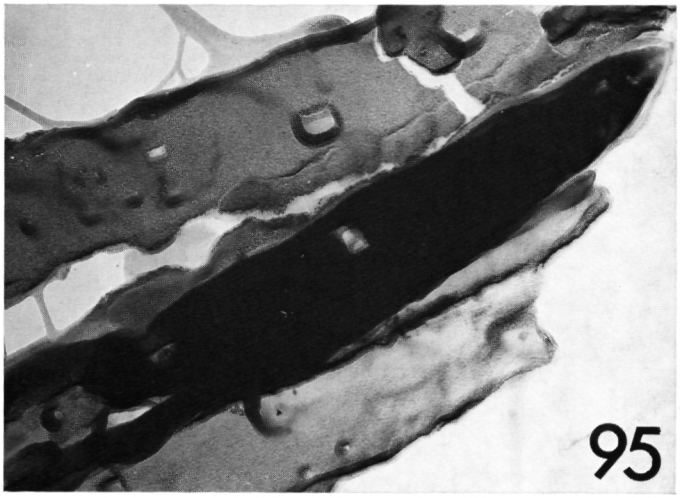

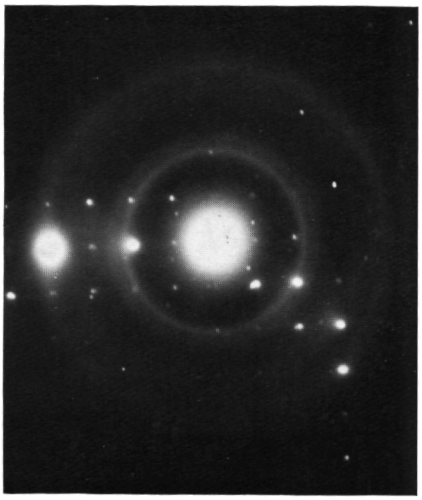

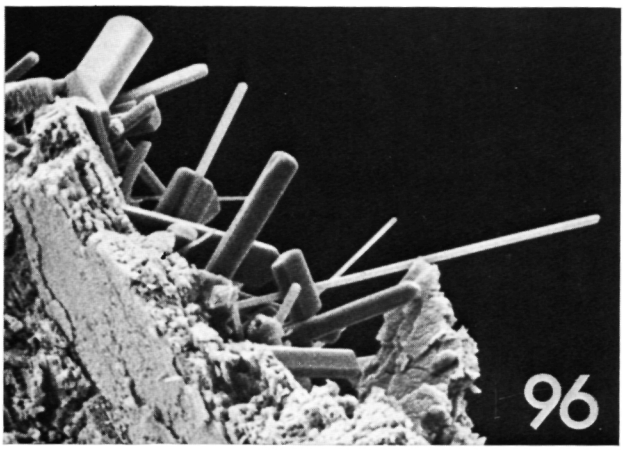

Ch. GREGOIRE. — Experimental alteration of the Nautilus shell.

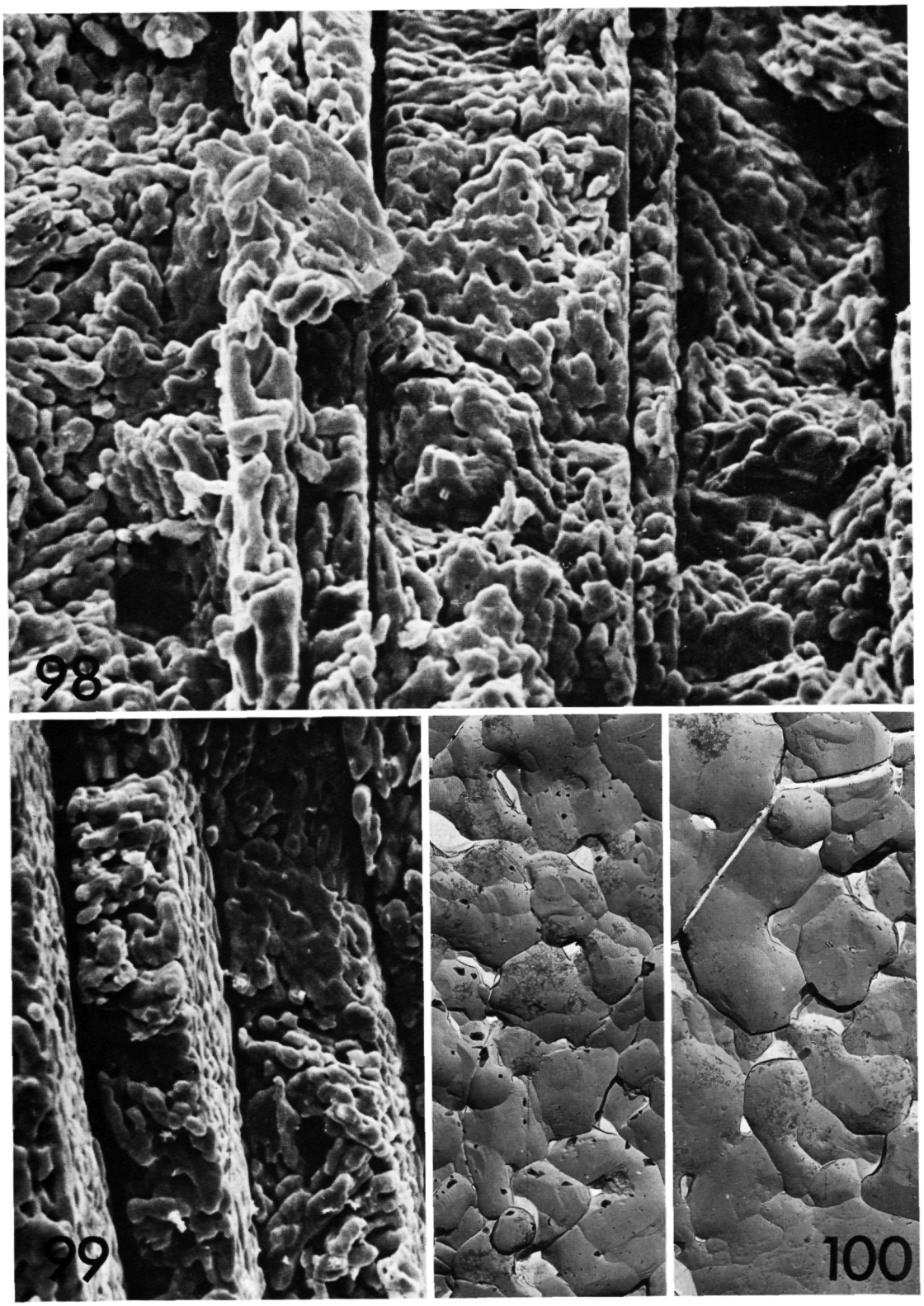

Ch. GREGOIRE. — Experimental alteration of the Nautilus shell.

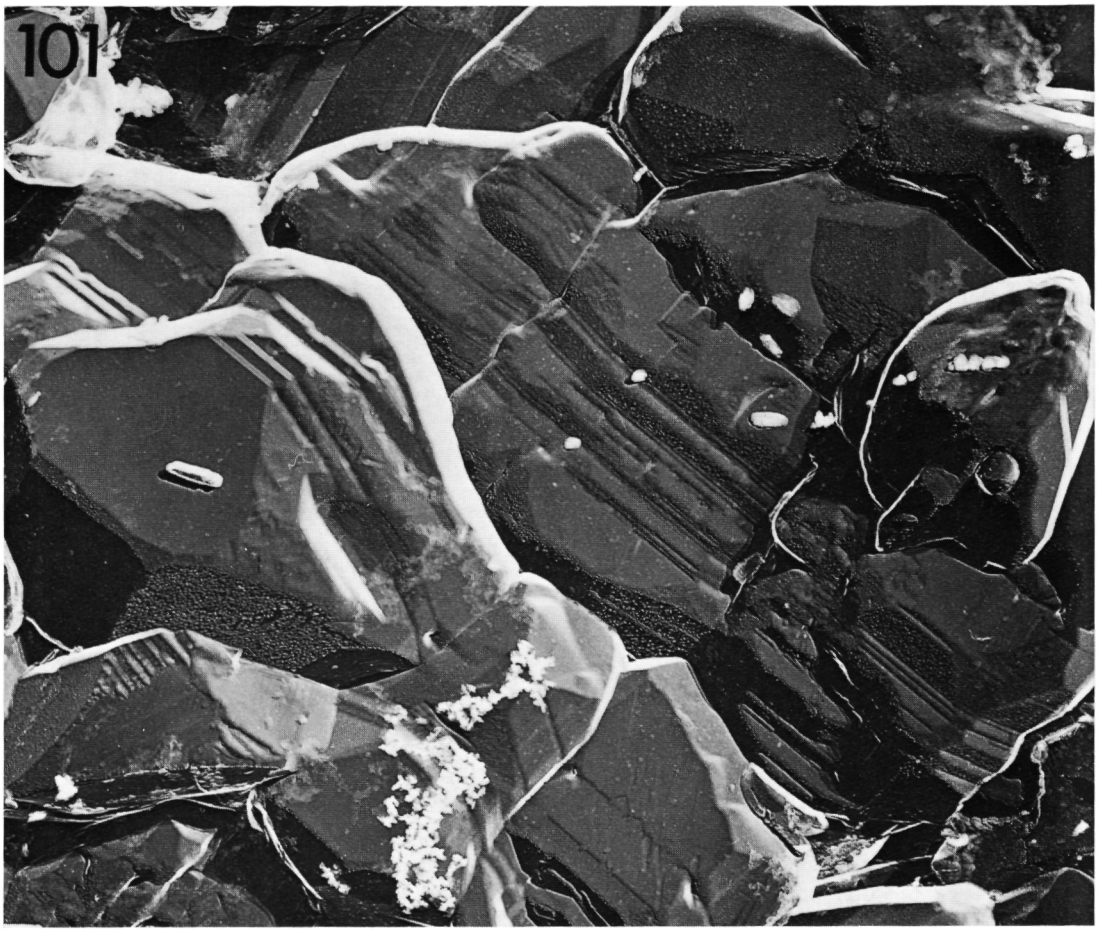

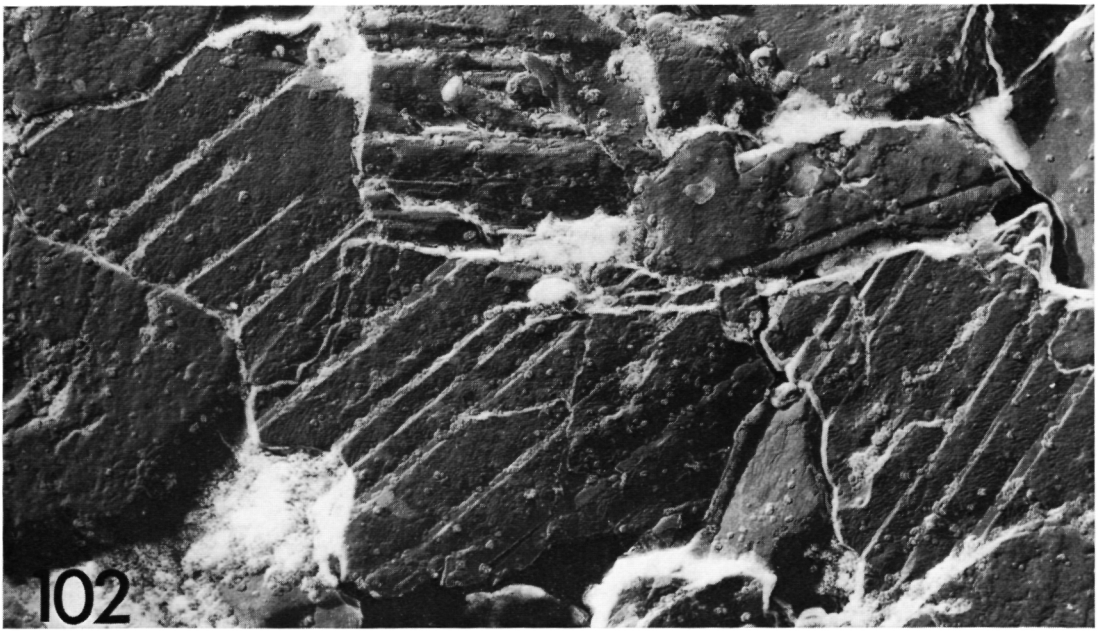

Ch. GREGOIRE. — Experimental alteration of the Nautilus shell.

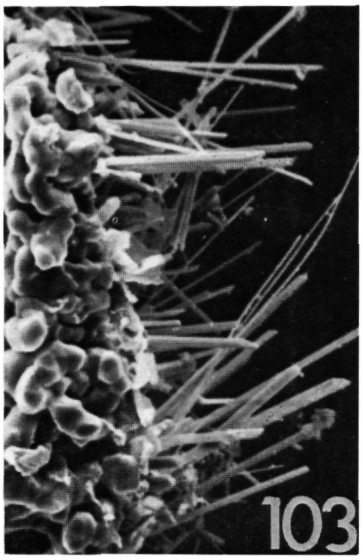

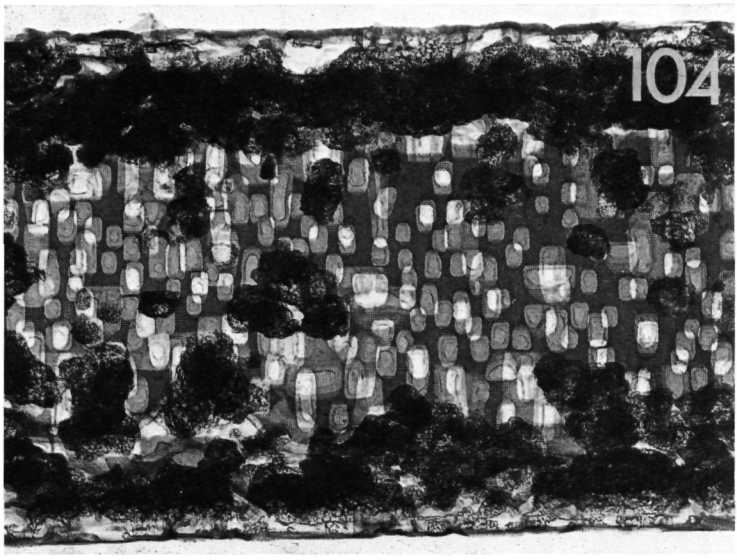

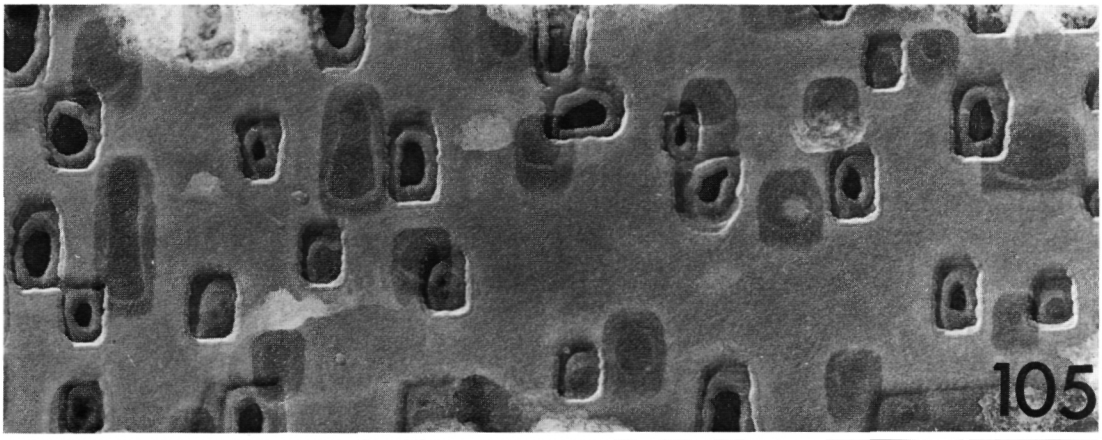

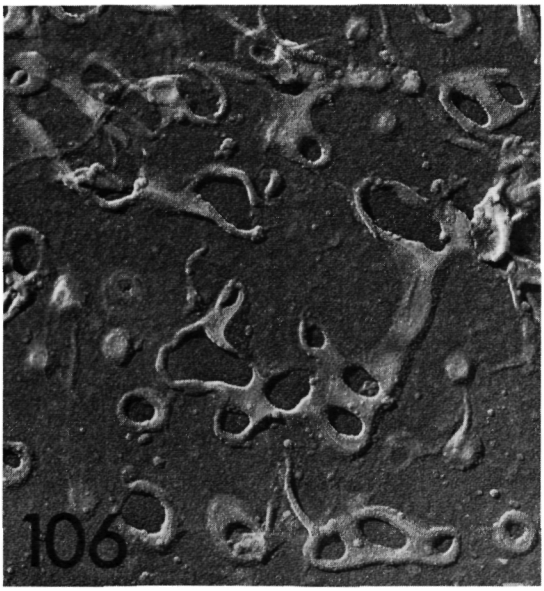

Ch. GREGOIRE. — Experimental alteration of the Nautilus shell.

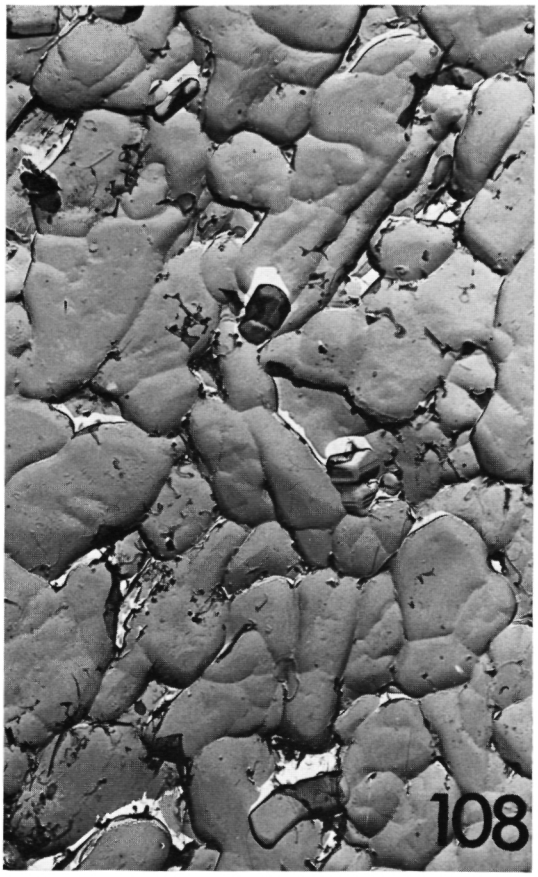

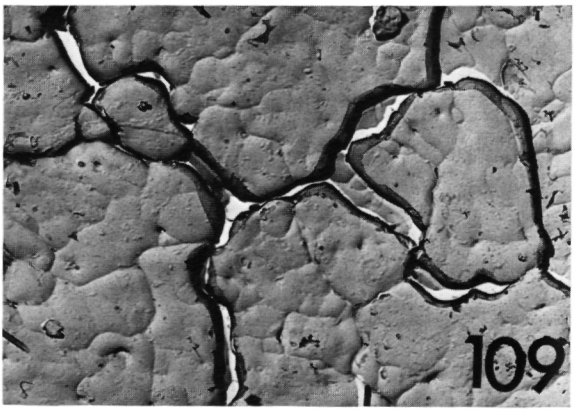

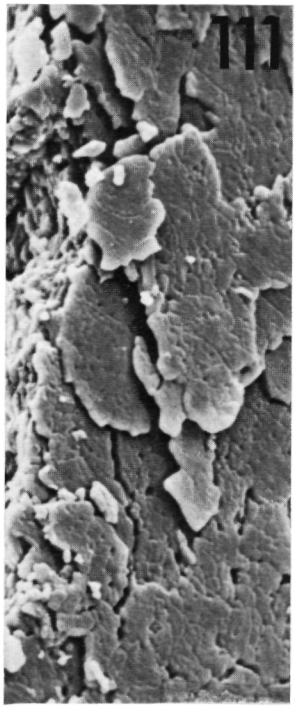

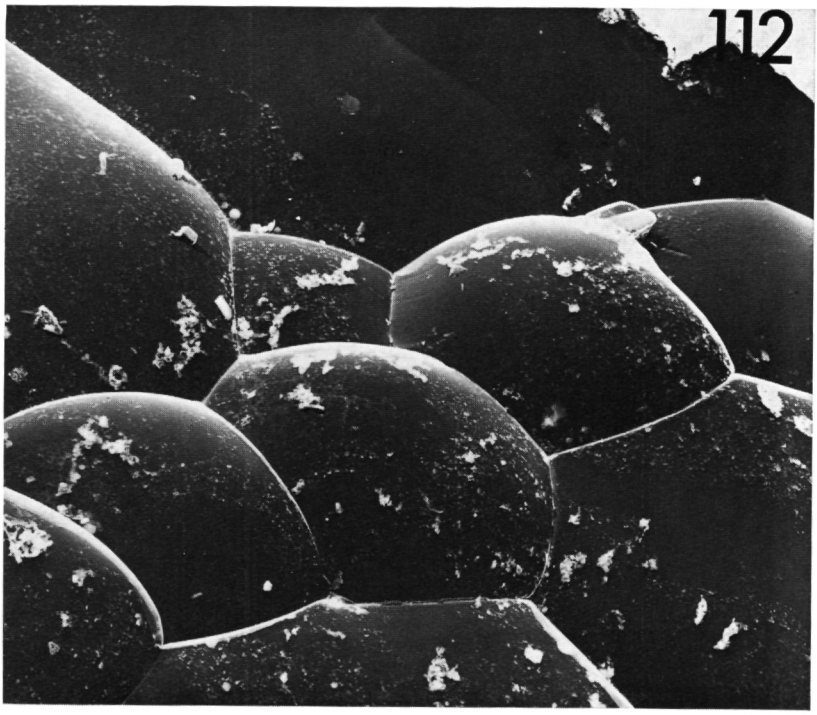

Ch. GREGOIRE. — Experimental alteration of the Nautilus shell.

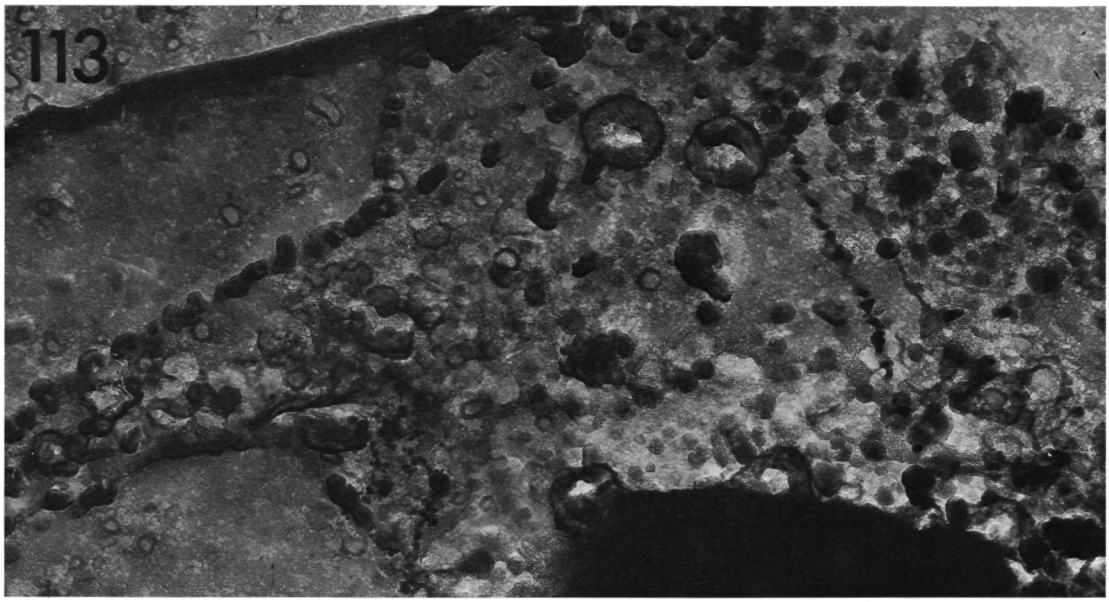

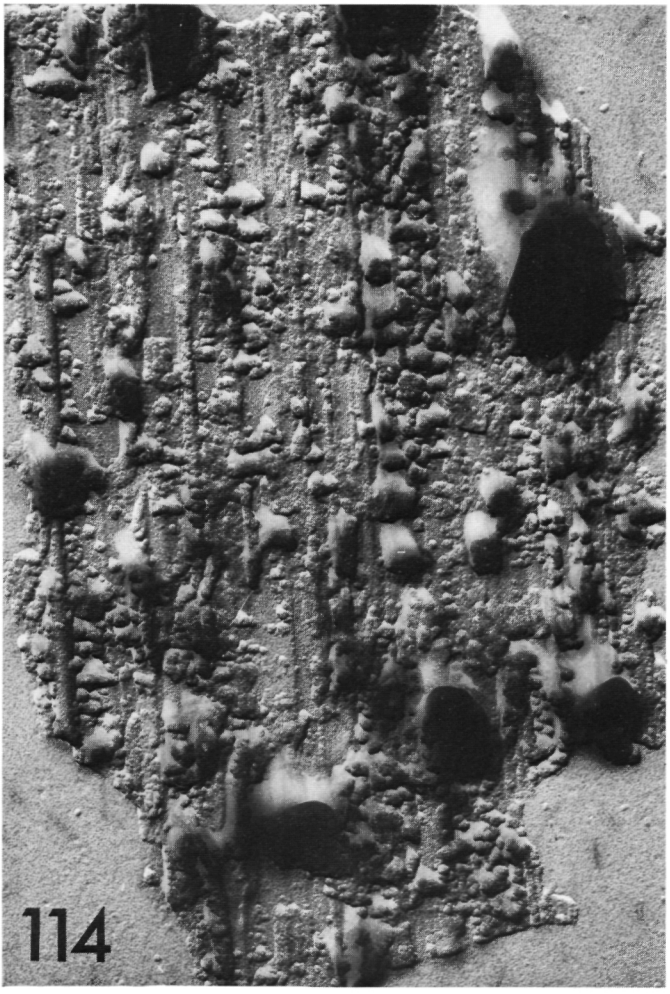

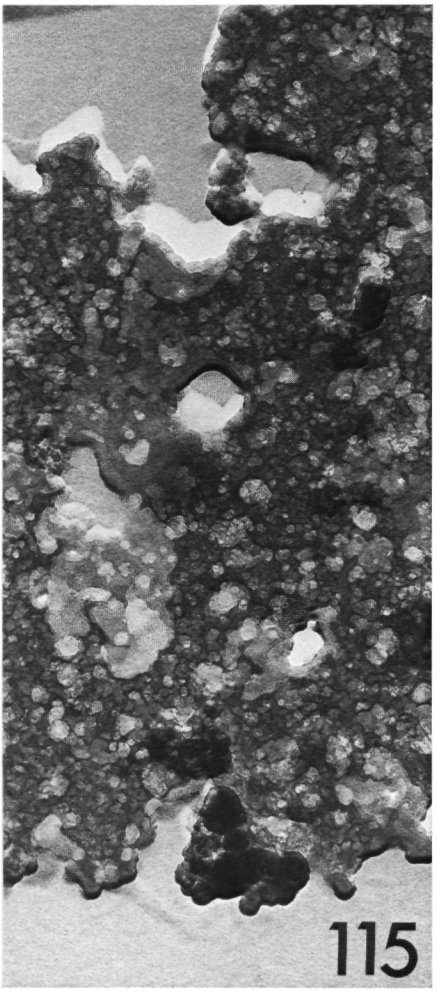

Ch. GREGOIRE. — Experimental alteration of the Nautilus shell.

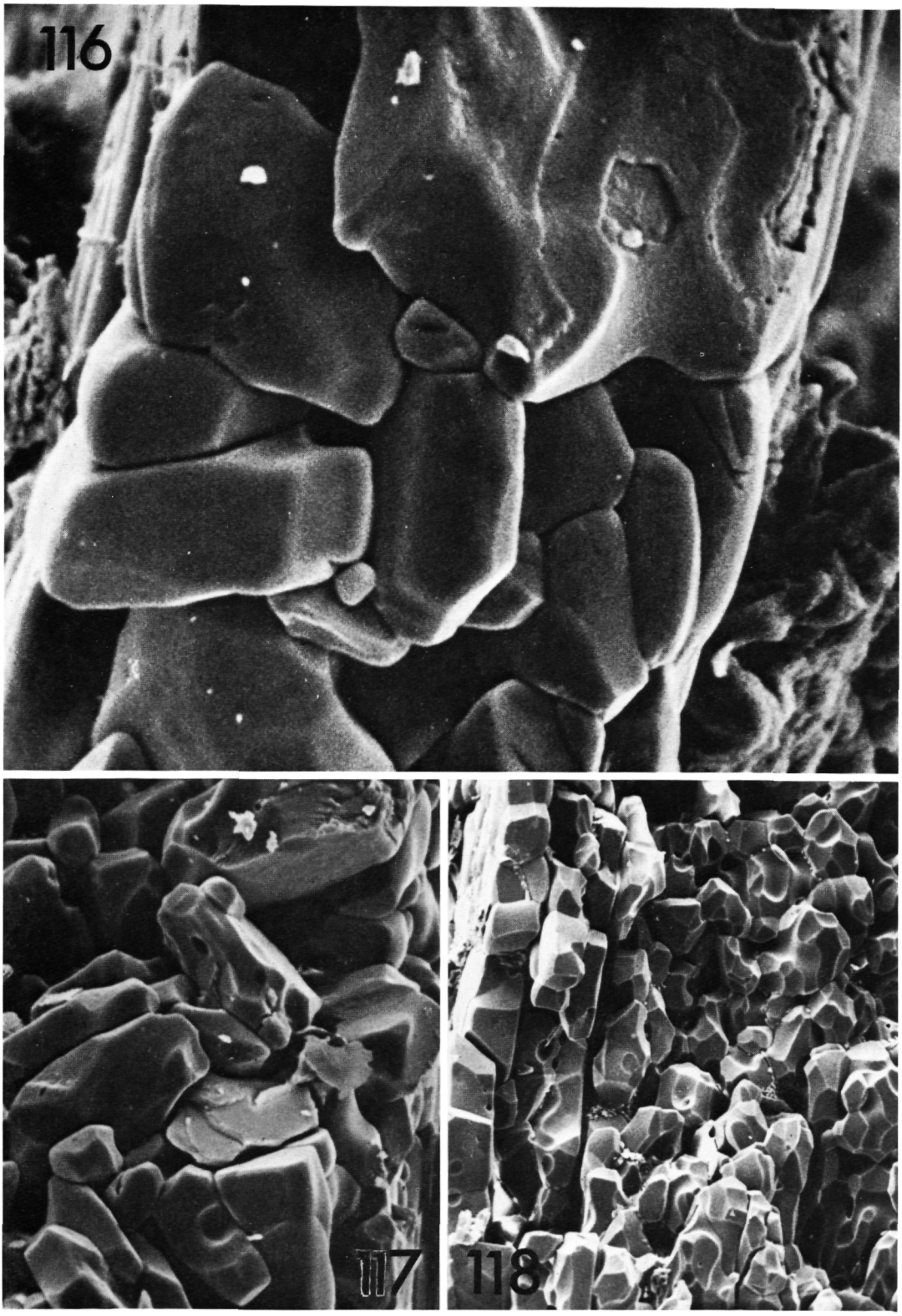

Ch. GREGOIRE. — Experimental alteration of the Nautilus shell.

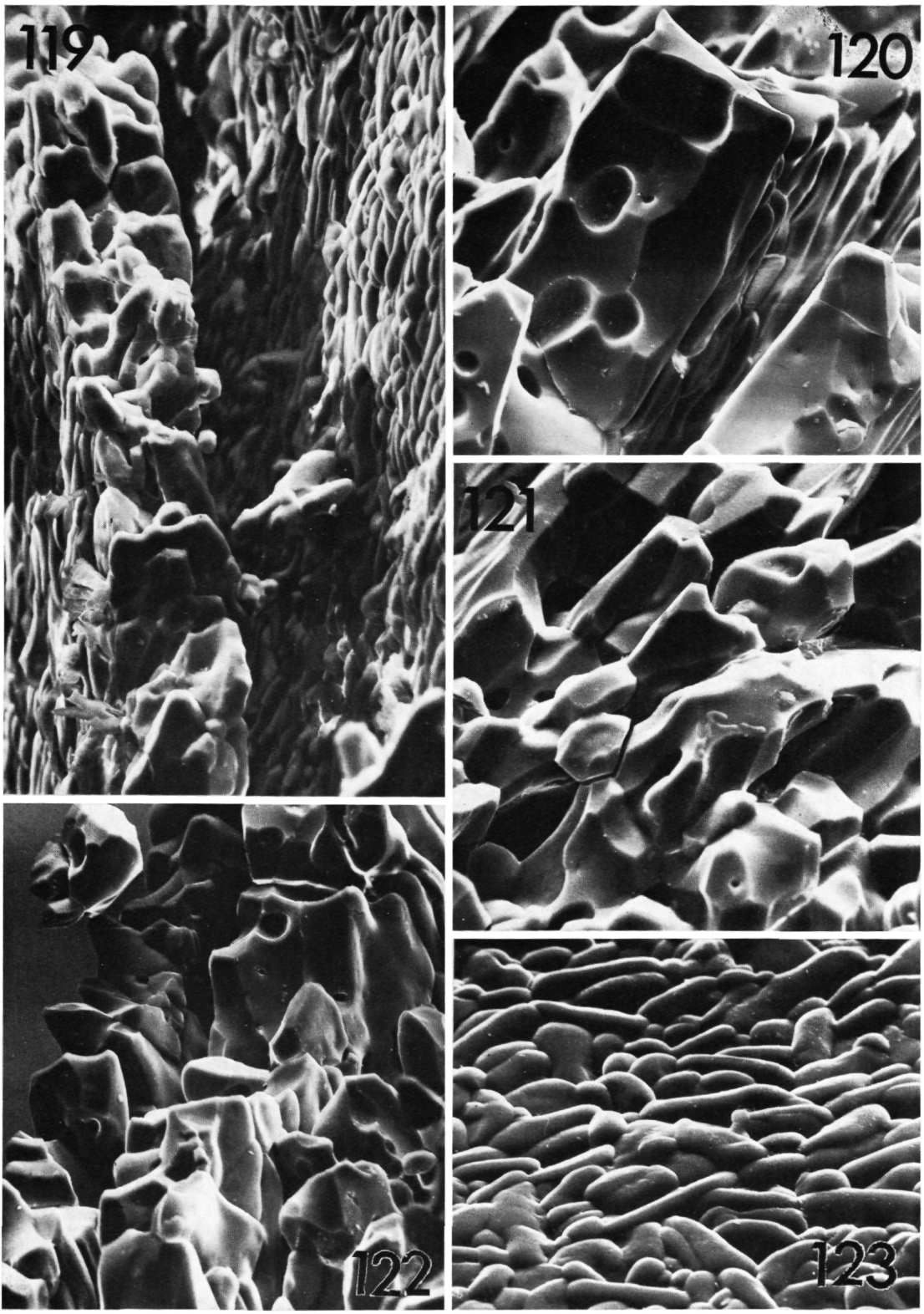

Ch. GREGOIRE. — Experimental alteration of the Nautilus shell.

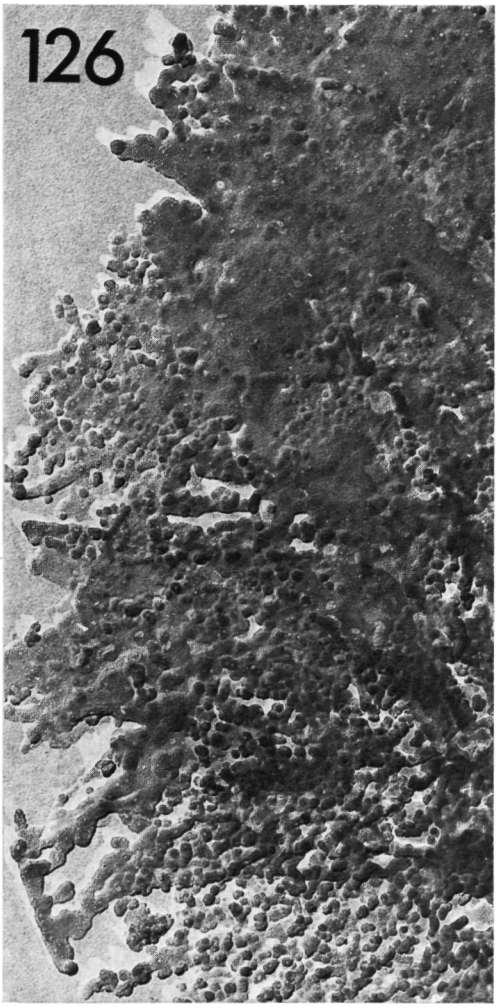

Ch. GREGOIRE. — Experimental alteration of the Nautilus shell.

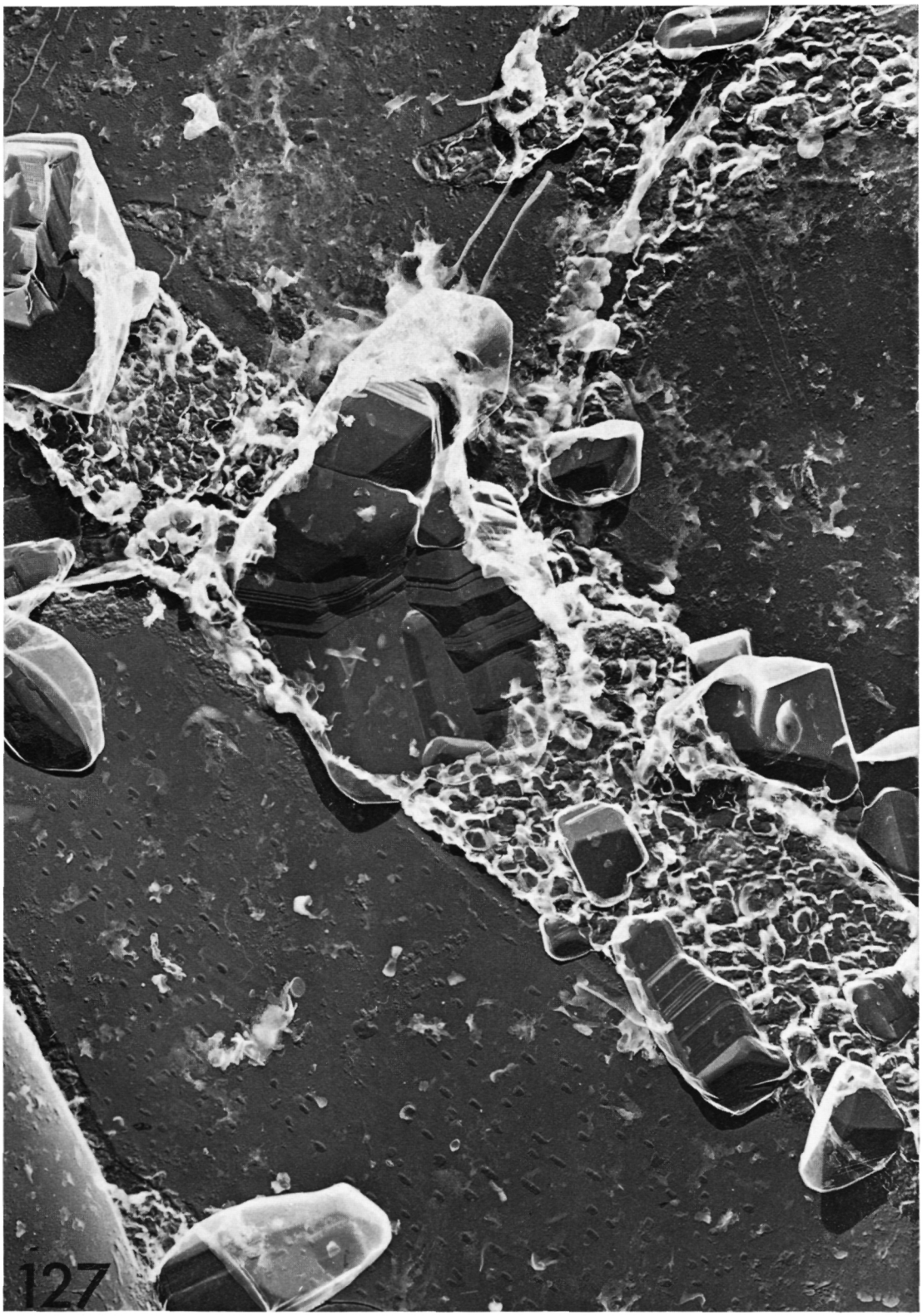

Ch. GREGOIRE. — Experimental alteration of the Nautilus shell.

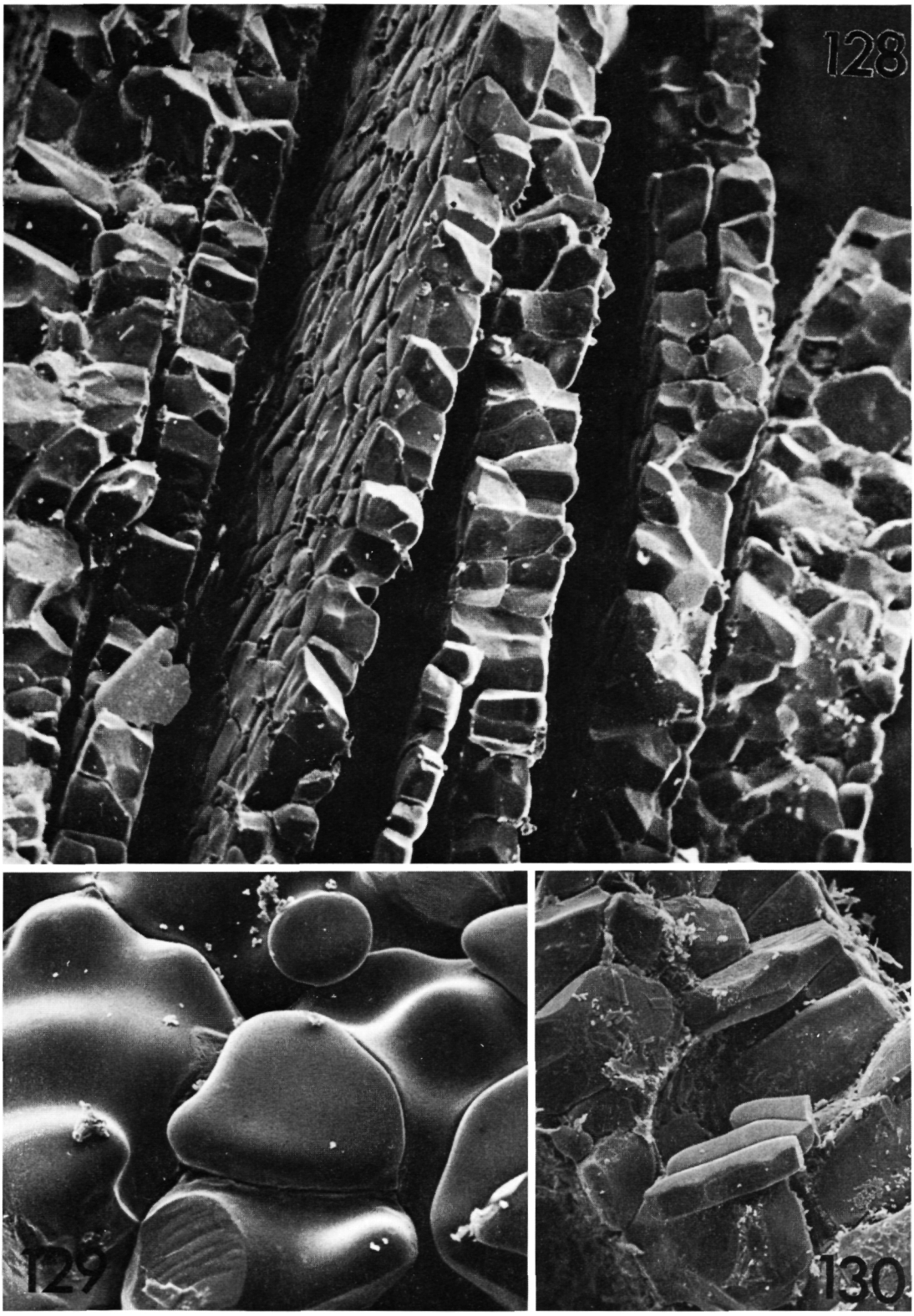

Ch. GREGOIRE. — Experimental alteration of the Nautilus shell.

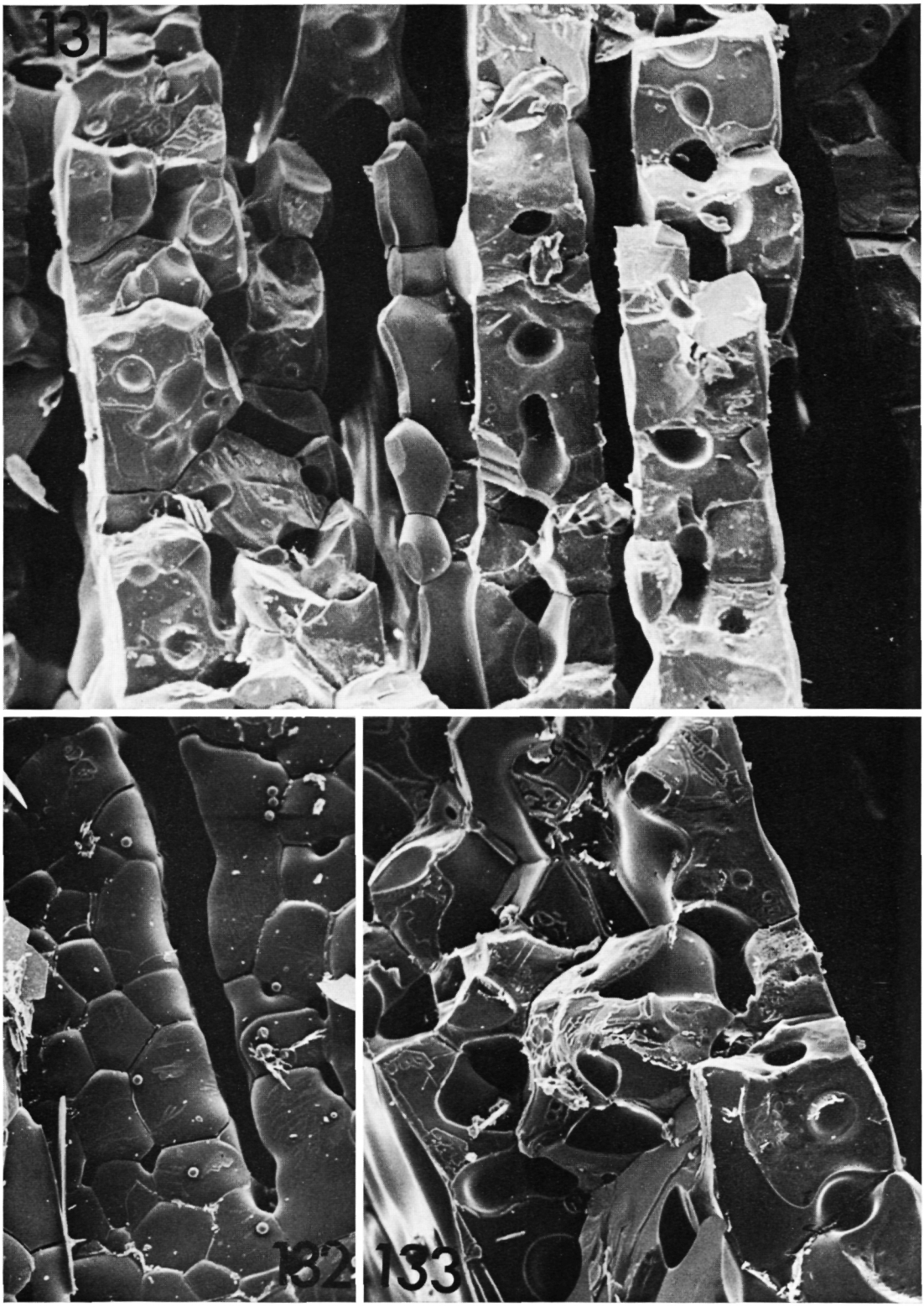

Ch. GREGOIRE. — Experimental alteration of the Nautilus shell.